

https://dspace.org/

Effects of binge alcohol consumption on the development of the femur of adolescent Sprague Dawley rats

Mngoma, Ndabenzinhle Ronald

2024

University of the Witwatersrand, Johannesburg

https://hdl.handle.net/10539/43067

Mngoma, Ndabenzinhle Ronald. (2024). Effects of binge alcohol consumption on the development of the femur of adolescent Sprague Dawley rats[Master's dissertation, University of the Witwatersrand, Johannesburg]. WireDSpace.

Downloaded from a DSpace repository. https://dspace.org/

Effects of binge alcohol consumption on the development of the femur of adolescent Sprague Dawley rats

Student name: Ndabenzinhle Ronald Mngoma

Student number: 1764364

Registered degree: Master of Science in Medicine

Faculty of Health Sciences, University of the Witwatersrand, Johannesburg

Supervisor 1

Dr Akaashni Bhika (BChD)

Lecturer (Morphological Anatomy)

School of Anatomical Sciences

Medical School

7 York Road Parktown

Faculty of Health Sciences

Tel: +27 11 717 2136

Email: Akaashni.bhika@wits.ac.za

Supervisor 2

Dr Diana Pillay (PhD)

Senior Lecturer

(Morphological Anatomy)

Sefako Makgatho Health Sciences

University

Medunsa

Tel: +27 12 521 4313

Email: Diana.pillay@smu.ac.za

A Dissertation submitted to the Faculty of Health Sciences, University of the Witwatersrand, Johannesburg, in fulfilment of the requirements for the degree of Master in Science in Medicine.

Johannesburg, 2023

DECLARATION

I, Ndabenzinhle Ronald Mngoma, declare that this Dissertation is my own, unaided work. It is being submitted for the Degree of Master in Science in Medicine at the University of the Witwatersrand, Johannesburg. It has not been submitted before for any degree or examination at any other University.



(Signature of candidate)

18th day of December 2023 in Parktown

ABSTRACT

Excessive alcohol consumption adversely affects bone metabolism, thus resulting in reduced bone length, density, and strength. While excessive alcohol consumption is an established risk factor for osteoporotic fractures, there remains a dearth of information in literature regarding bone effects of binge alcohol consumption in adolescents. Therefore, our study aimed to examine the effects of binge alcohol consumption in an acute and chronic binge model, on the development and growth of the adolescent femur. Forty-eight Sprague Dawley rats (24 male and 24 female) aged 7 weeks were randomly allocated to one of the 4 treatment groups (n= 12/group) receiving binge alcohol (3g/kg of 20% alcohol) or caloric equivalent of maltose dextrin (pair-fed control), via oral gavage. The treatment groups were; A1, receiving alcohol on 3 alternating days for one week, C1, receiving the caloric equivalent of maltose dextrin in the same manner as A1 (acute), A4 and C4 received treatments in the same manner as A1 and C1 for four consecutive weeks (chronic). Trabecular morphometry in both the proximal and distal epiphysis, and cortical dimensions were assessed by using three-dimensional Micro-Focus X-ray Computed Tomography (3D-µCT) and Volume Graphics Studio® software. The morphology of the epiphyseal growth plate was examined by Haematoxylin and Eosin staining, whereas Ki-67 immunostaining was employed to quantify the proliferation of chondrocytes in the proliferative zone of the growth plate. A three-point bending test was employed to examine the effects of alcohol on bone strength. Results showed that binge alcohol consumption causes thinner trabeculae that are more widely spaced and with a smaller bone to volume ratio (BV/TV). However, the tensile strength was similar in the alcohol exposed rats and paired fed groups in male rats, whereas it appeared improved in female rats exposed to alcohol. A binge model also affected the number of chondrocytes in the proliferative zone negatively. All the adverse changes observed in the osseous tissue in the current study were shown in the male rats. Our study found alcohol to have no adverse effects on female rats, which could be due to hormonal differences.

ACKNOWLEDGEMENTS

Firstly, I would like to extend my profound gratitude to my supervisors; Dr D Pillay, and Dr A Bhika, for their unwavering support, immense knowledge, motivation, and mentorship throughout my Master's journey. I consider myself fortunate to have had such dedicated and knowledgeable supervisors to guide me through this academic endeavour.

Special thanks to Mrs Ali and Mr Khoza for their invaluable technical support, together with the staff of the University of the Witwatersrand Research Animal Facility, for their assistance in caring and treatment of our study animals. I also wish to thank Mr Kobus and Mr Lunga who assisted me in scanning and reconstruction of rat bones used in this study. To Dr Nura Bello, I offer my sincere thanks for your valuable assistance.

I could not have completed this Master's dissertation without the funding from my supervisor's grant (NRF Thuthuka fund), NFR scholarship, TATA Africa postgraduate scholarship and the FRC grant. Special thanks to all my funders.

Lastly, I am deeply grateful to my family and friends for their unwavering support and prayers throughout my academic journey. Your encouragement has been invaluable to me.

CONTENTS

Declaration ii

Abstract.....iii

Acknowledgements iv

Table of Contents v

List of abbreviations ix

List of figures xi

List of tables ……xiii

Chapter 1: Introduction, Literature review, Aims and Objectives

1.1 Background to the research question…….2

1.2 **Literature review**

1.2.1. Overall effects of alcohol consumption…….4

1.2.2. Alcohol metabolism……...4

1.2.3. Drinking patterns……...5

1.2.4. Binge alcohol consumption……...5

1.2.5. Prevalence of binge alcohol consumption…….6

1.2.6. Adolescence growth phase ……...7

1.2.7. Bone structure and function …….8

1.2.8. Femur……..10

1.2.9. The epiphyseal growth plate……...11

1.2.10. Cortical and trabecular bone……...12

1.2.11. The effects of alcohol on the internal bone's architecture..……....13

1.2.12. Bone remodelling…….……...14

1.2.13. Bone biomechanical properties……...15

1.2.14. The role of Ki-67 antibody….……16

1.2.15. Animal model…….16

1.2.16. Alcohol administration techniques employed in animal studies investigating the developmental effects of alcohol consumption……17

1.3 **Aims and objectives**

1.3.1. Aim…….18

1.3.2. Objectives……...…18

Chapter 2: Methodology

2.1 Study animals……....……...20
2.2 Group treatment and allocation…….....20
2.3 Determination of Blood alcohol concentration…….21
2.4 Skeletal harvesting……21
2.5 Three-dimensional Micro-Focus X-ray Computed Tomography (3D-µCT)……21
2.6 Femoral osteometry and trabecular morphometry …….....22
2.7 Three-point bending test…….....23
2.8 Tissue processing for histology and immunohistochemical techniques (IHC)…25
2.9 Haematoxylin and Eosin staining of the epiphyseal growth plate…….……..26
2.10 Immunohistochemistry for Ki-67 in the femoral epiphyseal growth plate…26
2.11 Photography and quantification of chondrocytes.……..27
2.12 Data analysis ..……....28

Chapter 3: The effects of acute binge alcohol consumption on the development of the femur of adolescent Sprague Dawley rats

3.1 **Introduction** …….31
3.2 **Results**
3.2.1 Measurement reliability…….32
3.2.2 Blood alcohol concentration……..32
3.2.3 Body weight gain……...32
3.2.4 Food consumption……..33
3.2.5 Osteometric measurements of the femur……34
3.2.6 Femur Trabecular Morphometrics……..35
3.2.7 Femur cross-sectional area, medullary canal area and cortical area……...41
3.2.8 Three-point bend testing of the femur, tensile strength assessment……...46
3.2.9 Morphological assessment of the femoral epiphyseal growth plate……...47
3.2.10 Proliferative zone Ki-67 immuno-positive chondrocyte number……...49
3.3 **Discussion**……..52
3.4 **Conclusion**…….57

Chapter 4: The effects of chronic binge alcohol consumption on the development of the femur of adolescent Sprague Dawley rats

4.1 **Introduction** …….60

4.2 **Results**

4.2.1 Measurement reliability……61

4.2.2 Blood alcohol concentration……..61

4.2.3 Body weight gain .....….....……...61

4.2.4 Food consumption……..62

4.2.5 Osteometric measurements of the femur……63

4.2.6 Femur Trabecular Morphometrics……..65

4.2.7 Femur cross-sectional area, medullary canal area and cortical area……...71

4.2.8 Three-point bend testing of the femur, tensile strength assessment……76

4.2.9 Morphological assessment of the femoral epiphyseal growth plate……77

4.2.10 Proliferative zone Ki-67 immuno-positive chondrocyte number……79

4.3 **Discussion**……...82

4.4 **Conclusion**……..87

Chapter 5: General discussion and conclusion……...89

References……...93

Appendices

Appendix 1: Turnitin report……...102

Appendix 2: Ethical clearance certificate ……103

Appendix 3: Reagent used……104

Appendix 4: Equipment……106

Appendix 5: Software packages……107

Appendix 6: Calculation of the Alcohol (ethanol 20%) dosage administered……...108

Appendix 7: Calculation of the Maltose dextrin (isocaloric) dosage administered……...109

Appendix 8: Preparation of 10% Neutral Buffered Formalin (1000 ml)…….....110

Appendix 9: Preparation of 0.9% Saline solution (1000ml)…….....111

Appendix 10: Tissue decalcification; EDTA 14%.....112

Appendix 11: Tissue processing.……...113

Appendix 12: Paraffin wax embedding……114

Appendix 13: Silane coated slides……115

Appendix 14: Mayer's Haematoxylin and eosin staining……..116

Appendix 15: Immunohistochemistry for Ki-67 antibody (NB 500-170)…….118

Appendix 16: Measurement of cross-sectional area, medullary canal area and cortical area……..120

Appendix 17: Measuring the trabecular morphometry on VG studio……....121

NOMENCLATURE/LIST OF ABBREVIATIONS AND SYMBOLS

%	:	percent
µa	:	microampere (µa)
µm	:	micrometre
3D -µCT	:	three-dimensional micro-focus X-ray computed tomography
dl	:	decilitre
g	:	grams
kg	:	kilogram
kV	:	kilovolts
mg	:	milligram
ml	:	millilitre
mm	:	millimetre
mm^{-1}	:	per 1 millimetre unit
mm^2	:	area in millimetres
N	:	Newton
^{o} C	:	degree celsius
sec	:	second
vol/vol	:	volume per volume
w/v	:	weight per volume
A1	:	1-week alcohol-exposed rats
A4	:	4-week alcohol-exposed rats
ADH	:	Alcohol dehydrogenase
AESC	:	Animal Ethics Screening Committee
ALDH	:	Acetaldehyde dehydrogenase
APES	:	3-aminopropyltriexothysilan
BAC	:	Blood alcohol concentration
BT/TV	:	Bone volume to total volume
C1	:	1-week pair-fed control rats
C4	:	4-week pair-fed control rats
CA	:	Cortical area

CSA	:	Cross sectional area
DAB	:	3-3’ diaminobenzidine
EDTA	:	Ethylenediamine tetra acetic acid
Fig	:	Figure
H&E	:	Haematoxylin and eosin
H_2O_2	:	Hydrogen peroxide
HDL	:	High density lipoprotein
HZ	:	Hypertrophic zone
IHC	:	Immunohistochemistry
MCA	:	Medullary canal area
NIAAA	:	National institute on alcohol abuse and alcoholism
PBS	:	Phosphate buffer solution
pH	:	Potential of hydrogen
PZ	:	Proliferative zone
RZ	:	Resting zone
SD	:	Standard deviation
SPSS	:	Statistical package for social services
WRAF	:	University of the Witwatersrand research animal facility

LIST OF FIGURES

Figure	Description	Page
Figure 1.1	Schematic representation of endochondral ossification	9
Figure 1.2	Schematic representation of intramembranous ossification	10
Figure 1.3	Parts of a long bone	11
Figure 1.4	An illustration of an epiphyseal growth plate with chondrocytes progressing through the resting phase, proliferative phase, and hypertrophic phase	12
Figure 1.5	Illustration of types of bone; spongy bone and compact bone	13
Figure 1.6	Bone remodelling	15
Figure 2.1	A reconstructed 3D femur illustrating points analysed	23
Figure 2.2	3-point bend testing	24
Figure 2.3	An illustration of a load displacement curve showing bone strength parameters of compact bone	25
Figure 2.4	Serial sectioning of bone samples	26
Figure 2.5	A Haematoxylin and Eosin-stained section of the femur showing delineated growth plate zones namely, the hypertrophic, proliferative, and resting zones	28
Figure 3.1	Average body weight	33
Figure 3.2	Food consumption	33
Figure 3.3	Bone length	34
Figure 3.4	Femoral bicondylar breadth for the acute binge alcohol consumption model	35
Figure 3.5	Femoral bone to total volume ratio (BV/TV) for the acute binge alcohol consumption model	36
Figure 3.6	Femoral trabecular thickness (Tb.Th) for the acute binge alcohol consumption model	37
Figure 3.7	Femoral trabecular number (Tb.N) for the acute binge alcohol consumption model	38
Figure 3.8	Femoral trabecular spacing (Tb.Sp) for the acute binge alcohol consumption model	40
Figure 3.9	Trabecular morphology in the proximal and distal ends of the femora for the pair-fed control and alcohol groups in male rats	40
Figure 3.10	Trabecular morphology in the proximal and distal ends of the femora for the pair-fed control and alcohol groups in female rats	40
Figure 3.11	25^{th} percentile mark (proximal) dimensions of the femoral shaft.	42
Figure 3.12	50^{th} percentile mark (midshaft) dimensions of the femoral shaft.	44
Figure 3.13	75^{th} percentile mark (distal) dimensions of the femoral shaft.	45
Figure 3.14	Haematoxylin and Eosin-stained longitudinal sections of both the proximal and distal epiphyseal growth plates for two study groups in male rats	48
Figure 3.15	Haematoxylin and Eosin-stained longitudinal sections of both the proximal and distal epiphyseal growth plates for two study groups in female rats	49

Figure 3.16	Femoral epiphyseal growth plate proliferative zone number of chondrocytes	50
Figure 3.17	Photomicrographs depicting immunolabeled femur chondrocytes using the anti-Ki-67 antibody (male rats)	51
Figure 3.18	Photomicrographs depicting immunolabeled femur chondrocytes using the anti-Ki-67 antibody (female rats)	51
Figure 4.1	Average body weight	62
Figure 4.2	Food consumption	63
Figure 4.3	Bone length	64
Figure 4.4	Femoral bicondylar breadth for the acute binge alcohol consumption model	65
Figure 4.5	Femoral bone to total volume ratio (BV/TV) for the acute binge alcohol consumption model	66
Figure 4.6	Femoral trabecular thickness (Tb.Th) for the acute binge alcohol consumption model	67
Figure 4.7	Femoral trabecular number (Tb.N) for the acute binge alcohol consumption model	68
Figure 4.8	Femoral trabecular spacing (Tb.Sp) for the acute binge alcohol consumption model	69
Figure 4.9	Trabecular morphology in the proximal and distal ends of the femora for the pair-fed control and alcohol groups in male rats	70
Figure 4.10	Trabecular morphology in the proximal and distal ends of the femora for the pair-fed control and alcohol groups in female rats	71
Figure 4.11	25^{th} percentile mark (proximal) dimensions of the femoral shaft.	72
Figure 4.12	50^{th} percentile mark (midshaft) dimensions of the femoral shaft.	74
Figure 4.13	75^{th} percentile mark (distal) dimensions of the femoral shaft.	75
Figure 4.14	Haematoxylin and Eosin-stained longitudinal sections of both the proximal and distal epiphyseal growth plates for two study groups in male rats	78
Figure 4.15	Haematoxylin and Eosin-stained longitudinal sections of both the proximal and distal epiphyseal growth plates for two study groups in female rats	79
Figure 4.16	Femoral epiphyseal growth plate proliferative zone number of chondrocytes	80
Figure 4.17	Photomicrographs depicting immunolabeled femur chondrocytes using the anti-Ki-67 antibody (male rats)	81
Figure 4.18	Photomicrographs depicting immunolabeled femur chondrocytes using the anti-Ki-67 antibody (female rats)	81

LIST OF TABLES

Table	Description	Page
Table 2.1	Scanning parameters	22
Table 2.2	Femoral osteometric description	23
Table 2.3	Trabecular morphometric parameters description	23
Table 2.4	Parameters derived from a load displacement curve	24
Table 3.1	Weight measurements and tensile strength parameters of the male rat femur	47
Table 3.2	Weight measurements and tensile strength parameters of the female rat femur	47
Table 4.1	Weight measurements and tensile strength parameters of the male rat femur	76
Table 4.2	Weight measurements and tensile strength parameters of the female rat femur	77

Chapter 1

Introduction, Literature review, Aims and Objectives

1.1 INTRODUCTION

1.1 Background to the research question

Excessive alcohol consumption is known to have a range of detrimental effects on public health. These include alcohol-related accidents, violence, crime and may disturb the integrity of bone development and internal architecture of the osseous tissue (Morojele and Ramsoomar, 2016; Reed et al., 2002). South Africa, in particular, has a high prevalence of dangerous drinking practices, with one in three individuals reported consuming alcohol, while one in seven reported binge drinking on an average day on which alcohol is consumed (Morojele and Ramsoomar, 2016, Vellios and Van Walbeek, 2017). This poses a significant public health concern, as high levels of binge drinking are observed among the adolescent population globally (Morojele and Ramsoomar, 2016, Vellios and Van Walbeek, 2017).

The adolescent stage is critical in the development of bone and attaining peak bone mass (Weaver, 2002). Hence, the consumption of alcohol during this period may cause interruptions in bone growth and development (Lauing et al., 2008). Alcohol is known to decrease peak bone mass causing an increased risk of fractures and the early onset of osteoporosis (Reed et al., 2002; Sampson, 1998).

Previous studies on the effects of chronic alcohol consumption on the skeleton of young rats have shown significant reductions in cancellous and periosteal bone formation, trabecular thickness, and bone compressive strength (Lauing et al., 2008; Manolagos et al., 2013; Reed et al., 2002; Turner, 2000). Additionally, a study by Föger-Samwald et al, (2018) conducted on prepubescent pigs suggested that the effects of binge alcohol consumption on bone are site-specific. However, there has been limited research investigating the effects of binge alcohol consumption specifically on the development of the adolescent femur. Therefore, further investigation is warranted in this niche to understand the specific effects of binge alcohol consumption on the development and integrity of the adolescent femur.

Considering the above, the current study aimed to investigate the effects of binge alcohol consumption on the development of the adolescent Sprague Dawley rat femur. The study incorporated the use of three-dimensional micro-focus X-ray computed tomography (3D-µCT) to assess the effects of binge drinking on trabecular parameters and femoral osteometrics. Haematoxylin and Eosin (H&E) staining were employed to study the morphological changes of the epiphyseal growth plate. Immunohistochemistry was used to assess the proliferation of chondrocytes in the epiphyseal growth plate using the anti-Ki-67 antibody. The effects of binge

alcohol consumption on bone strength were assessed using a 3-point bending test. These comprehensive assessments provided insights into the specific effects of binge alcohol consumption on the development of the adolescent femur, shedding light on potential structural and functional alterations associated with this behaviour.

1.2 Literature Review

1.2.1 Overall effects of alcohol consumption

The relationship between alcohol consumption and health is multifaceted. Extensive research has provided evidence that consuming alcohol plays a substantial role in contributing to the overall burden of diseases (Griswold et al., 2018; Reed et al, 2002). Numerous studies have specifically identified links between alcohol consumption and the development of various acute and chronic illnesses (Rehm et al., 2011). Acute illnesses can occur after a single episode of heavy drinking and encompass alcohol poisoning, accidental injuries due to impaired coordination and judgment, gastrointestinal issues like gastritis and ulcers, pancreatitis, and cardiovascular events like heart attacks. On the other hand, chronic illnesses often result from long-term, excessive alcohol use which include conditions like liver disease, cardiovascular disease, pancreatitis, alcoholic neuropathy, secondary osteoporosis, and alcoholic dementia. These conditions can have severe long-term effects on the body's organs, particularly the liver, heart, pancreas, and skeletal system (Morojele and Ramsoomar, 2016; Reed et al., 2002; Shield et al., 2014).

1.2.2 Alcohol metabolism

The effects of alcohol on various tissue depend on its concentration in the blood (blood alcohol concentration) over time. Blood alcohol concentration is determined by how quickly alcohol is absorbed, distributed, metabolised, and excreted (Zakhari, 2006). Following ingestion, alcohol is primarily absorbed from the small intestines to the liver via the hepatic vein (Zakhari, 2006). The liver plays a crucial role as the primary site for alcohol metabolism. Alcohol dehydrogenase (ADH) catalyses the enzymatic conversion of alcohol into acetaldehyde, a toxic metabolite (Ramchandani et al., 2001). Subsequently, acetaldehyde is further metabolized by acetaldehyde dehydrogenase (ALDH) into acetic acid, which is then oxidized into carbon dioxide and water (Zakhari, 2006; Ramchandani et al., 2001).

Generally, the liver maintains a relatively constant rate of alcohol metabolism, averaging around one standard drink per hour (Zakhari, 2006). However, it is important to consider individual variations such as age, sex, genetics, liver function, and alcohol tolerance, can affect the rate of metabolism and increase susceptibility to adverse effects associated with excessive alcohol consumption (Zakhari, 2006). Moreover, the rate of alcohol metabolism also differs

across various species (Cederbaum, 2019). While all mammalian species possess the necessary enzymes to metabolize alcohol, the efficiency of these enzymes in eliminating alcohol from the system varies (Ramchandani et al., 2001). Rodents, such as rats and mice, metabolize alcohol much more rapidly, typically within approximately 1.5 hours, compared to humans. Conversely, larger animal species like sheep and non-human primates exhibit similar rates of alcohol metabolism to humans, taking around 4 hours (Zorzano and Herrera, 1990).

1.2.3 Drinking patterns

Drinking patterns play a significant role in influencing the association between alcohol consumption and related health consequences (Rehm, 2016). This is primarily because these patterns determine both the extent of harmful effects resulting from toxic substances, leading to chronic illnesses and the degree of intoxication which then influences the propensity of injuries and social issues (Rehm, 2011). Many alcohol-related conditions exhibit a dose-response correlation between volume of alcohol consumption and risk of adverse outcomes (Rehm, 2011; Turner, 2000). This suggests that occasions involving heavy alcohol consumption have a greater risk for both toxic effects and greater intoxication (Astudillo et al., 2010). By definition, heavy alcohol consumption refers to the act of regularly consuming significant quantities of alcoholic beverages over a continuous period of time (Astudillo et al., 2010). On the other hand, moderate alcohol consumption refers to the consumption of one standard alcoholic drink per day for women and two drinks per day for men, according to the National Institute on Alcohol Abuse and Alcoholism (2004). Consuming alcohol at low to moderate levels is more likely to have beneficial effects such as anti-fibrillatory properties, increased high density lipoprotein (HDL) cholesterol levels, enhanced heart energy metabolism, and the activation of protective mechanisms (Editorial Staff, 2018) When investigating the effects of alcohol consumption, particularly in developmental studies, it is essential to consider drinking patterns. Another drinking pattern of interest, particularly in the current study is the binge alcohol consumption.

1.2.4 Binge alcohol consumption

Binge alcohol consumption is defined as the consumption, on one occasion, of ≤ 5 standard drinks for men and ≤ 4 standard drinks for women, resulting in a blood alcohol concentration of 80 mg/dL or above (Föger-Samwald et al, 2018; National Institute on Alcohol Abuse and

Alcoholism, 2004). This pattern of alcohol ingestion is increasingly gaining attention as this pattern tends to occur mainly in the adolescent and young adult populations (Chung et al, 2018). Among adolescents and young adults, binge drinking is often observed on weekends, while moderate or no drinking is common on most weekdays (Kuntsche and Gmel, 2013). This drinking pattern is strongly associated with an increased risk of short and long-term consequences, such as permanent disabilities resulting from injuries or even death (Anderson, 2007; Courtney and Polich, 2009; Dawson et al., 2008; Gmel et al., 2003; Ham and Hope, 2003; Gilmore, 2007). These consequences also encompass direct effects of intoxication, including hangovers, blackouts, memory loss, nausea, and vomiting. In extreme cases, excessive doses of alcohol can lead to alcohol poisoning, which can occasionally be fatal (Kuntsche et al., 2017).

1.2.5 Prevalence of binge alcohol consumption

Worldwide prevalence of binge drinking

On a global scale, the rates of binge drinking prevalence varies significantly among countries due to cultural differences, measurement methods and age restrictions (Chung et al., 2018) According to data from the World Health Organization (2014), when considering individuals aged 15 and older, standardized global estimates indicate that approximately 7.5% of the population engages in binge drinking at least once a week. However, this proportion varies widely across regions with only 0.1% in the Eastern Mediterranean Region containing mainly Islamic states and 1.6% in the South-East Asian Region (mainly India) to 13.7% in the American region and 16.5% in Europe (Kuntsche et al., 2017). Additionally, there is evidence to suggest that countries with lower legal drinking ages tend to experience a greater prevalence of binge alcohol consumption among adolescents, as opposed to countries with higher legal drinking ages (Chung et al., 2018).

Prevalence of binge drinking in South Africa

South Africa has the highest rates of risky alcohol consumption with the prevalence in the adolescent population ranging from 11.2% to 56.9% (Föger-Samwald et al., 2018; Lauing et al., 2008). Additionally, data from the South African Youth Risk Behavior Survey, showed that nationally, 25.1% (with a confidence interval of 23.3–27.0) of Grade 8–11 learners had

consumed five or more alcoholic drinks within a short period of time on one or more occasions in the month before the survey was conducted (Mmereki et al., 2022). This poses a significant public health concern, as the adolescent phase represents a critical period of growth, particularly in terms of skeletal maturation.

1.2.6 Adolescence growth phase

Adolescence is a critical growth phase marked by rapid skeletal development, essential for the attainment of peak bone mass (Weaver, 2002). Peak bone mass corresponds to the maximum amount of osseous tissue present at the end of skeletal maturation and it is a determinant of overall bone health and fragility fractures later in life (Weaver, 2002; Zhu and Zheng, 2021). The attainment of peak bone mass during adolescence, is influenced by various factors including genetics, gender, level of physical activity, hormonal balance, and risky lifestyle choices such as smoking and alcohol consumption (Zhu and Zheng, 2021; Rizzoli et al., 2010).

Genetics play a pivotal role in determining an individual's bone mass. Family and twin studies have consistently demonstrated that bone mass density exhibits a high heritability, with estimates ranging from 50% to 85% (Ralston, 2005; Zhai et al., 2009). Gender differences in the accrual of peak bone mass exist, with the female individuals typically exhibiting a lower peak bone mass compared to their male counterparts, resulting in a 2-4 fold higher incidence of fragility fractures (Gordon et al., 2017). In addition, physical activity such as weight-bearing exercises promote bone development and strength (Nilsson et al., 2009). The production of testosterone in males and oestrogen in females also contribute to bone health and integrity (Zhu and Zheng, 2021). Lifestyle choices, especially excessive alcohol consumption may interfere with the attainment of peak bone mass and may adversely impacting bone health.

Bone mass gradually declines throughout the course of life as a part of the senescence, which increases the risk of developing osteoporosis. Osteoporosis is a prevalent bone disease characterized by a deterioration of bone micro-architecture and a decrease in bone mass (Lauing et al., 2008; Rachner et al., 2011). Attaining a high peak bone mass during adolescence is advantageous as this is likely to endure a longer period of bone loss before reaching a fracture threshold, thus delaying the onset of osteoporosis (Sampson, 1998). In agreement with the latter, research indicates that 10% increase in peak bone mass gain during adolescence can delay the onset of osteoporosis by at least 13 years. Conversely, a 6.4% reduction in peak bone mass is associated with a twofold increase in the risk of low trauma fractures (Zhu and Zheng,

2021). This finding provides further evidence that the bone mass accumulated during adolescence plays a crucial role in determining bone health in adulthood.

1.2.7 Bone structure and function

To investigate the effects of binge alcohol consumption on adolescent bone, an insight on bone function, structure and development is crucial. The skeletal system forms a central framework, giving the body shape, allowing movement, and providing protection for vital organs and storage for minerals (Caballero et al., 2003). Throughout life, bones develop through two cell-mediated processes namely, endochondral (Fig 1.1) and intramembranous ossification (Fig 1.2). Endochondral ossification involves the formation of a cartilage model, which is gradually replaced by bone throughout foetal and postnatal developmental phases. This process is responsible for interstitial growth of long bones (Boskey and Coleman., 2010; Mackie et al., 2008). However, bone is formed directly from mesenchymal cells during intramembranous ossification. This process is involved in the formation of flat bones (Boskey and Coleman, 2010). Adolescence entails physical changes of the body, such as an increase in height and weight (Soliman et al., 2014), and considering that long bones are crucial for height, the current study paid attention to long bones, specifically the femur.

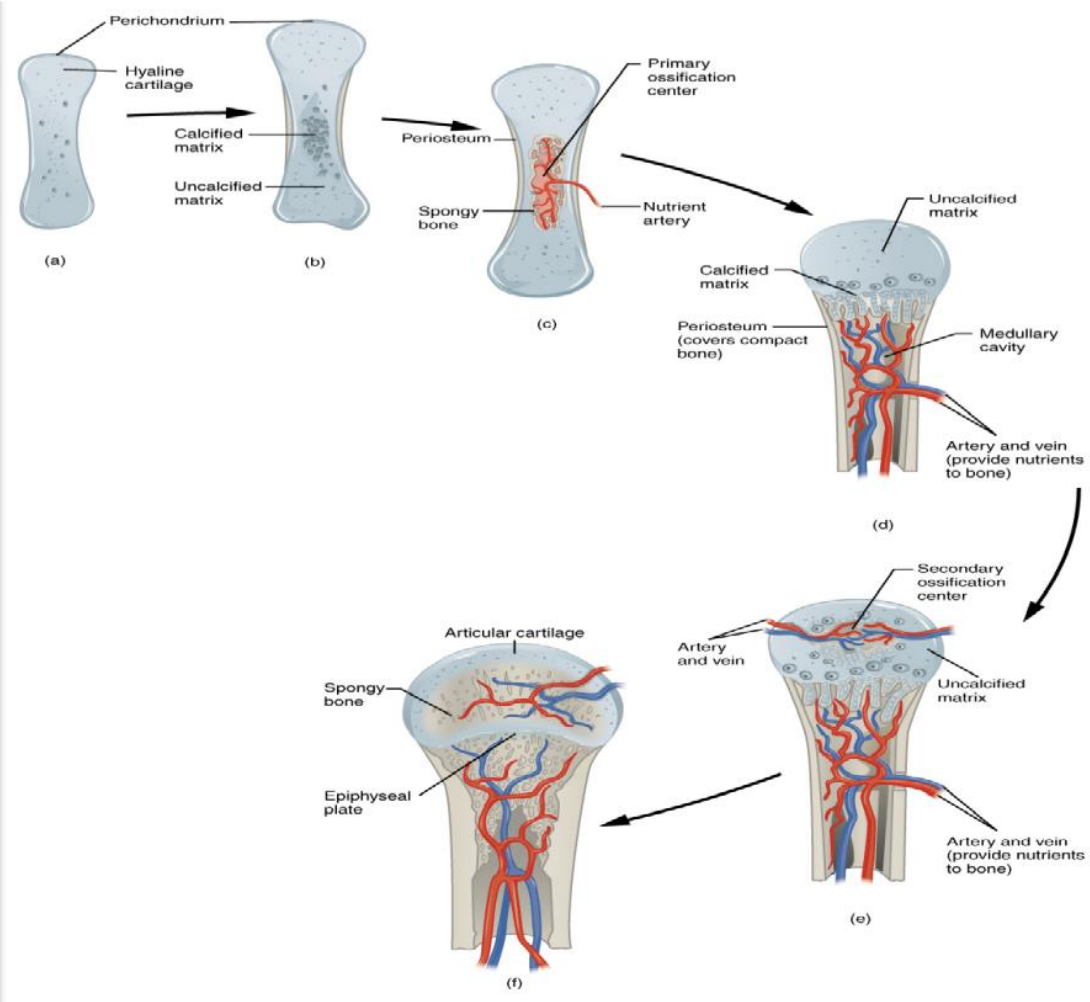


Figure 1.1: Schematic representation of endochondral ossification. (a)Mesenchymal cells differentiate into chondrocytes thus form; (b) a hyaline cartilage model of the bone , (c) blood vessels penetrate the cartilage and perichondrium is transformed into periosteum. The primary ossification centre develops. (d) Hyaline cartilage and chondrocytes continue to grow at the distal ends of the bone. (e) The secondary ossification centre develops. (f) The cartilage remains at the epiphyseal growth plate as the bone grows longitudinally (Sourced from OpenStax College, 2020).

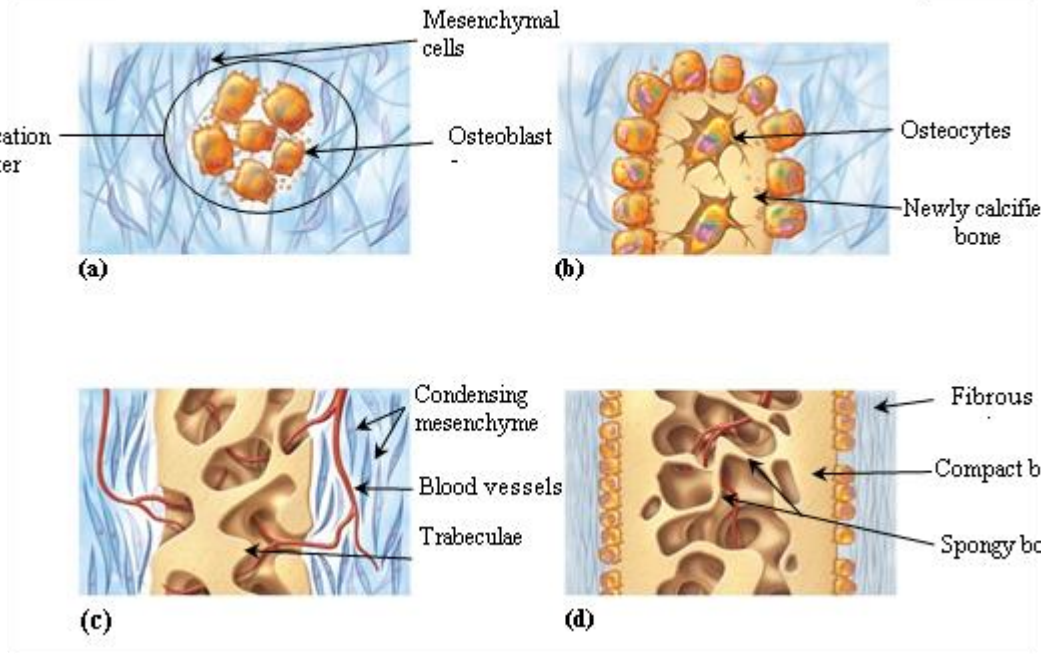


Figure 1.2: Schematic representation of intramembranous ossification. (a) Mesenchymal cells cluster and differentiate into osteoblasts, thus forming an ossification centre, **(b)** Osteoblasts secrete osteoid which then calcifies to form bone. Osteoblasts trapped in the bone, differentiate into osteocytes **(c)** Secreted osteoid accumulates randomly between embryonic blood vessels, forming a network trabecula (woven bone). Vascularised mesenchyme condenses on the peripheral surface of the woven bone to **form** the periosteum **(d)** Trabeculae deep to the periosteum thickens and is replaced with mature lamella (compact bone). Internally, distinctive trabeculae persist, forming the spongy bone and the vascular tissue becomes the red marrow. **(**Adapted from Quizlet, 2012).

1.2.8 Femur

The femur (Fig 1.3), also known as the thigh bone, is the largest and heaviest bone in the human body. Located in the lower limb, the femur articulates proximally with the acetabulum of the pelvic bone forming the hip joint, and distally with the tibia and patella bones forming the knee joint (White and Folken, 2015). It plays a critical role in bearing the weight of the body and ensuring stability during the gait process (Chang et al., 2022). Structurally, the femur is a long bone with a cylindrical shaft (diaphysis), two extremities (proximal and distal epiphyses) and a development zone (metaphysis) (Fig 1.3) (White and Folken, 2015). In a developing bone, the epiphysis and metaphysis are separated by a cartilaginous layer, the epiphyseal growth plate which plays a critical role in the longitudinal growth of long bones (Cashman and Ginty, 2003).

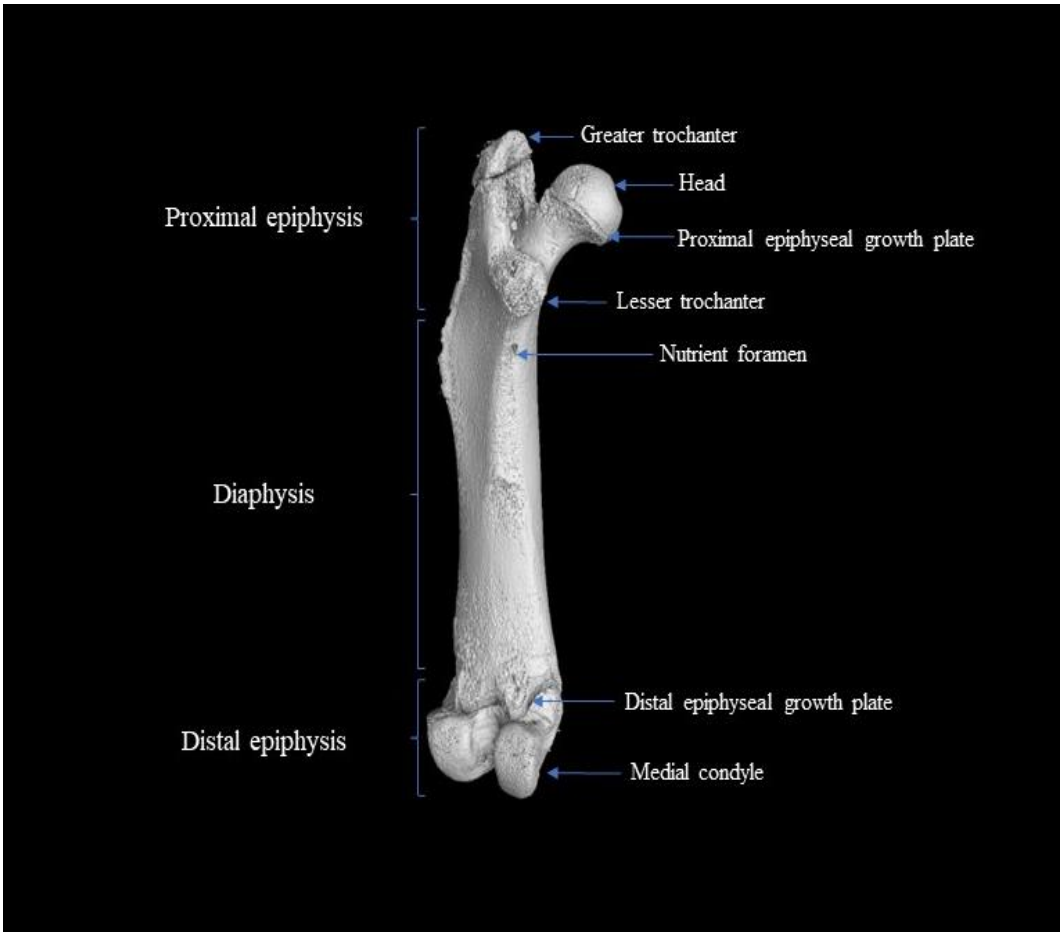


Figure 1.3: Parts of a long bone. A longitudinal view of an 8-week-old rat's right femur, reconstructed in 3D using Micro focus X-Ray Computed Tomography.

1.2.9 The epiphyseal growth plate.

The growth plate (physis) (Fig 1.4) is made up of chondrocytes which are specialized cells suspended in a collagen matrix. These cells undergo several phases of maturation, and are replaced by osteoblasts, osteoclasts, and lamellar bone, as part of bone remodelling (Ağırdil, 2020). The maturation of chondrocytes occurs in a coordinated stepwise process, which entails the resting phase, proliferative phase, hypertrophic phase, and terminal phase (Fig 1.4). This process is essential in facilitating the longitudinal growth of long bones and is intricately regulated by an array of humoral factors such as growth factors, oestrogen, growth hormone, parathyroid hormone, and other signalling cascades (Ağırdil, 2020; Setiawati and Rahardjo., 2018). Most studies (Hogan et al., 1997; Lauing et al., 2008; Pillay and Ndou, 2022; Sampson et al., 1996; Sampson, 1997) have consistently indicated that alcohol consumption exerts detrimental effects on osseous tissue development. Specifically, these studies have demonstrated a reduction in the length of long bones (tibia and femur). This may be due to

alcohol disrupting signalling pathways crucial for longitudinal growth. In the present study, we examined the impact of binge alcohol consumption on the morphology of the growth plate, specifically focusing on chondrocyte density, arrangement, and the presence of proliferating chondrocytes within the proliferative zone. By testing this hypothesis, we aimed to determine the effects of binge alcohol consumption on these specific aspects.

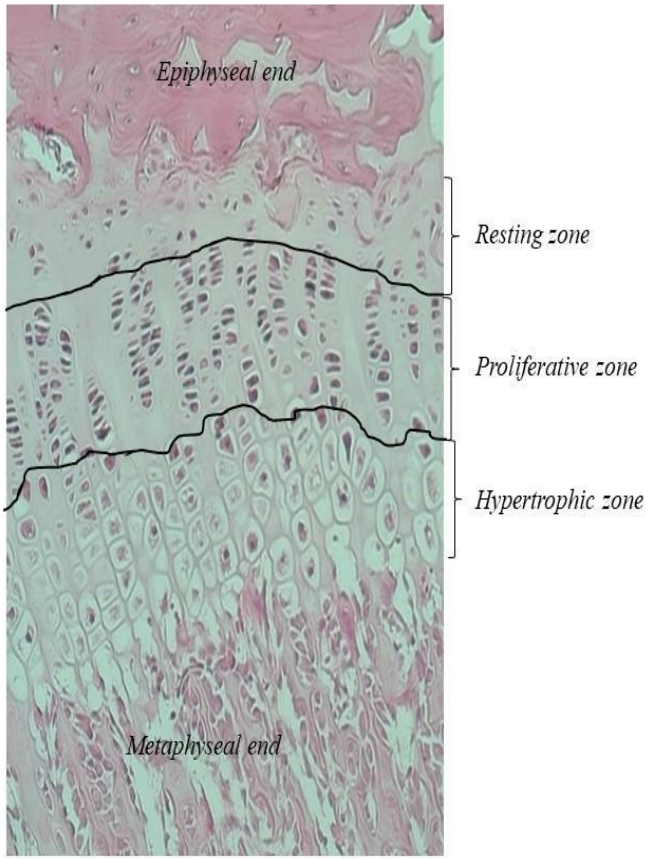


Figure 1.4: An illustration of an epiphyseal growth plate, with chondrocytes progressing through the resting phase, proliferative phase, and hypertrophic phase.

1.2.10 Cortical and trabecular bone

Bone tissue is classified structurally and functionally into two types namely, the cortical (compact) bone and spongy (trabecular) bone (Marieb and Hoehn, 2013). The cortical bone which appears homogenous, dense, and strong, forms the outer layer of most skeletal elements in the body (Fig 1.5). It is tightly packed with several osseous subunits called the osteons or Haversian systems, which consist of concentric layers of bone matrix surrounding a central canal. The central canal houses blood vessels, nerves, and connective tissue, ensuring sufficient

supply of nutrients, oxygen, and innervation to the bone (Kierszenbaum and Tres, 2015). The cortical bone mainly serves a mechanical function, providing strength to the skeletal system (Setiawati and Rahardjo, 2018). On the other hand, the spongy bone is porous, has a honeycomb-like structure and predominantly found between two layers of cortical bone (Setiawati and Rahardjo, 2018) (Fig 1.5). It consists of a network of thin trabeculae and marrow spaces filled with red bone marrow (Hsu et al., 2013; Setiawati and Rahardjo, 2018). The cancellous bone is essential for support and flexibility of the bone (Setiawati and Rahardjo, 2018).

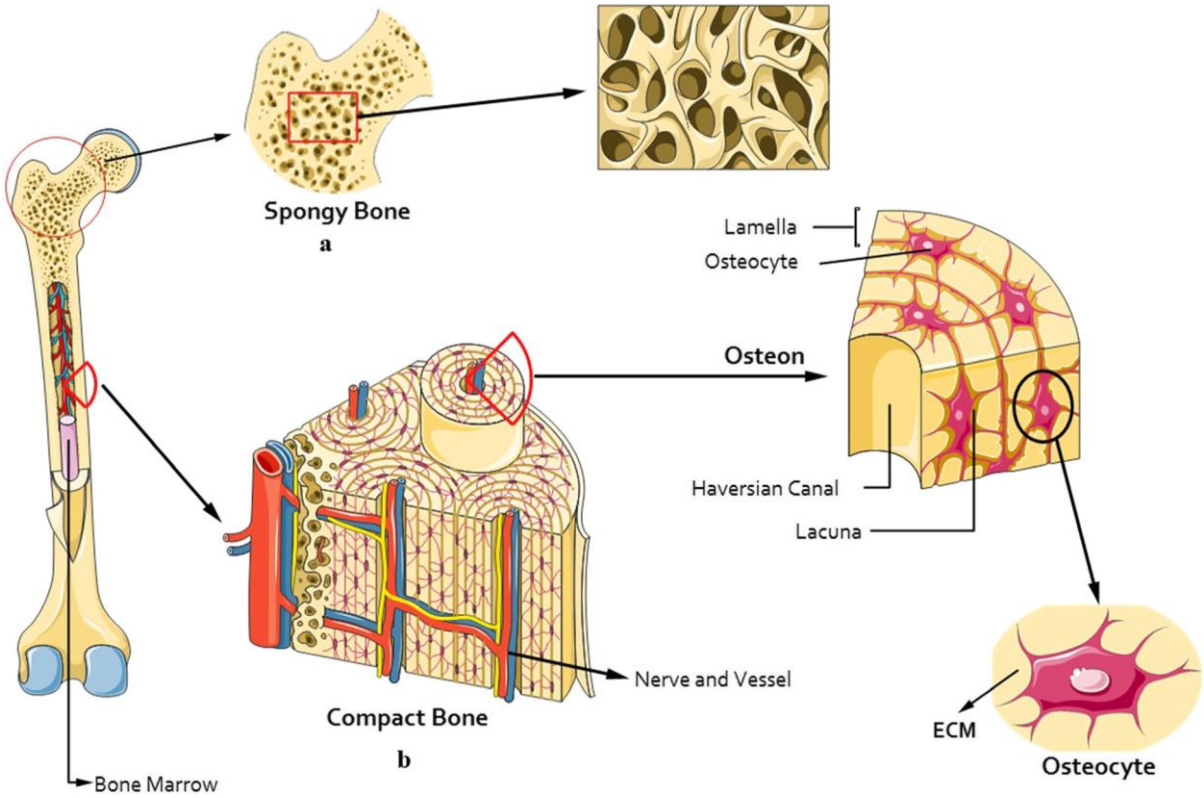


Figure 1.5: Illustration of types of bone, spongy bone, and compact bone (Adapted from Amirazad et al., 2022).

1.2.11 The effects of alcohol on the internal bone architecture

The consumption of alcohol negatively impacts bone formation, leading to weakened bones that are more susceptible to conditions like osteoporosis and an increased risk of fractures due to their diminished strength (Mikosch, 2014; Turner, 2000). Consequently, the microarchitecture of osseous tissue becomes a crucial structural characteristic of bone,

influenced by various factors that contribute to its strength. These factors include, bone morphology, encompassing size, shape, and internal architecture; bone tissue material properties, such as density, degree of mineralization, presence of micro-damage, and collagen characteristics; and bone remodelling processes.

Research indicates that alcohol-induced bone disease in postnatal life leads to a reduction in cortical and trabecular thickness, as well as a decrease in bone formation rate (Diamond et al., 1989; Hogan et al., 1997; Maurel et al., 2012). Alcohol consumption alters the process of bone remodelling by diminishing bone formation (Diamond et al., 1989; Maurel et al., 2011). This decrease in bone formation rate may arise from disruptions in the proliferation and activity of osteoblasts, which can impact the internal integrity of the bone (Sampson et al., 1996; Hogan et al., 1997). Despite the established evidence of the detrimental effects of alcohol consumption on cortical and trabecular parameters, there is a lack of research on the effects of binge alcohol consumption on the microarchitecture of long bones in adolescents. Therefore, the objective of the current study was to address this research gap and provide further insight into the consequences of binge alcohol consumption on adolescent osseous microarchitecture.

1.2.12 Bone remodelling

Bone remodelling confers continuous adaption and maintenance of the skeletal system. This process entails, the resorption of old osseous tissue, followed by the deposition of new osseous tissue (Raggatt and Partridge, 2010). It also requires tight coordination and synchronization of bone cells such as bone-resorbing osteoclasts and bone-forming osteoblasts (Raggatt and Partridge, 2010). However, an imbalance of bone resorption and deposition has been reported to increase the risk of bone fracture and osteoporosis (Langdahl et al, 2016). Binge alcohol exposure may interfere with the balance of bone resorption and deposition thus disturbing the bone's internal architecture which, increases the risk of bone fractures. However, the mechanism involved is still warranted, and more particularly during the adolescent growth phase.

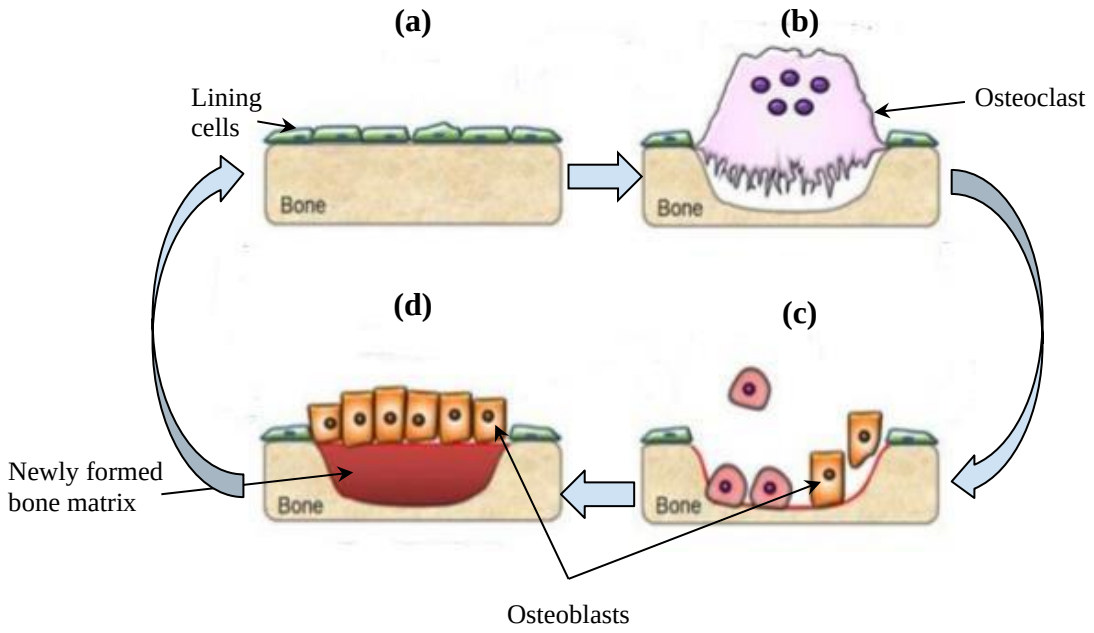


Figure 1.6: Bone remodelling. A Schematic illustration of bone remodelling. (Adapted from Del Fattore et al. 2012). **(a)** The activation phase, the detection of remodelling initiation signal triggers the activation of osteoclast precursors, thus differentiating into functional osteoclast. These are responsible for the removal/resorption of damaged bone tissue in the resorption phase **(b)**, therefore generating cavities. **(c)** Reversal phase, osteoblast precursors are recruited to the bone remodelling site (BMS), proliferate, and differentiate into functional osteoblasts, **(d)** Formation phase, osteoblast secrete new organic bone matrix which undergoes mineralization to become calcified bone.

1.2.13 Bone biomechanical properties

It is established that alcohol abuse has detrimental effects on bone's biomechanical properties, thus, increasing the risk of fragility fractures (Turner et al, 2001). The incidence of fractures is related to a deterioration in bone's strength, which is predominantly determined by the bone's structural properties and intrinsic material properties (Augat and Schorlemmer, 2006). Structural properties include, bone geometry (size and shape), trabecular orientation and cortical porosity, whereas, bone mineral density, the amount of hydroxyapatite (HA) crystal and the chemical composition, constitute the bone's intrinsic material properties (Augat and Schorlemmer, 2006; Martin and Correa, 2010). An increased propensity of fragility fractures is associated with an early onset of osteoporosis, a common skeletal disease characterised by a systemic impairment in bone's micro-architecture and mass (Augat and Schorlemmer, 2006; Kanis et al., 2008; Rachner et al., 2011).

Various experimental testing techniques, such as compression testing (McCalden et al., 1993; Yeni et al., 2004), tensile testing (Kotha and Guzelsu, 2007), and bending testing (Bagi et al., 2006; Leppanen et al., 2008; Margolis et al., 2006), have been employed to quantify the mechanical properties of bone. Among these techniques, the three-point bending test is the most commonly used method for determining the biomechanical properties of long bones (Leppanen et al., 2008; Margolis et al., 2006). In this test, the entire bone is placed in a fixture attached to a material testing machine and subjected to loading until it fractures. The three-point bending test yields various parameters that characterize different aspects of bone fragility.

1.2.14 The role of Ki-67 antibody

Ki-67 is a protein associated with cellular proliferation, and is present in the nucleus of cells during active phases of the cell cycle, such as the G1, S, G2, and M phases, but downregulated in resting cells (G0 phase) (Sun and Kaufman, 2018). The Ki-67 antibody specifically targets the Ki-67 protein and is commonly employed in immunohistochemistry (IHC), a technique used to visualize and measure specific proteins in tissue samples. By staining tissue sections with the Ki-67 antibody, scientists can evaluate the rate of cell proliferation. In the case of bone growth, particularly in the epiphyseal plate, chondrocytes undergo rapid cellular proliferation. Hence, by utilizing the Ki-67 antibody, we can examine the impact of binge alcohol consumption on the proliferation rate.

1.2.15 Animal model

Due to ethical considerations such as administration of alcohol to humans for experimental purposes and difficulties in assessing the organs non-invasively, various animal models are used to examine the mechanism by which alcoholism induces organ damage. Among these animal models, rats have been extensively utilized (Lauing et al., 2008; Hogan et al., 1997; Sampson et al., 1996, Sampson, 1997). Rat models are easy to handle, have a short experimental period and permit the examination of bone's micro-architecture and histomorphometry parameters, which are difficult to assess in humans (Föger-Samwald et al, 2018). Therefore, this study used a Sprague Dawley (SD) rat model.

1.2.16 Alcohol administration techniques employed in animal studies investigating the developmental effects of alcohol consumption.

It is challenging for a single animal model to replicate the full spectrum of effects observed in humans due to alcohol consumption. As a result, in animal studies, particularly rodents, the effects of alcohol on bone metabolism are dependent on the peak blood alcohol concentration and the duration of exposure (Turner et al., 2012). To achieve a desired peak blood alcohol concentration, alcohol can be delivered to study animals via various techniques. These techniques include oral gavage, intraperitoneal injections, total intragastric infusion, provision through drinking water, and incorporation into a liquid diet (French, 2001; Turner et al., 1998; Lieber et al., 1989). Total intragastric infusion confers precise control over the delivery of nutrients (substance) and specially employed to deliver extremely high amounts of alcohol, enabling induction of a specific pathological response (Turner et al., 2012). However, it is worth noting that this technique is labour intensive and highly invasive. The provision of alcohol through drinking water is the simplest method, however, it has disadvantages such as, difficulties in managing both macro and micronutrient levels between study groups. In addition, it is important to note that high concentrations of alcohol can potentially trigger alcohol intolerance in study animals. This may potentially decrease fluid intake, leading to dehydration among study animals (Turner et al., 2012). The commonly utilized methods of delivering alcohol in binge models are via oral gavage and intraperitoneal injections (Turner et al., 2012). Intraperitoneal injection is a convenient method for delivering alcohol in short duration studies (Turner et al., 1998). However, it is important to note that this technique may not replicate the same pathological responses observed with oral administration of alcohol (Turner et al., 2012). To accurately simulate binge alcohol consumption in adolescents, it is crucial to consider the route of alcohol administration, which is typically oral. Therefore, the technique utilized in this study was oral gavage. This method allows for precise control over the dosage and mimics the oral consumption pattern observed in binge drinking scenarios.

1.3 Aims and Objectives

1.3.1 Aim

This study aims to investigate the effects of binge alcohol consumption on the development of the adolescent Sprague Dawley rat femur during two phases, acute and chronic alcohol ingestion.

1.3.2 Objectives

1. To determine the effects of binge alcohol consumption on trabecular parameters such as trabecular thickness (Tb.Th), spacing (Tb.Sp), number (Tb.N), and bone to tissue volume (BV/TV) as well as density in the proximal and distal epiphysis of the rat femur by using a 3D micro-focus X-ray computed tomography (3D-μCT).

2. To determine whether binge alcohol consumption weakens the femur, 3-point bending tests were be performed.

3. To determine whether binge alcohol consumption affects adolescent bone growth and development by inhibiting the proliferation of epiphyseal growth plate chondrocytes, Ki-67 protein immunolabelling will be done.

Chapter 2

Methodology

2.0 METHODOLOGY

2.1 Study animals

A total of 48 adolescent (female and male) rats aged 49 days (7 weeks) and weighing between 150-320g were used in this study (*2020/11/02/C*). These form part of the 72 adolescent rats from a Ph.D. study carried out by Dr. Bhika. The age of rats in this study (49 postnatal days) was equivalent to 14.5 human years(Sengupta, 2013). All study animals were bred and kept at the University of Witwatersrand Research Animal Facility (WRAF), University of the Witwatersrand. These animals were maintained under controlled conditions that are free of most pathogens, temperature-controlled environment (26-28°C) and a 12-hour light/dark cycle. 2 Male rats were paired together, and 2 female rats were also paired together, with free movement within the cages (Length 430mm *x* width 220mm *x* height 200mm). All study animals had unrestricted access to tap water and a standard rodent diet.

2.2 Group treatment and allocation

A 20% (vol/vol) alcohol solution at a dose of 3g/kg was administered to study animals, as a single dose via oral gavage. This alcohol dose is known to achieve a peak blood alcohol concentration (BAC) of approximately 300mg/dL (Nation et al., 1993). A single dose of alcohol was chosen to prevent alcohol withdrawal symptoms that arise due to administration of high alcohol doses twice a day (Penland et al., 2001). Control animals were given an isocaloric equivalent of maltose dextrin via oral gavage. The treatment groups were as follows:

Group A1 (1-week alcohol-exposed rats): Rats in this group were administered alcohol for 3 days of the week (Every alternate day). These are known as the acute binge alcohol-exposed rats.

Group C1 (1-week pair-fed control rats): As a caloric equivalent control (pair-fed), these rats were given maltose dextrin instead of alcohol for 1 week (3 days of the week), on the same days as Group A1.

Group A4 (4 weeks alcohol-exposed rats): These rats were administered alcohol for 4 weeks (3 days/week), in the same manner as Group A1. These are known as the chronic binge alcohol-exposed rats.

Group C4 (4 weeks pair-fed control rats): Rats (pair-fed) in this group were given maltose dextrin for 4 weeks (3days/week), in the same manner as Group C1.

Parameters such as weight and food consumed were recorded to track the health of the study animals.

2.3 Determination of blood alcohol levels (BAC)

To monitor BAC, weekly tail vein blood samples were obtained an hour after treatment, when peak BAC is achieved (Livy et al., 2003). An Alcohol Calorimetric assay kit was used to record BAC (Sigma-Aldrich , USA). BAC readings were taken using a Microplate Absorbance Reader (Bio-Rad Laboratories Inc, USA) at 540nm wavelength.

2.4 Skeletal harvesting

Pentobarbital intraperitoneal injection was used to terminate the animals. Immediately after termination, all femora were dissected, the left bone was then individually wrapped with 0.9% saline-soaked gauze and stored at -20°C for biomechanical analysis. The right bone was placed in 10% buffered formalin for fixation, these bones were used for immunohistochemistry. The right femora were scanned and used for microtomography. Subsequently, the entire animal was immersed in 10% buffered formalin after an abdominal incision was made to permit penetration of the fixative.

2.5 Three-dimensional Micro-Focus X-ray Computed Tomography (3D-µCT)

A Nikon XTH 225/320 LC X-ray microtomography was used for 3D-µCT of the femora. Bone samples were placed in plastic tubes to enhance stability, and mounted in low density Styrofoam, thus permitting X-rays to permeate the sample with insignificant absorption. The scanning settings used are shown in **Table 2.1.**

Table 2.1: Scanning parameters

Parameter	Value
X-ray voltage	70kV
X-ray current	400µa
Filter	1mm aluminium
Scanning resolution	15µm
Tomographic rotation	360 degrees
Rotation step	1 degree
Frame averaging	4
Scan duration	8 minutes

2.6 Femoral osteometry and trabecular morphometry

Following reconstruction, the VG studio Max® 3.2 software was employed for data analysis. A VG studio software built-in calliper was used to determine femoral osteometric parameters (Fig 2.1 and Table 2.2). Cross-sectional slices from selected percentile marks (Fig 2.1), were saved for further analysis using Fiji image J software. The percentile marks selected were the proximal (25^{th}), distal (75^{th}) as well as the midshaft (50^{th}) of the femur. From these slices, cross-sectional area, medullary canal area of the shaft and cortical area were determined. The VG studio Max® 3.2 software was used to assess trabecular morphometric parameters in both the proximal and distal epiphysis of the femur (Table 2.3). These determined bone volume fraction (BV/TV), trabecular number (Tb.N), trabecular thickness (Tb.Th) and trabecular spaces (Tb.Sp). (See appendix 16 and 17).

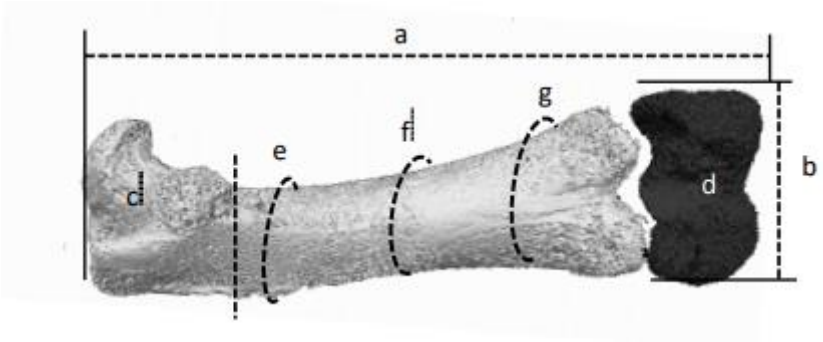


Figure 2.1: A reconstructed 3D femur illustrating points analysed. (a) full femur length; (b) bicondylar breath; (c) and (d) proximal and distal epiphysis of the bone; (e), (f), (g): 25^{th} (proximal), 50^{th} (midshaft), 75^{th} (distal) percentile marks, respectively (Image courtesy of Dr D Pillay).

Table 2.2: Femoral osteometric description (Adapted from Pillay and Ndou, 2022**)**

Osteometric parameter	**Description**
Full femur length (mm)	Measures the maximum length between the top surface of the greater trochanter and the bottom surface of the distal condyle.
Bicondylar breadth (mm)	Measures the mediolateral distance of the epicondyles.
Cross sectional area (mm^2)	The total area from the peripheral margins, covering the shaft of the bone, at each percentile mark (25^{th}, 50th and 75^{th}).
Medullary canal area (mm^2)	The total area from the outer margins, covering the medullary canal of the bone, at each percentile mark (25^{th}, 50th and 75^{th}).
Cortical area(mm^2)	Measured in difference between the cross sectional area and medullary canal area of the bone at each percentile mark (25^{th}, 50^{th} and 75^{th}).

Table 2.3: **Trabecular morphometric parameter description** (Adapted from Bouxsein et al., 2010)

Parameter	**Description**	**Units**
Bone volume fraction **($\frac{BV}{TV}$)**	A ratio representing bone volume to total volume of the region of interest.	%
Trabecular number **(Tb.N)**	Measures the mean number of trabeculae per unit length.	mm^{-1}
Trabecular thickness **(Tb.Th)**	Mean thickness of trabeculae	mm
Trabecular spacing **(Tb.Sp)**	Mean distance between trabeculae	mm

2.7 Three-point bending test

As previously mentioned, the left bones were individually wrapped with gauze soaked in 0.9% saline solution and stored at a temperature of -20°C. On the day of the three-point bending test, these bones were thawed. The three-point bending test was performed on the left femora of

each rat. The load was applied at the midshaft, which is the point halfway between two supports measuring 15mm apart (Fig 2.2). Prior to conducting the mechanical test, various osteometric measurements were taken using a digital calliper. The femora were positioned to ensure that bending occurred along the anteroposterior plane. Load-displacement curves were recorded with a constant speed of 3mm/min until failure occurred.

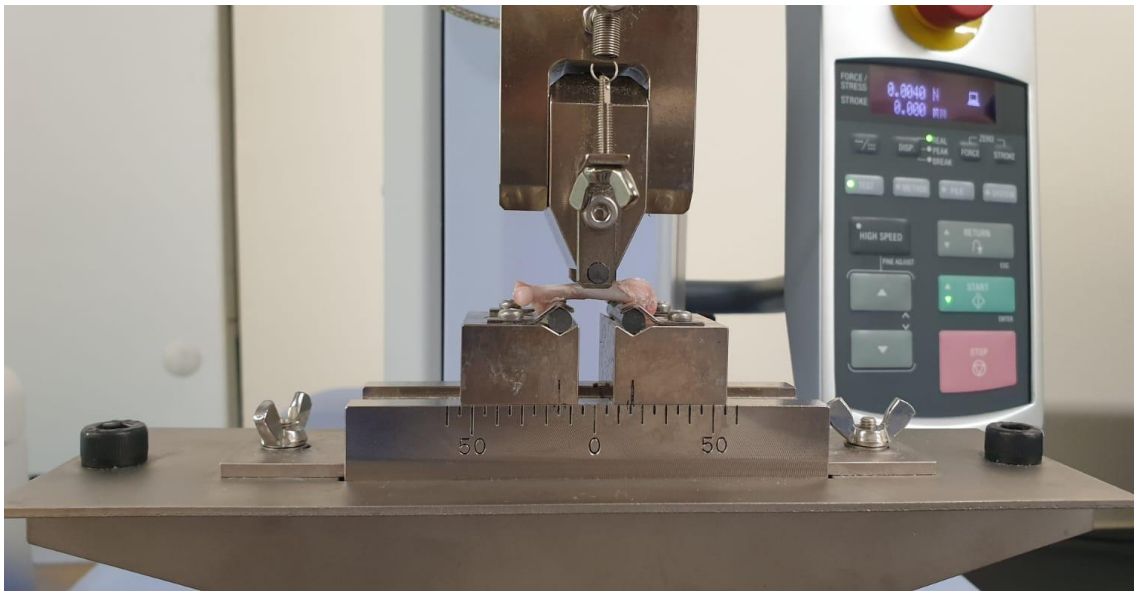


Figure 2.2: Three-point bend testing. The load was applied at the midshaft of the femur in an antero-posterior direction.

Table 2.4: Parameters derived from a load displacement curve (Adapted from Pillay, and Ndou, 2022)

Parameter	**Definition**
Displacement	The amount of vertical deviation from the horizontal plane required to fracture the bone.
Maximum force	The amount of force/load required to deform a bone
Break force	The amount of force/load required to fracture the bone
Yield point	Represents the value of the load at which the load displacement curve deviates from linearity
Time	Represents the duration of the bone resisting the load/force until failure
Energy to fracture	The total energy input required to fracture the bone, represented by the total area under the curve.

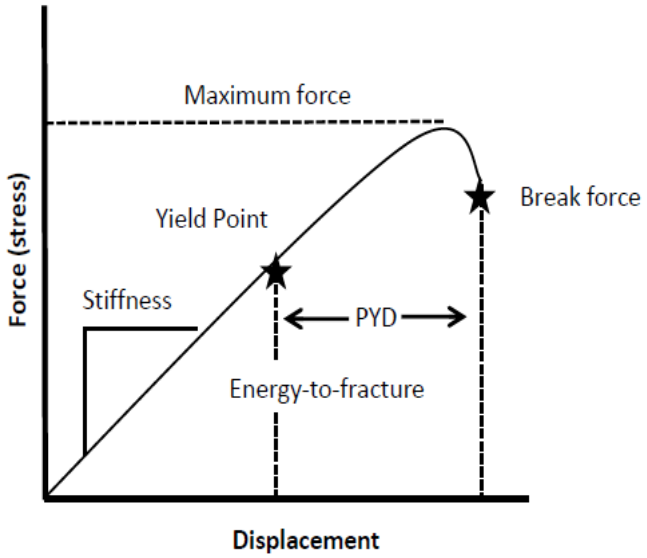


Figure 2.3: An illustration of a load displacement curve, showing bone strength parameters of compact bone. (PYD: post yield displacement) (Pillay and Ndou 2022).

2.8 Tissue processing for histology and immunohistochemical techniques (IHC)

Right femora were used for immunohistochemistry. Formalin fixed bone samples were decalcified in 14% w/v ethylenediaminetetraacetic acid (EDTA, pH 7.4) in an incubator with continuous shaking at 45ºC for 8 days. Thereafter, bone samples were rinsed, divided into proximal and distal portions, and immersed in 10% buffered formalin for 24hrs. Bone samples were processed through ascending grades of alcohol overnight using an automatic tissue processor (Citadel 2000, Thermo Fisher Scientific, USA), before embedding in paraffin. Serial sections were cut with a microtome at 5µm thickness in a longitudinal plane and placed on silane coated slides (Fig 2.3). The first sections were stained with haematoxylin and eosin (H&E) to assess epiphyseal growth plate morphology (see section 2.8). Every second and third sections were immunolabeled with Ki-67 antibody (NB 500-170) and its negative control, respectively. This method was employed to assess the effects of binge alcohol on the proliferation of epiphyseal growth plate chondrocytes (see section 2.9). This process was repeated after discarding the first 20 sections and hence each experiment was done in duplicate for both the proximal and distal extremities of the femora.

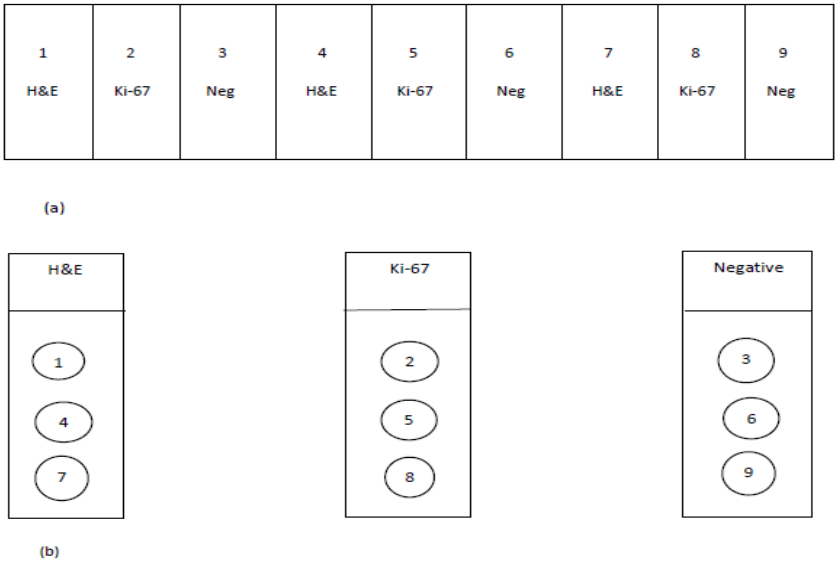


Figure 2.4: Serial sectioning of bone samples (a) an illustration of how serial sections were obtained **(b)** the manner in which slides were labelled and sections chosen.

2.9 Haematoxylin and Eosin staining of the epiphyseal growth plate.

For normal morphology evaluation of the epiphyseal growth plate, haematoxylin and eosin staining was performed. To do this, sections placed on silane-coated slides were dewaxed in xylene for 2 x 10 minutes, hydrated in graded series of alcohol and washed in running tap water for 5 minutes. Thereafter sections were stained with Meyer's haematoxylin for 20 minutes, washed in running tap water for 5 minutes and differentiated in 1% acid alcohol. Sections were washed in running tap water for 5 minutes prior to staining in Scott's tap water, serving as a bluing agent, for 5 minutes and washed again in running water for 5 minutes. Thereafter, sections were stained with Eosin for 2 minutes, briefly washed in running water, dehydrated in graded series of alcohols, cleared in xylene, and mounted in entellen (see appendix 14).

2.10 Immunohistochemistry for Ki-67 in the femoral epiphyseal growth plate.

Immunolabeling of epiphyseal growth plate chondrocytes in the proliferative zone expressing Ki-67 protein, was done using a Ki 67 antibody (NB 500-170), sourced from Whitehead Scientific. To do this, sections placed on silane coated slides were deparaffinized in xylene for 20 minutes, rehydrated in graded series of alcohol and washed in running tap water for 5 minutes. Thereafter, sections were immersed in a citrate buffer (pH 6) and kept overnight in a

water bath at 60℃. This was the antigen retrieval step. On the following day, sections were left to cool at room temperature for 20 minutes and washed in phosphate buffer solution (PBS) (pH 7.4) for 5 minutes. Subsequently, endogenous peroxidase was blocked with 1% hydrogen peroxide in alcohol for 30 minutes and washed in PBS for 3 x 5 minutes. The sections were incubated with a protein block (Ab156024) for 20 minutes and washed in PBS for 3 x 5 minutes. Thereafter, sections were incubated with primary antibody (Anti-Ki 67 in 1:200 dilution factor) overnight at 4℃. On the following day, sections were allowed to reach room temperature, washed in PBS for 4 x 5 minutes and incubated with a biotinylated secondary antibody (Biotinylated Goat Anti-Rabbit IgG (H+L) (Ab64256) for 10 minutes. Thereafter, sections were washed with PBS for 4 x 5 minutes and incubated with Strept-Avidin HRP (Ab64269) for 10 minutes to reduce nonspecific background staining and enhance antibody binding. Sections were washed in PBS for 4 x 5 minutes prior to incubation with 3-3' diaminobenzidine (DAB) working solution for 10 minutes. This step was performed to aid with tissue visualization under a light microscope. Sections were rinsed in running tap water, briefly stained with Haematoxylin (about 2 minutes), and rinsed in running tap water for 5 minutes. Thereafter sections were dehydrated through graded alcohols, cleared in xylene, and mounted with entellen (see appendix 15)

2.11 Photography and quantification of chondrocytes

Photomicrographs of stained slides were taken using a light microscope fitted with an axiocam HRC digital camera (Zeiss Axioscope 2 plus). These were imported into Fiji Image J software and epiphyseal growth plate zones were delineated based on cell morphology (Fig 2.5). The proliferative zone (region of interest) was delineated by the first flattened chondrocyte on the distal end and the first hypertrophic chondrocyte on the metaphyseal side.

For quantification of chondrocytes, the manual counting method on photomicrographs of stained slides was employed. The counting was conducted on the entirety of the proliferative zone of the epiphyseal growth plate.

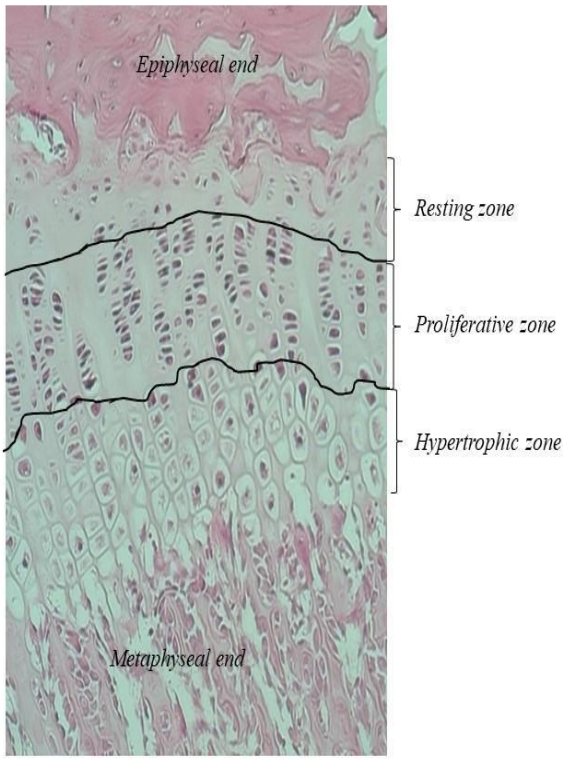


Figure 2.5. A Haematoxylin and Eosin-stained section of the femur showing delineated growth plate zones namely, the hypertrophic, proliferative, and resting zones. (Image courtesy of NR, Mngoma).

2.12 Data analysis

Data obtained was managed in Microsoft Excel 2016 (Microsoft Corporation) and statistically analysed using the Statistical Package for Social Services (SPSS) version 23 (IBM) software. To assess the reliability of the data, Lin's concordance correlations for reliability were employed. Normality of the data was examined using the Shapiro-Wilk's test. Given the parametric nature of the data, the Levene's test for equality of variances was employed alongside the Independent Samples t-test for comparing means between the study groups. The significance level was set at $p < 0.05$.

Chapter 3

The effects of acute binge alcohol consumption on the development of the femur of adolescent Sprague Dawley rats

ABSTRACT

Chronic alcohol consumption has a detrimental impact on bone metabolism, leading to a decrease in bone length, density, and strength. These deficiencies in bone density and strength may increase the risk of fractures and the early onset of osteoporosis. While chronic alcohol consumption is an established risk factor for osteoporotic fractures, there remains a dearth of information in literature about the effects of binge alcohol consumption in adolescents' bones. Therefore, our study aimed to examine the effects of acute binge alcohol consumption on the development of the adolescent femur. Twenty-four Sprague Dawley rats (12 male and 12 female) aged 7 weeks were randomly placed in 2 groups: alcohol (n = 12), receiving alcohol (3g/kg) and pair-fed control (n =12), receiving an isocaloric equivalent of maltose dextrin via oral gavage for 3 days of the week(on alternative days). The duration of the acute binge alcohol model was 7 days. Trabecular morphometry in both the proximal and distal epiphysis, as well as cortical dimensions were assessed by using three-dimensional Micro-Focus X-ray Computed Tomography (3D-µCT) and Volume Graphics Studio® software. The morphology of the epiphyseal growth plate was examined by Haematoxylin and Eosin staining, whereas Ki-67 immunostaining was employed to quantify the proliferation of chondrocytes in the proliferative zone of the growth plate. A three-point bending test was employed to examine the effects of alcohol on bone strength. Results showed trabecular parameters to be affected in the male rats in the distal epiphysis of the femur. Osteometric measurements, remained unaffected in both the male and female rats. However, the trabecular morphometry was similar in the proximal region in the male rats among the alcohol and pair-fed control groups. Conversely, the microarchitecture was negatively affected in the distal extremity of the male alcohol exposed rats. The female rats exhibited no detrimental effects of alcohol on both extremities. Tensile strength remained unaffected in both male and female rats. A decrease in proliferation of chondrocytes was observed in both the extremities (proximal and distal) of the femur in male alcohol exposed rats. Again, no harmful effects of alcohol were seen in the female rats with regards to chondrocyte proliferation. These findings may suggest that acute binge alcohol consumption has detrimental effects on the trabeculae of the distal epiphysis as well as proliferation of chondrocytes in the epiphyseal growth plate in male rats.

3.1 INTRODUCTION

Drinking alcohol is a common practice globally in various social and cultural settings. The patterns of alcohol drinking differ from occasional, heavy chronic, and binge drinking. The binge drinking pattern is known to be the most common drinking practice amongst adolescents and young adults (Morojele and Ramsoomar, 2016). Binge alcohol consumption is defined as the consumption, on one occasion, of ≤ 5 standard drinks for men and ≤ 4 standard drinks for women, resulting in a blood alcohol concentration of 80 mg/dL or above (Föger-Samwald et al, 2018; National Institute on Alcohol Abuse and Alcoholism, 2004). This pattern of alcohol consumption poses numerous risks for adolescents since this period of growth is essential for the attainment of peak bone mass (Abrams, 2003). Although this is the case, there is a dearth in literature regarding the detrimental effects of binge alcohol on the skeletal system of adolescents therefore warrants further investigations.

To date, the effects of acute binge drinking on adolescent long bones have been investigated in a limited number of studies. Much of the literature on the effects of alcohol on bone development have focused on chronic alcohol consumption rather than acute binge drinking episodes. These studies have demonstrated that alcohol inhibits bone growth, decreases bone mineral density, and adversely affects the trabecular bone architecture (Hogan, et., 1997; Sampson, et al., 1996, 1997). Hogan et al, (1997) reported reduced biomechanical strength in bone following chronic alcohol exposure. Additionally, Lauing et al. (2008) reported a decrease in tibial cancellous bone mineral density after acute alcohol exposure. However, little research has been done to explore the effects of acute binge alcohol consumption on the development of adolescent bone with reference to the femur. A better understanding of the effects of acute binge drinking on the adolescent femur could provide interventions and education aimed to reducing underage alcohol consumption and promoting healthy bone development.

Thus, the aim of the study was to evaluate the effect of acute binge alcohol consumption in growing rats on longitudinal growth of the femur and parameters of bone quality. This was achieved by using three-dimensional micro-focus X-ray computed tomography (3D- μCT) to assess the bone to total volume ratio, trabecular thickness, spacing and trabecular number in both the proximal and distal epiphysis of the femur. We then, analysed femur osteometrics, cortical dimensions, and assessed the morphology of both the proximal and distal growth plates Additionally, we employed Ki-67 immunostaining to investigate whether acute binge alcohol

consumption affected bone growth by inhibiting the proliferation of chondrocytes in the proliferative zone of the growth plate, examining both the proximal and distal growth plates.

3.2 RESULTS

3.2.1 Measurement reliability

Measurement reliability was assessed using Lin's concordance correlation coefficient (pc), which yielded values above 0.7 for all osteometric measurements. These results indicate a high degree of measurement reliability, suggesting that the measurement error from the data collected are low enough to be considered reliable.

3.2.2 Blood alcohol concentration

The average blood alcohol concentration was 108.04 mg/dL (± 16.60) in alcohol groups.

3.2.3 Body weight gain

The acute binge alcohol consumption model showed a similar weight gain in the male rats between the alcohol (mean = 12.16% ± 1.69) and the pair-fed control groups (mean = 12.29% ± 1.59) ($p = 0.890$) (Fig 3.1). In female rats, the alcohol group (mean = 4.98% ± 1.59) experienced less weight gain compared to the pair-fed control group (mean = 7.00% ± 1.24), however no statistical significance was detected (Fig 3.1) ($p = 0.064$).

Regarding pair-fed control groups, the male rats exhibited a significantly higher percentage of weight gained (mean = 12.29% ± 1.59) than the female pair-fed control group (mean = 7.00% ± 1.24) (Fig 3.1) ($p < 0.001$). A similar pattern was observed in animals exposed to alcohol, with the male alcohol group (mean = 12.16% ± 1.69) gaining more weight in comparison to the female alcohol group (mean = 4.98% ± 1.59) ($p < 0.001$) (Fig 3.1).

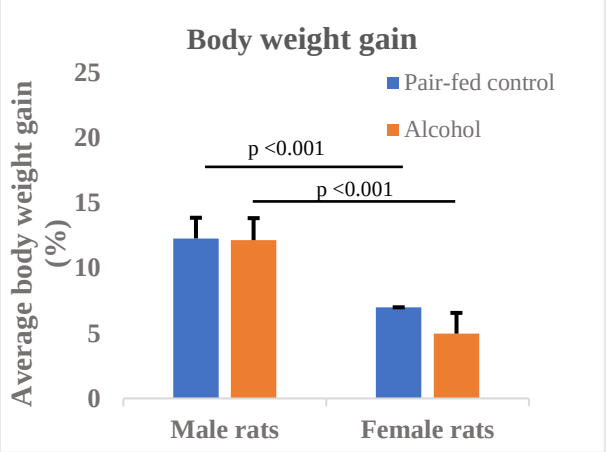


Figure 3.1: Average body weight gain. Mean body weight gain values are represented as a percentage. Error bars represent standard deviation.

3.2.4 Food consumption

With regards to food consumption, group comparisons were similar across study groups. Male rats showed similar daily food consumption between the alcohol group (mean = 48.6g ± 2.77) and pair-fed control group (mean = 48.4g ± 2.86) (p = 0.946) (Fig 3.2). This pattern continued in the female rats, with the alcohol and pair-fed control groups consuming similar amounts of food (mean = 29.2g ± 0.11 and 31.2g ± 0.82, respectively) (p = 0.051) (Fig 3.2).

A comparison in daily food consumption between male and female rats showed that the male pair-fed control group (mean = 48.4g ± 2.86) consumed more food than the female pair-fed control group (mean = 31.2g ± 0.82) (Fig 3.2) (p < 0.001). This pattern was also observed in animals exposed to alcohol, with male rats (mean = 48.6g ± 2.77) consuming more food than female rats (mean = 29.2g ± 0.11) (Fig 3.2) (p < 0.001).

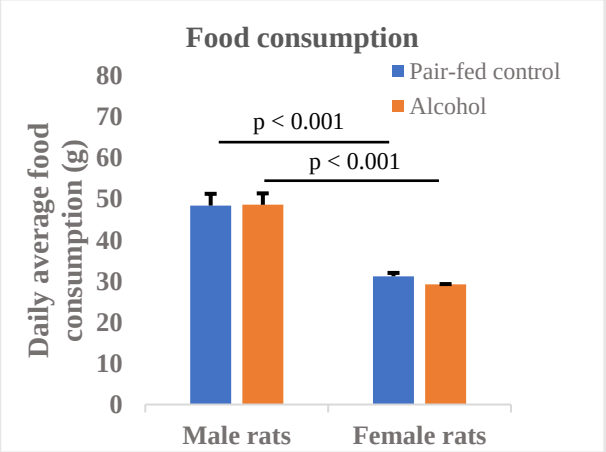


Figure 3.2: Food consumption. Daily average food consumption shown for pair-fed control and alcohol groups in both male and female rats. Error bars represent standard deviation.

3.2.5 Osteometric measurements of the femur

Full bone length

No differences in bone length were observed amongst the study groups in the acute binge alcohol consumption model. Similar bone length was displayed in the male rats in the alcohol and the pair-fed controls (mean = 33.28mm ± 0.77 and mean = 33.11mm ± 0.59, respectively) (Fig 3.3) ($p = 0.660$). This pattern continued in the female rats, (mean = 30.72mm ± 0.84 and mean = 30.84mm ± 0.21, alcohol and pair-fed control, respectively) ($p = 0.700$).

Male rats had longer femora in both pair-fed control (mean = 33.11mm ± 0.59) and alcohol groups (mean = 33.28mm ± 0.77) when compared to the pair-fed control (mean = 30.84mm ± 0.21) and alcohol groups (mean = 30.72mm ± 0.84) in female rats (Fig 3.3). These differences were statistically significant ($p \leq 0.001$ for both comparisons).

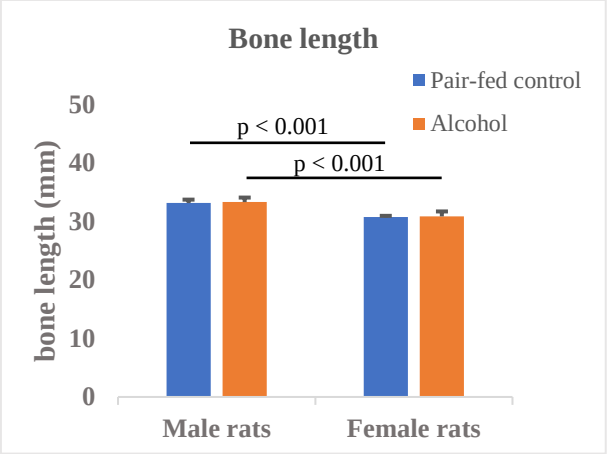


Figure 3.3: Femur length for the acute binge consumption model. The mean values for femur length are represented for the pair-fed control and alcohol groups in both male and female rats. Error bars represent standard deviation.

Bicondylar breadth

The bicondylar breadth amongst the study groups were similar. In males, the alcohol group had a marginally larger bicondylar breadth (mean = 7.45mm ± 0.15) compared to the pair-fed

control group (mean = 7.32mm ± 0.21), however, no significance was detected (p = 0.240) (Fig 3.4). Again, the bicondylar breadth in the alcohol group was similar to the pair-fed control group in the female rats (mean = 8.77mm ± 1.55 and mean = 8.79mm ± 0.56, respectively) (p = 0.980) (Fig 3.4).

A comparison among pair-fed control groups revealed that the bicondylar breadth was significantly greater in female rats (mean = 8.79mm ± 0.56) compared to male rats (mean = 7.32mm ± 0.21) (p < 0.001) (Fig 3.4). Similarly in alcohol exposed animals, female rats had a greater bicondylar breadth (mean = 8.77mm ± 1.55) compared to male rats (mean = 7.45mm ± 0.15). However, this difference was not statistically significant (p = 0.065).

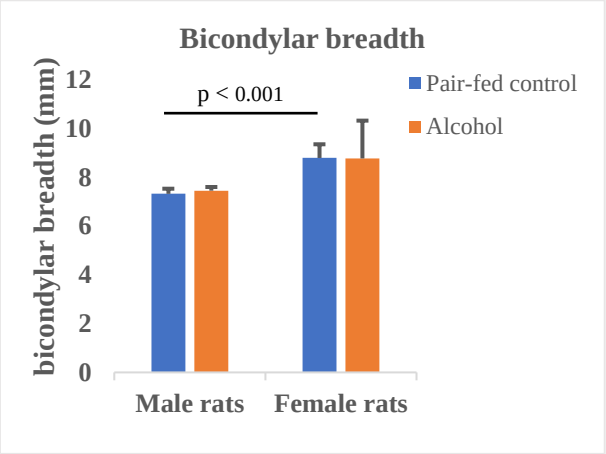


Figure 3.4: Femur bicondylar breadth for the acute binge alcohol consumption model. The mean values for femur bicondylar breadth are represented for the pair-fed control and alcohol groups in both male and female rats. Error bars represent standard deviation.

3.2.6 Femur Trabecular Morphometrics

Femoral bone to total volume ratio (BV/TV)

With regards to bone to total volume (BV/TV) ratio in the proximal epiphysis, no significant differences were observed among study groups. The alcohol group in the male rats, had a marginally lower BV/TV (mean = 52.44% ± 1.2) compared to the pair-fed control group (mean = 55.29% ± 3.44) (p = 0.080) (Fig 3.5a). The female rats exhibited slightly a higher BV/TV in the alcohol group (mean = 68.95% ± 3.98) than the pair-fed control group (mean = 66.52% ± 3.22). However, this difference was not significant (p = 0.270) (Fig 3.5a).

A comparison between male and female pair-fed control groups, exhibited a higher BV/TV in the female pair-fed control (mean = 66.52% ± 3.22) than the male pair-fed control group (mean

= 55.29% ± 3.44) ($p < 0.001$) (Fig 3.5a). This pattern was also observed in alcohol groups, with the female rats (mean = 68.95% ± 3.98) having a higher BV/TV compared to the male rats (mean = 55.29% ± 3.44) ($p < 0.001$) (Fig 3.5a).

In the distal epiphysis, male rats displayed a significantly lower BV/TV in the alcohol group (mean = 20.69% ± 1.77) than the control group (mean =28.51% ± 2.4) ($p = 0.002$) (Fig 3.5b). The female rats showed a contrasting pattern, with the alcohol group having a marginally higher BV/TV (mean = 29.05% ± 5.19) compared to the pair-fed control group (mean = 25.59% ± 2.50) (Fig 3.5). However, this difference was not statistically significant ($p = 0.180$) (Fig 3.5b).

Regarding pair-fed controls, male rats (mean =28.51% ± 2.4) had a marginally higher BV/TV compared to the female rats (mean = 25.59% ± 2.50), however this difference was not statistically different ($p = 0.105$) (Fig 3.5b). In contrast, a significantly higher BV/TV in animals exposed to alcohol was observed in female rats (mean = 29.05% ± 5.19) than the male rats(mean = 20.69% ± 1.77) ($p = 0.009$) (Fig 3.5b).

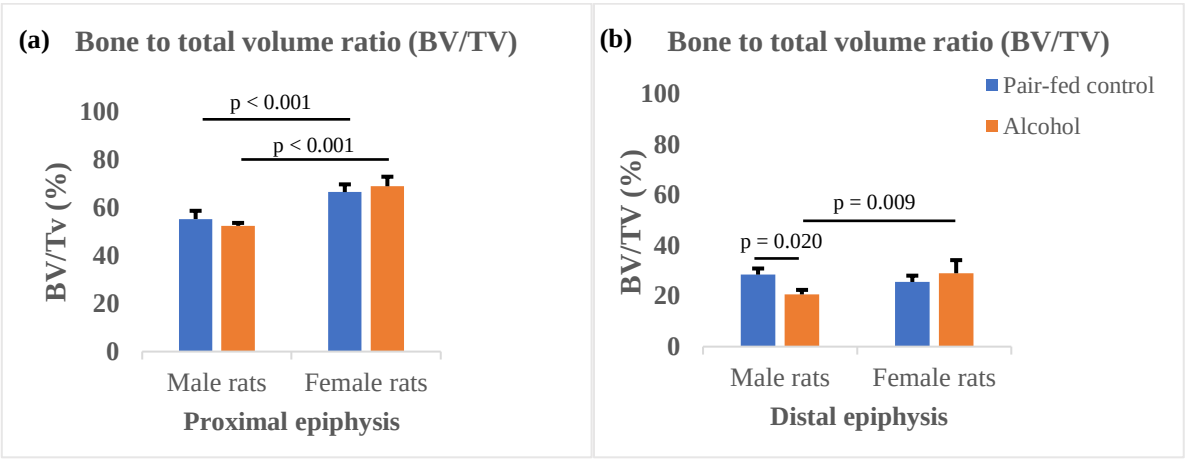


Figure 3.5: Femoral bone to total volume ratio (BV/TV) for the acute binge alcohol consumption model. The mean values for BV/TV are given for both the **(a)**; proximal and **(b)**; distal epiphysis for the alcohol and pair-fed groups of the male and female rats. Error bars represent standard deviation.

Femur trabecular thickness (Tb.Th)

The trabeculae of the proximal epiphysis were significantly thinner in the alcohol group (mean = 0.086mm ± 0.006) than the pair-fed control group (mean = 0.098mm ± 0.010) in male rats ($p = 0.033$) (Fig 3.6a). Conversely, the trabeculae in female rats were marginally thicker in the

alcohol group (mean = 0.136mm ± 0.022) compared to the pair-fed control group (mean = 0.124mm ± 0.014), however no significance was detected (p = 0.311) (Fig 3.6a).

Regarding the trabecular thickness between the pair-fed controls, it was significantly higher in female rats (mean = 0.124mm ± 0.014) than the male rats (mean = 0.098mm ± 0.010) (p = 0.005) (Fig 3.6a). A similar comparison was observed in the alcohol groups, with the female rats (mean = 0.136mm ± 0.022) having thicker trabeculae than male rats (mean = 0.086mm ± 0.006) (p = 0.002) (Fig 3.6a).

In the distal region, the alcohol group (mean = 0.066mm ± 0.002) had significantly thinner trabeculae than the pair-fed control group (mean = 0.080mm ± 0.006) in male rats (p = 0.023) (Fig 3.6b). Female rats exhibited thicker trabeculae in the alcohol group (mean = 0.074mm ± 0.004) than the pair-fed controls (mean = 0.069mm ± 0.002). This difference was significant (p = 0.041) (Fig 3.6b).

When comparing the pair-fed control groups, trabecular thickness was significantly thicker in male rats (mean = 0.080mm ± 0.006) than female rats (mean = 0.069mm ± 0.002). (p = 0.044)(Fig 3.6b). Conversely, in the alcohol exposed groups, female rats (mean = 0.074mm ± 0.004) had thicker trabeculae compared to the male rats (mean = 0.066mm ± 0.002). This difference was significant (p = 0.004) (Fig 3.6b).

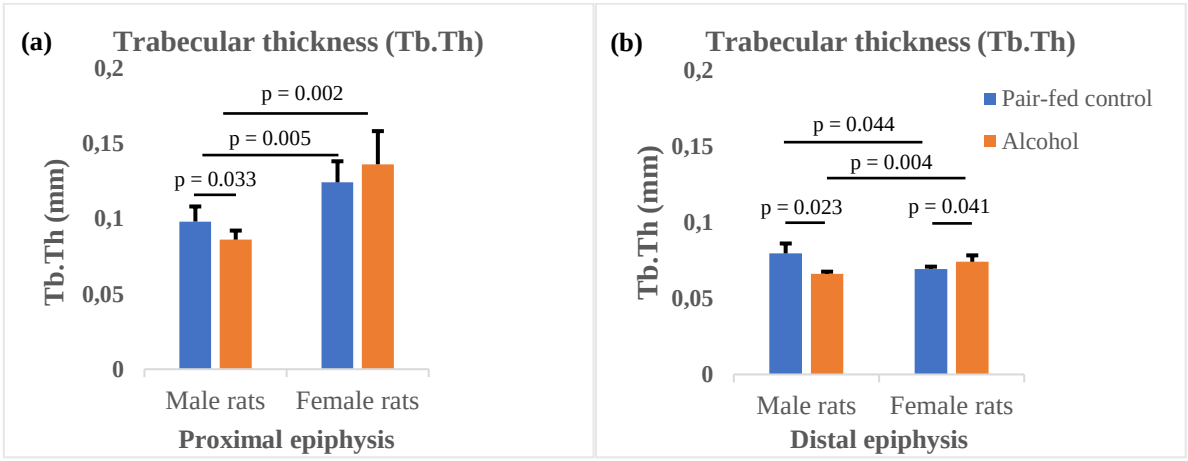


Figure 3.6: Femoral trabecular thickness (Tb.Th) for the acute binge drinking model. The mean values for Tb.Th are given for both the **(a)**; proximal and **(b)**; distal epiphysis for the alcohol and pair-fed groups of the male and female rats. Error bars represent standard deviation.

Femur trabecular number (Tb.N)

Regarding the trabecular number in the proximal epiphysis, group differences were observed. The alcohol group in male rats had a marginally higher trabecular number (mean = 6.122mm^{-1} ± 0.312) compared to the pair-fed control group (mean = 5.669mm^{-1} ± 0.479) (p = 0.044) (Fig 3.7a). However, female rats showed similar trabecular numbers between the two study groups (alcohol mean = 5.153mm^{-1} ± 0.616 and pair-fed control mean = 5.381mm^{-1} ± 0.357) (p = 0.450) (Fig 3.7a).

No group difference was observed between the male pair-fed control (mean = 5.669mm^{-1} ± 0.479) and female pair-fed control (mean = 5.381mm^{-1} ± 0.357) (p = 0.277) (Fig 3.7a). However, in animals exposed to alcohol, the male rats (mean = 6.122mm^{-1} ± 0.312) exhibited a higher trabecular number than the female rats (mean = 5.153mm^{-1} ± 0.616). This difference was significant (p = 0.006) (Fig 3.7a).

In the distal region, the male rats exhibited a significantly reduced trabecular number in the alcohol group (mean = 3.128mm^{-1} ± 0.248) compared to the pair-fed control (mean = 3.675mm^{-1} ± 0.298) (p = 0.030) (Fig 3.7b). The female rats showed a similar trabecular number between the alcohol group (mean = 3.903mm^{-1} ± 0.509) and the pair-fed control (mean = 3.587mm^{-1} ± 0.311) (p = 0.400) (Fig 3.7b).

The male pair-fed control (mean = 3.675mm^{-1} ± 0.298) and female pair-fed control groups (mean = 3.587mm^{-1} ± 0.311) showed similar trabecular number (p = 0.952) (Fig 3.7b). However, the male alcohol group (mean = 3.128mm^{-1} ± 0.248) had fewer trabeculae compared to the female alcohol group (mean = 3.903mm^{-1} ± 0.509) (p = 0.013) (Fig 3.7b).

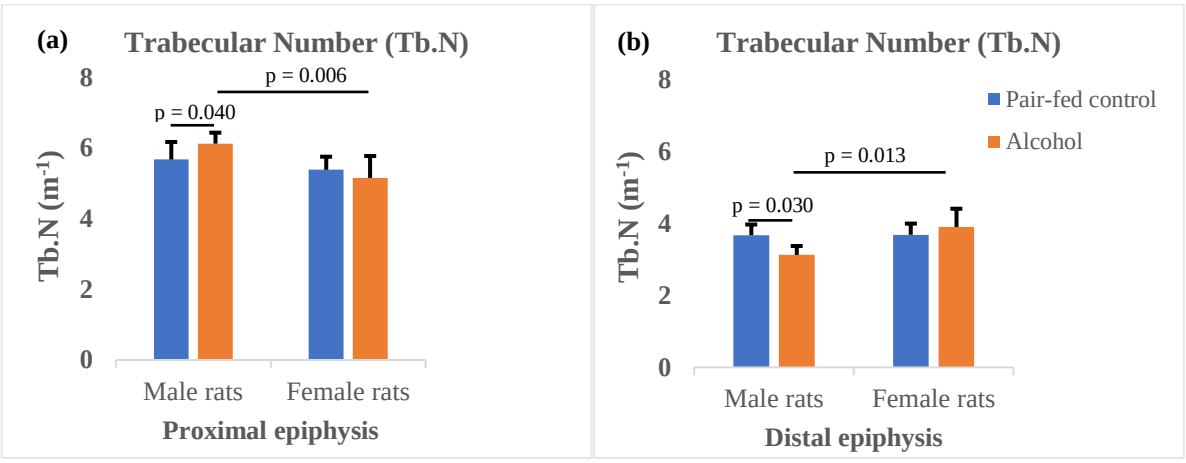


Figure 3.7: Femoral trabecular number (Tb.N) for the acute binge drinking model. The mean values for Tb.N are given for the **(a)**; proximal and **(b)**; distal epiphysis for the two study groups in both male and female rats. Error bars represent standard deviation.

Femur trabecular spacing (Tb.Sp)

Male rats showed similar trabecular spacing in the proximal epiphysis between the alcohol group (mean = 0.078mm ± 0.002) and the pair-fed control (mean = 0.079mm ± 0.008) (p = 0.70) (Fig 3.8a). This pattern was also observed in female rats, with the alcohol (mean = 0.061mm ± 0.005) and the pair-fed control (mean = 0.062mm ± 0.003) showing similar trabecular spacing in the proximal epiphysis (p = 0.55) (Fig 3.8a).

A comparison between the pair-fed control groups, showed wider trabeculae in male rats (mean = 0.079mm ± 0.008) than female rats (mean = 0.062mm ± 0.003) (p = 0.002) (Fig 3.8a). This pattern continued in alcohol exposed animals, with the male rats (mean = 0.078mm ± 0.002) exhibiting wider trabecular spacing than the female rats (mean = 0.061mm ± 0.005) (p < 0.001) (Fig 3.8a).

In the distal epiphysis, male rats showed significantly wider trabeculae in the alcohol group (mean = 0.255mm ± 0.024) compared to the pair-fed control group (mean = 0.196mm ± 0.018) (p = 0.008) (Fig 3.8b). While, the female rats had less spacing in the alcohol group (mean = 0.186mm ± 0.037) than the pair-fed control (mean = 0.204mm ± 0.024) (Fig 3.8b). However, no significance was detected (p = 0.360).

When comparing the pair-fed control groups, both male rats (mean = 0.196mm ± 0.018) and female rats (mean = 0.204mm ± 0.024) had a similar trabecular spacing (p = 0.594) (Fig 3.8b). However, male rats (mean = 0.255mm ± 0.024) had a significantly wider spacing in trabeculae than the female rats (mean = 0.186mm ± 0.037), in alcohol exposed groups (p = 0.012) (Fig 3.8b).

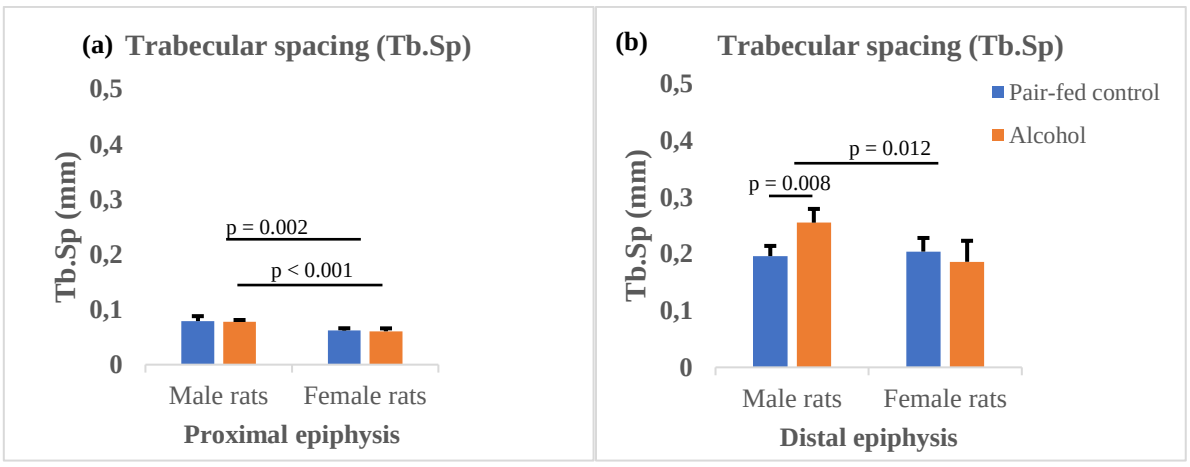


Figure 3.8: Femoral trabecular spacing (Tb.Sp) for an acute binge drinking model. The mean values for Tb.Sp are given for both the **(a)**; proximal and **(b)**; distal epiphysis for the two study groups in both male and female rats. Error bars represent standard deviation.

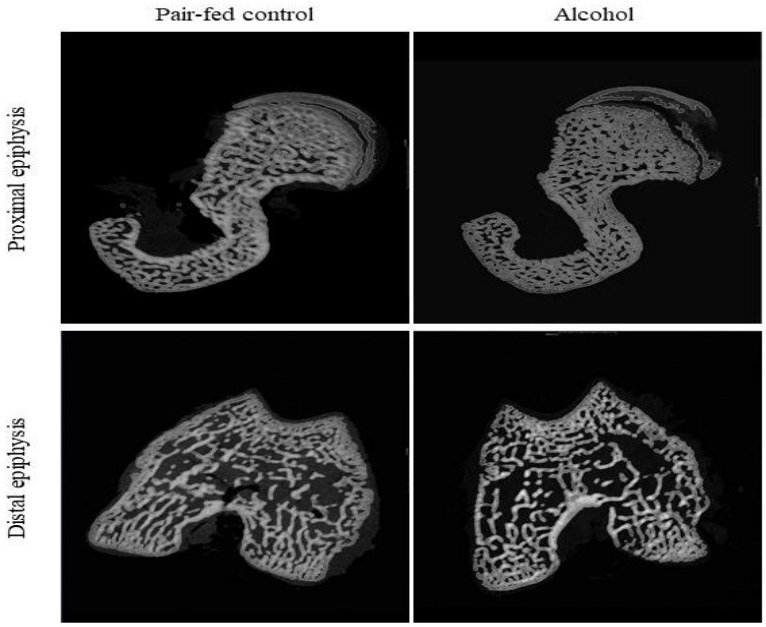


Figure 3.9: Trabecular morphology in the proximal and distal ends of femora for the pair-fed control and alcohol groups in male rats. Representative slices, show similar trabecular morphometry in the proximal epiphysis between the pair-fed control and alcohol groups. In the distal epiphysis, the alcohol group appears to have less BV/TV, trabecular thickness, and trabecular number, with wider trabecular spacing.

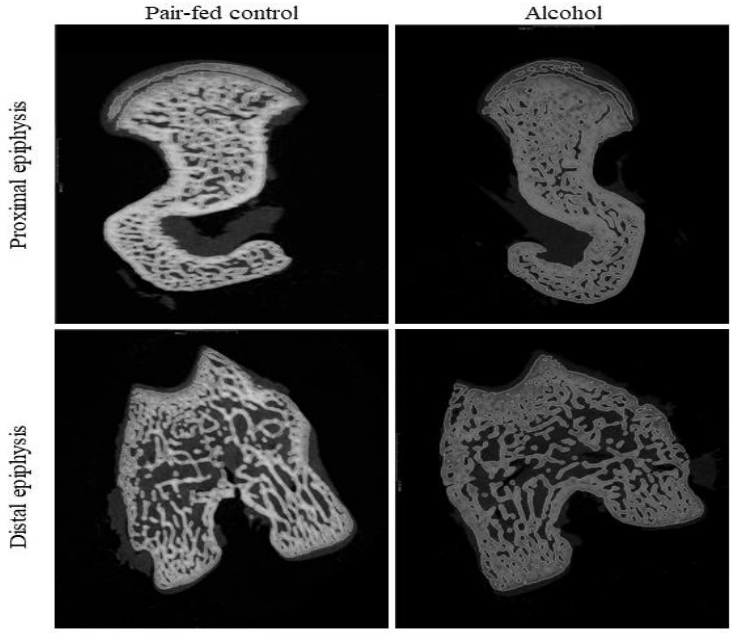


Figure 3.10: Trabecular morphology in the proximal and distal ends of femora for the pair-fed control and alcohol groups in female rats. Representative slices, show no significant difference in

trabecular morphometry between the alcohol and pair-fed control groups, both in the proximal and distal ends of the femur. The exception was the trabecular thickness in the distal epiphysis, which appeared to be increased in the alcohol group compared to the pair-fed control group.

3.2.7 Femur cross-sectional area, medullary canal area and cortical area

25th percentile mark (proximal)

In the male rats, both the cross-sectional area (CSA) and the cortical area (CA) were marginally lower in the alcohol group (CSA mean =13.363mm^2 ± 0.986; CA mean = 7.600mm^2 ± 0.519) compared to the pair-fed control group (CSA mean = 14.240mm^2 ± 0.545; CA mean = 8.485mm^2 ± 0.819), however, no significance was observed (p = 0.440 and 0.680, respectively) (Fig 3.11a,c). Regarding the medullary canal area (MCA), similar values were observed between alcohol (mean = 5.762mm^2 ± 0.550) and pair-fed control groups (mean = 5.754mm^2 ± 0.506) (p = 0.310) (Fig 3.11b). A similar pattern was also observed in female rats, as the CSA (mean =11.321mm^2 ± 0.555), MCA (mean = 4.400mm^2 ± 0.228), and CA (mean = 6.921mm^2 ± 0.529) in the alcohol group were similar to the pair-fed control groups' CSA (mean =10.938mm^2 ± 0.890), MCA (mean = 4.191mm^2 ± 0.364) and CA (mean = 6.746mm^2 ± 0.730) (p = 0.44; 0.31 and 0.68 respectively) (Fig 3.11).

Regarding pair-fed controls, male rats had a significantly higher CSA (mean = 14.240mm^2 ± 0.545), MCA (mean = 5.754mm^2 ± 0.506) and CA (mean = 8.485mm^2 ± 0.819) compared to female rats' CSA (mean =10.938mm^2 ± 0.890), MCA (mean = 4.191mm^2 ± 0.364) and CA (mean = 6.746mm^2 ± 0.730) (p < 0.001, p < 0.001 and p = 0.003, respectively) (Fig 3.11). This pattern continued in the alcohol groups, with male rats exhibiting a higher CSA (mean = 13.363mm^2 ± 0.986), MCA (mean = 5.762mm^2 ± 0.550) and CA (mean = 7.600mm^2 ± 0.519) than the female rats' CSA (mean =11.321mm^2 ± 0.555), MCA (mean = 4.400mm^2 ± 0.228), and CA (mean = 6.921mm^2 ± 0.529) (Fig 3.11). These differences were statistically significant (p = 0.001, p < 0.001 and p = 0.049, respectively).

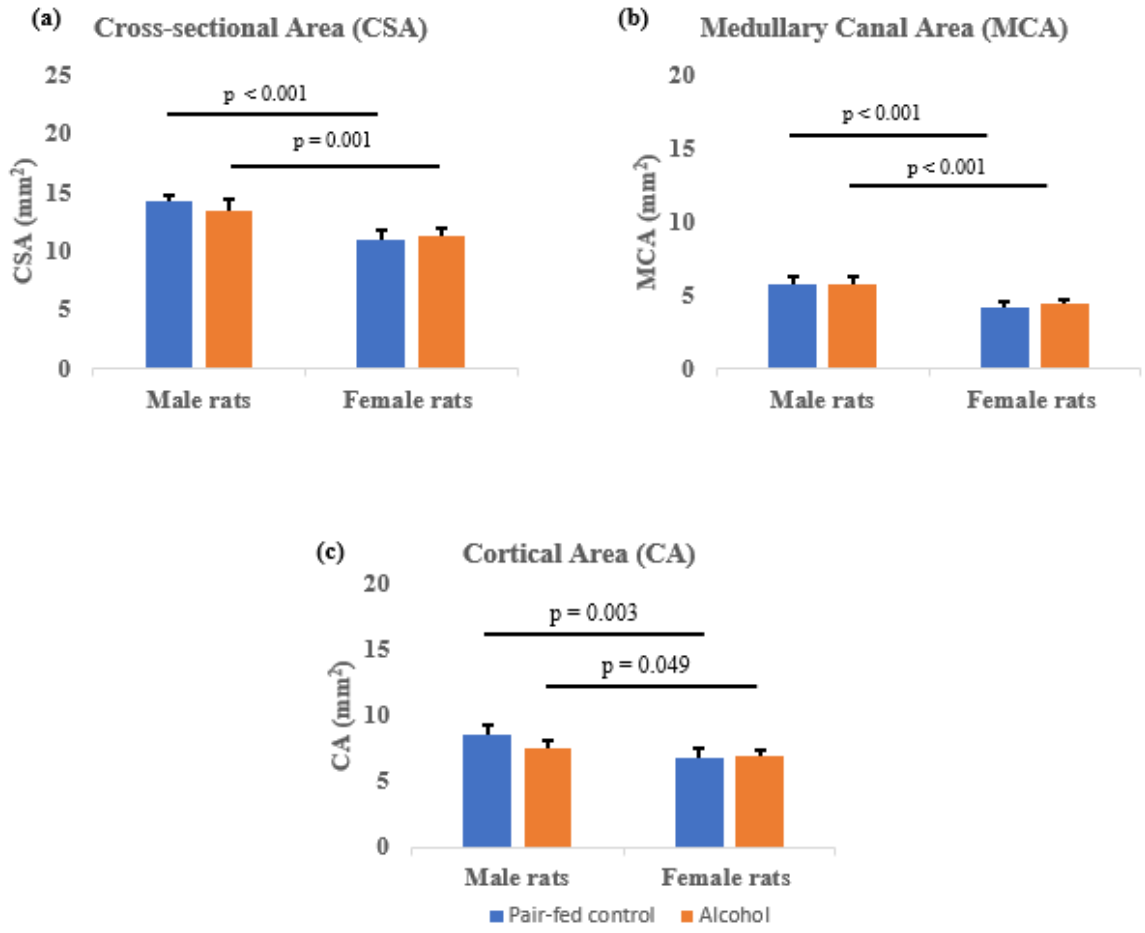


Figure 3.11: 25th percentile mark (proximal) dimensions of the femoral shaft. The mean **(a)**; cross-sectional area (CSA), **(b)**; medullary canal area (MCA) and **(c)**; cortical area (CA) are shown for the two groups studied in both male and female rats. Error bars represent standard deviation.

50th percentile mark (midshaft)

The midshaft showed a similar pattern to that of the proximal region, with no significant group differences. The CSA (mean = 11.538mm^2 ± 0.842) and MCA (mean = 5.390mm^2 ± 0.470) was marginally lower in the alcohol group compared to the pair-fed control group (CSA mean = 13.073mm^2 ± 0.297 and MCA mean = 6.479mm^2 ± 0.552), however no significance was detected (p = 0.060 and 0.210 respectively) (Fig 3.12a,b). Similarly, the alcohol group had a lower CA (mean =6.148mm^2 ± 0.402) compared to the pair-fed control group (mean = 6.594mm^2 ± 0.776) (Fig 3.12c). Again, no significance was detected (p = 0.29). Similar trends were also observed in female study groups, as the CSA was marginally lower in the alcohol group (mean = 9.629mm^2 ± 0.576) compared to the pair-fed control group (mean = 10,595mm^2 ± 0.838) (Fig 3.12a). However, this difference was not significant (p = 0.070). The MCA and

CA were also found to be lower in the alcohol group (MCA mean = 4.575mm^2 ± 0.462 and CA mean = 5.054mm^2 ± 0.241) than the pair-fed control group (MCA mean = 4.994mm^2 ± 0.542 and CA mean = 5.601mm^2 ± 0.460) (Fig 3.12b,c). However, no significance was detected ($p = 0.23$ and 0.06 respectively).

With respect to pair-fed controls, a group comparison showed that male rats had significantly greater CSA (mean = 13.073mm^2 ± 0.297) and MCA (mean = 6.479mm^2 ± 0.552) in comparison to female rats' CSA (mean = 10.595mm^2 ± 0.838) and MCA (mean = 4.575mm^2 ± 0.462) ($p < 0.001$ for both comparisons) (Fig 3.12a,c). Similarly, the male rats' pair-fed control group had a greater cortical area (mean = 6.594mm^2 ± 0.776) than that of the female rats' pair-fed control (mean = 5.054mm^2 ± 0.241) ($p = 0.011$). Similar to group comparisons observed in pair-fed control groups, male rats appeared to have a higher CSA (mean = 11.538mm^2 ± 0.842) than female rats (mean = 9.629mm^2 ± 0.576) in alcohol exposed animals ($p = 0.001$). This pattern was also observed in MCA and CA, with male rats having significantly higher cortical dimensions (MCA mean = 5.390mm^2 ± 0.470 and CA mean = 6.148mm^2 ± 0.402) compared to female rats (MCA mean = 4.575mm^2 ± 0.462 and CA mean = 5.054mm^2 ± 0.241) ($p = 0.001$ and $p = 0.013$, respectively) (Fig 3.12b,c).

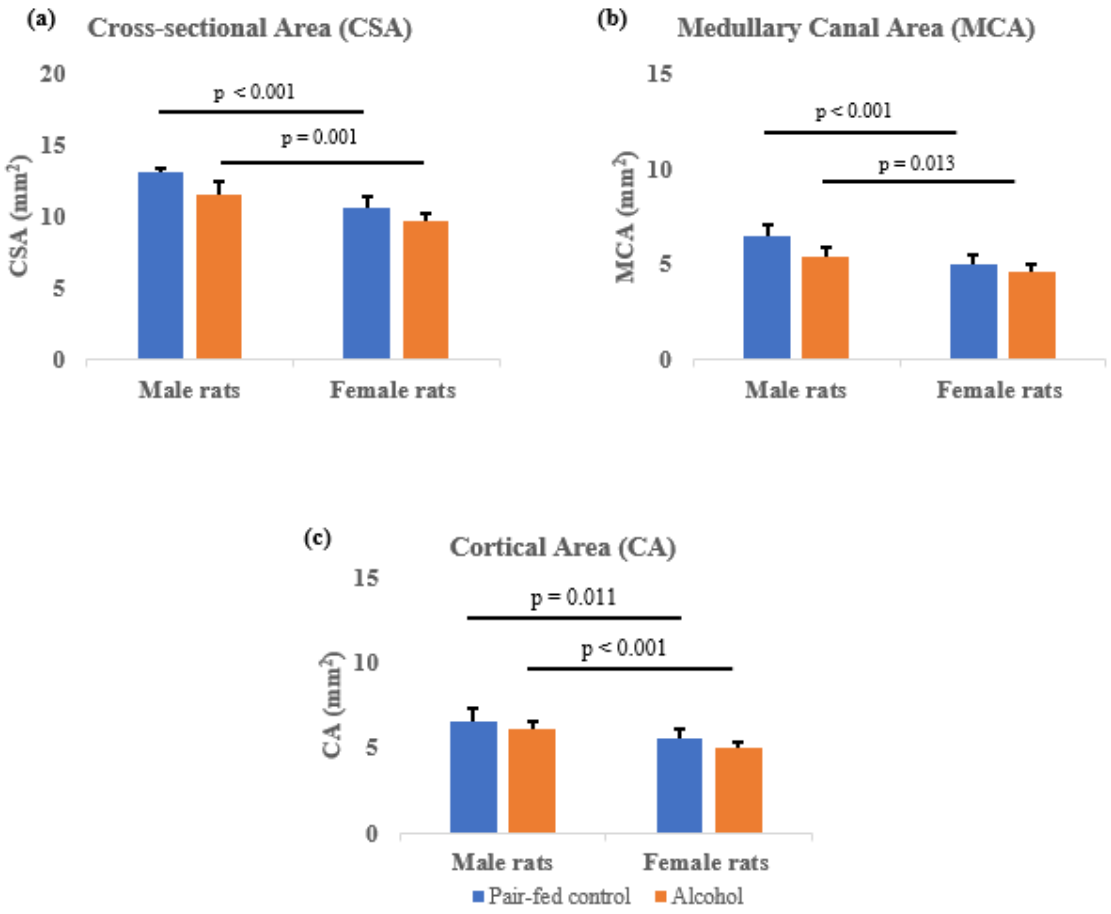


Figure 3.12: 50th percentile mark (midshaft) dimensions of the femoral shaft. The mean **(a)**; cross-sectional area (CSA), **(b)**; medullary canal area (MCA) and **(c)**; cortical area (CA) are shown for the two groups studied in both male and female rats. Error bars represent standard deviation.

75th percentile mark (distal)

The cortical dimensions in the distal region of the bone were similar amongst groups. In male rats, the alcohol group's CSA (mean =18.251mm^2 ± 2.015), MCA (mean = 11.400mm^2 ± 1.684) and CA (mean = 6.852mm^2 ± 0.335) values and the pair-fed control group's CSA (mean = 18.252mm^2 ± 2.056), MCA (mean = 11.490mm^2 ± 1.698) and CA (mean = 6.761mm^2 ± 0.439) values were similar (Fig 3.13) (p = 0.410; 0.670 and 0.110, respectively). In female rats, the alcohol group had a higher CSA (mean = 14.378mm^2 ± 1.446) and MCA (mean = 8.450mm^2 ± 1.235) compared to the pair-fed control group's CSA (mean = 13.770mm^2 ± 0.839) and MCA (mean = 8.057mm^2 ± 0.570), however no significance was detected (p = 0.44 and 0.54, respectively) (Fig 3.13a,b). Again, the cortical area was similar between the alcohol

(mean = 5.928mm^2 ± 0.251) and the pair-fed control (mean = 5.713mm^2 ± 0.276) (p = 0.23) (Fig 3.13c).

Regarding pair-fed controls, male rats had a significantly higher CSA (mean = 18.252 mm^2 ± 2.056), MCA (mean = 11.490mm^2 ± 1.698) and CA (mean = 6.761mm^2 ± 0.439) compared to female rats' CSA (mean =13.770mm^2 ± 0.839), MCA (mean = 8.057mm^2 ± 0.570) and CA (mean = 5.713mm^2 ± 0.276) (p < 0.001 for all differences) (Fig 3.13). This pattern continued in alcohol groups, with male rats exhibiting higher CSA (mean = 18.251mm^2 ± 2.015), MCA (mean = 11.400mm^2 ± 1.684) and CA (mean = 6.852mm^2 ± 0.335) than female rats' CSA (mean =14.378mm^2 ± 1.446), MCA (mean = 18.450mm^2 ± 1.235), and CA (mean = 5.928mm^2 ± 0.251). These differences were statistically significant (p = 0.003, p = 0.006 and p < 0.001, respectively) (Fig 3.13).

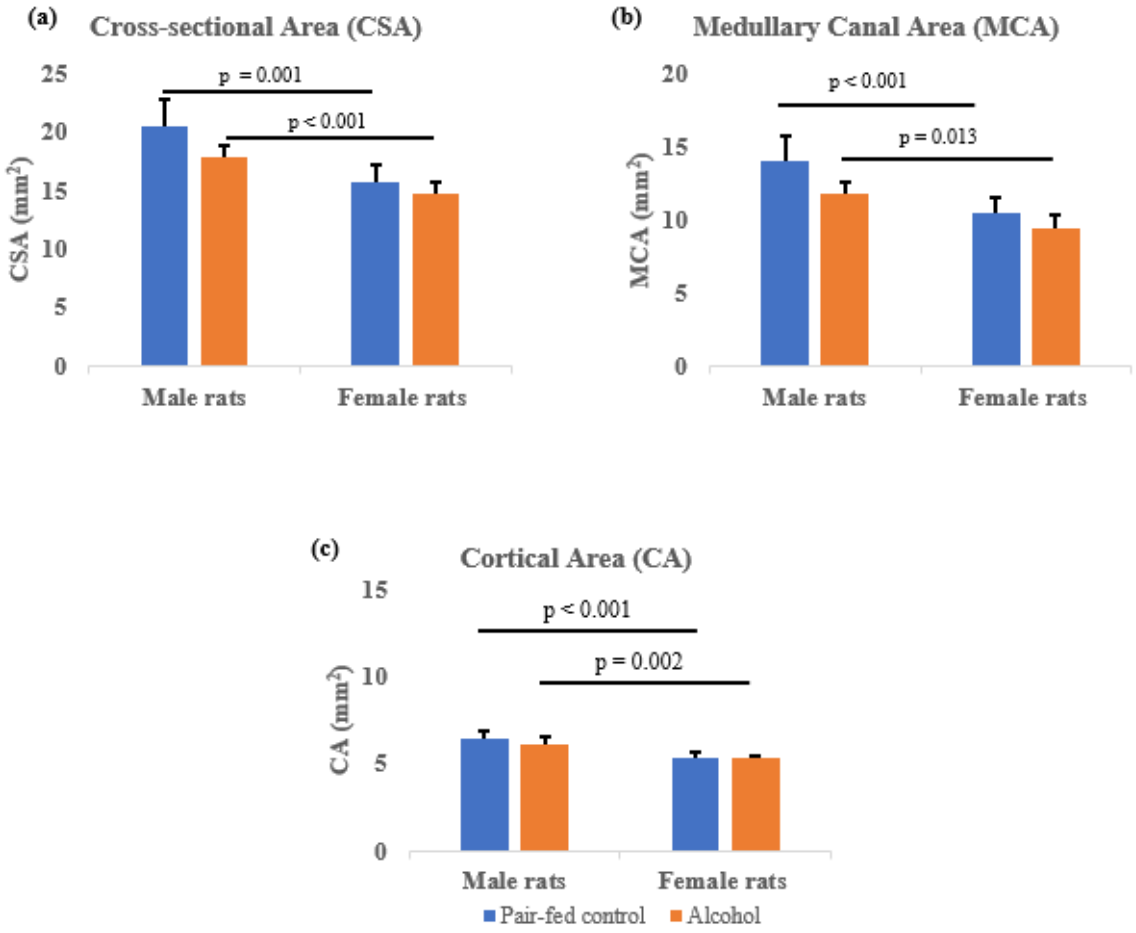


Figure 3.13: 75th percentile mark (distal) dimensions of the femoral shaft. The mean **(a)**; cross-sectional area (CSA), **(b)**; medullary canal area (MCA) and **(c)**; cortical area (CA) are shown for the two groups studied in both male and female rats. Error bars represent standard deviation.

3.2.8 Three-point bend testing of the femur, tensile strength assessment.

In the acute binge alcohol consumption model, no significant bone weight differences were observed between the alcohol and pair-fed control groups, in both male and female rats ($p = 0.743$ and 0.916 respectively) (Table 3.1 and 3.2). However, bone weight appeared to be increased in male rats, for both the pair-fed control group (mean = 0.872g ± 0.088) and alcohol group (mean = 0.887g ± 0.065) in comparison to female pair-fed control (mean = 0.688 ± 0.060) and alcohol group (mean = 0.692 ± 0.044) ($p = 0.002$ and <0.001, respectively).

With respect to bone biomechanical parameters, male rats exhibited similar maximum force, maximum displacement, and maximum time, between the alcohol and pair-fed control groups ($p = 0.871$, 0.973 and 0.972, respectively) (Table 3.1). Furthermore, the break force was marginally lower in the alcohol group compared to the pair-fed control group, again, this difference was not significant ($p = 0.634$) (Fig 3.1).

In female rats, the pair-fed control group had a marginally higher maximum force and break force compared to the alcohol group (Table 3.2), however these differences were not statistically significant ($p = 0.613$ and 0.671, respectively). Maximum time and break force were marginally higher in the pair-fed control group than the alcohol group and again no statistical significance was observed ($p = 0.673$ and $p = 0.286$, respectively) (Table 3.2).

When comparing tensile strength parameters across pair-fed control groups, no differences in maximum force, maximum displacement, maximum time, and break force were detected between male pair-fed control and female pair-fed control groups ($p = 0.693$, $p = 0.898$, $p = 0.908$ and $p = 0.840$, respectively). Similarly, in alcohol groups, no differences in tensile parameters were observed between male rats and female rats. ($p = 0.826$, $p = 0.747$, $p = 0.747$ and $p = 0.619$, respectively).

Table 3.1: Weight measurements and tensile strength parameters of the male rat femur.

Parameter		*n*	*Mean*	*SD*
Bone weight (g)	Pair-fed control	6	0.872	0.088
	Alcohol	6	0.887	0.065
Maximum force (N)	Pair-fed control	6	83.527	14.336
	Alcohol	6	84.692	9.047
Maximum displacement (mm)	Pair-fed control	6	1.200	0.457
	Alcohol	6	1.192	0.363
Maximum time (sec)	Pair-fed control	6	23.993	9.145
	Alcohol	6	23.823	7.257
Break force	Pair-fed control	6	81.663	13.993
	Alcohol	6	78.379	8.543

Table 3.2: Weight measurements and tensile strength parameters of the female rat femur.

Parameter		*n*	*Mean*	*SD*
Bone weight (g)	Pair-fed control	6	0.688	0.060
	Alcohol	6	0.692	0.044
Maximum force (N)	Pair-fed control	6	86.610	11.840
	Alcohol	6	83.605	7.595
Maximum displacement (mm)	Pair-fed control	6	1.174	0.169
	Alcohol	6	1.140	0.098
Maximum time (sec)	Pair-fed control	6	23.473	3.369
	Alcohol	6	22.783	1.958
Break force	Pair-fed control	6	83.457	10.732
	Alcohol	6	75.027	13.503

3.2.9 Morphological assessment of the femoral epiphyseal growth plate

Male study group

The proximal epiphyseal growth plate of the femur showed disturbances in the alcohol group. The pair-fed control group had more chondrocytes which were closely arranged in distinct rows, compared to the alcohol group (Fig 3.14). Furthermore, the alcohol group showed a diminished hypertrophic zone (HZ), whereas the pair-fed control showed a gradual increase in cellular size which denoted a hypertrophic zone (Fig 3.14). In the distal epiphyseal growth plate, similar morphology was observed between the alcohol and pair-fed control groups. Both study groups appeared to have a distinct proliferative zone (PZ), with similar chondrocyte distributions, tightly arranged in prominent rows (Fig 3.14). The hypertrophic zone was prominently elongated in both groups (Fig 3.14).

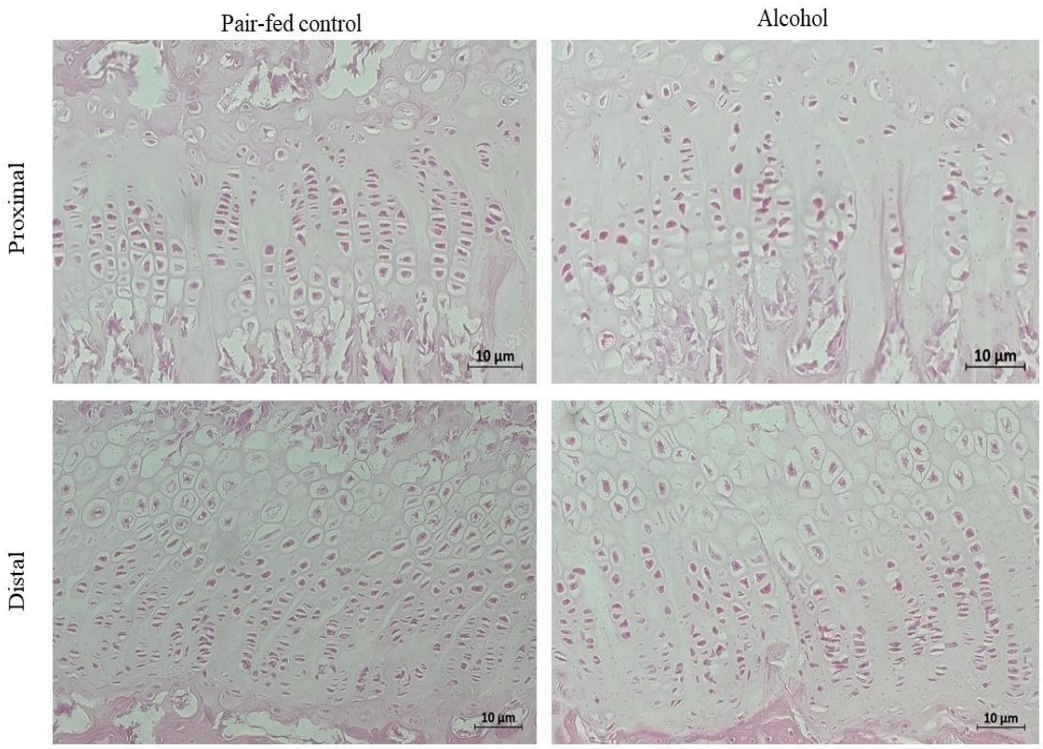


Figure 3.14: Haematoxylin and Eosin-stained longitudinal sections of both the proximal and distal epiphyseal growth plates of femora for the two study groups in male rats.

Female study groups

No morphological differences were observed in the proximal epiphyseal growth plate between study groups. Both the alcohol and pair-fed control groups showed a similar chondrocyte density and columnar arrangement. Gaps of varying width dimensions were observed between chondrocyte columns, connecting the epiphysis and the metaphysis (Fig 3.15). However, in the distal epiphyseal plate, minor differences were observed between study groups. The alcohol group appeared to have a greater chondrocyte density compared to the pair-fed control group (Fig 3.15). The chondrocyte columnar arrangement was more compact and prominent in the alcohol group than the pair-fed control group (Fig 3.15). The spacing between chondrocyte columns was less in the alcohol group compared to the pair-fed control group. Nevertheless, similar configurations were observed in the hypertrophic and resting zones of the growth plate (Fig 3.15).

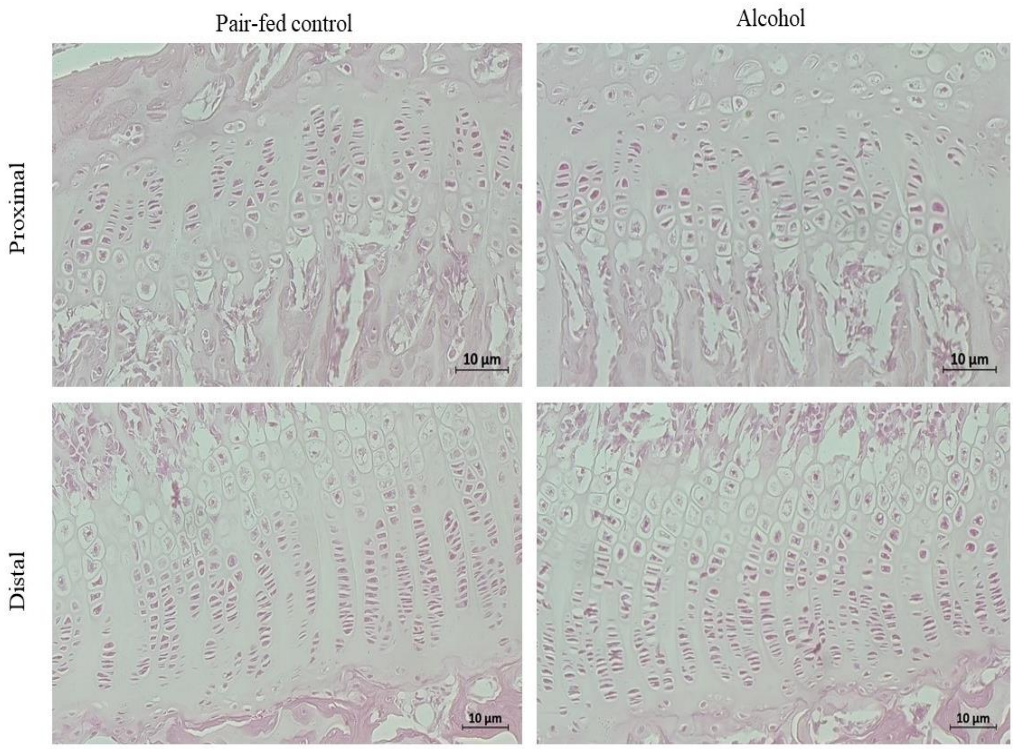


Figure 3.15: Haematoxylin and Eosin-stained longitudinal sections of both the proximal and distal epiphyseal growth plates of femora for the two study groups in female rats.

3.2.10 Proliferative zone Ki-67 immuno-positive chondrocyte number

In the proliferative zone of the proximal growth plate, the alcohol group (mean = 1 748 ± 61) had significantly fewer immunolabeled chondrocytes compared to the pair-fed control (mean = 2 194 ± 387) in male rats ($p = 0.019$) (Fig 3.16a). However, female rats showed a similar chondrocyte number in the proximal epiphysis between the pair-fed control and the alcohol groups (mean = 1 513 ± 103, and 1 585 ± 99, respectively) ($p = 0.245$) (Fig 3.16a).

Regarding the pair-fed control groups, the male rats (mean = 2 194 ± 387) had more proliferating chondrocytes compared to female rats (mean = 1 513 ± 103), in the proximal epiphyseal growth plate. ($p < 0.001$) (Fig 3.16a). This pattern continued in alcohol groups, with male rats (mean = 1 748 ± 61) having more proliferating chondrocytes than female rats (mean = 1 585 ± 99) ($p = 0.006$) (Fig 3.16a).

In the distal epiphysis, male rats had a lower chondrocyte number in the alcohol group (mean = 2 421 ± 284) than the pair- fed control group (mean = 2 913 ± 202) (Fig 3.16b). Again, this difference was statistically significant ($p =0.006$). Contrarily, the alcohol group in female rats

had more chondrocytes in the proliferative zone (mean = 2 117 ± 166) than the pair-fed control (mean = 1 827 ± 189) (p = 0.018) (Fig 3.16b).

Both male rats' pair-fed control (mean = 2 913 ± 202) and alcohol group (mean = 2 421 ± 284) had fewer proliferating chondrocytes than the female rats' pair-fed control (mean = 1 827 ± 189) and alcohol groups (mean = 2 117 ± 166) in the distal epiphyseal growth plate (p < 0.001 and p = 0.047, respectively) (Fig 3.16b).

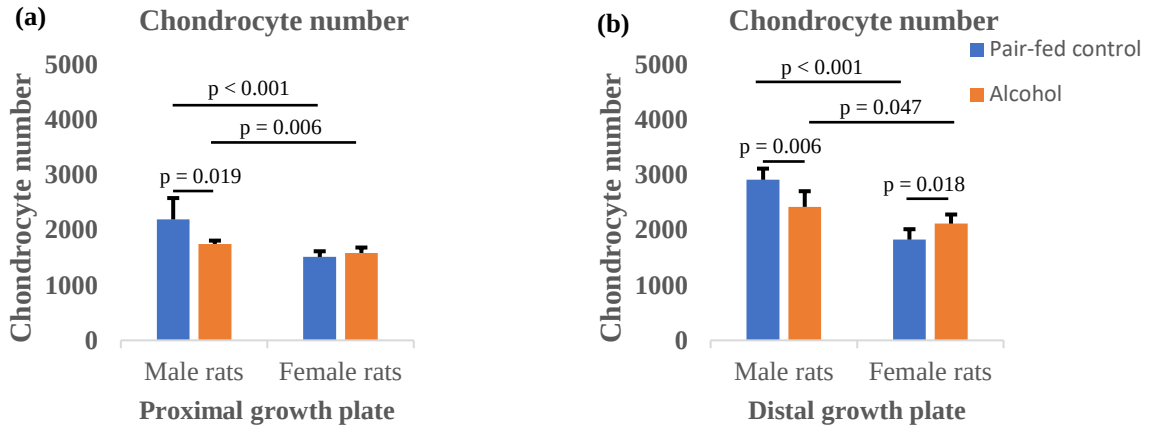


Figure 3.16: Femoral epiphyseal growth plate proliferative zone number of chondrocytes. The mean values are shown for the proliferative zone in the **(a);** proximal and **(b);** distal epiphyseal growth plate for the pair-fed control and the alcohol groups in both male and female rats. Error bars represent standard deviation.

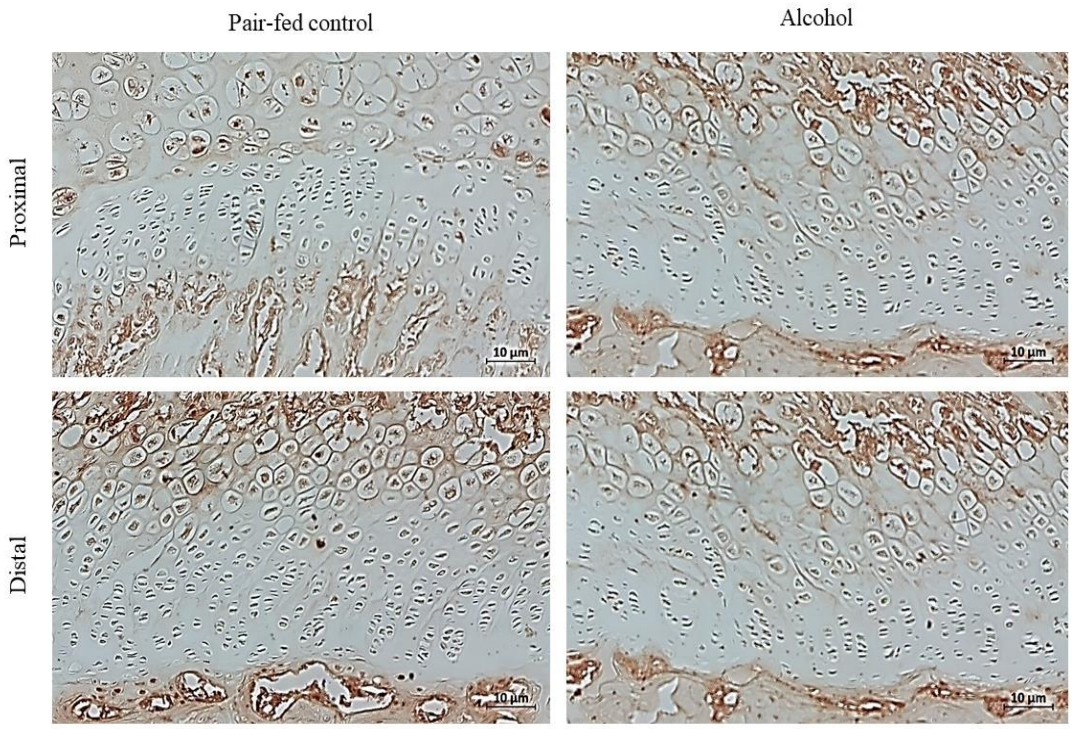


Figure 3.17: Photomicrographs depicting immunolabeled femur chondrocytes using the anti-Ki-67 antibody. The images represent the proximal and distal epiphyseal growth plates for the pair-fed control and alcohol groups in male rats.

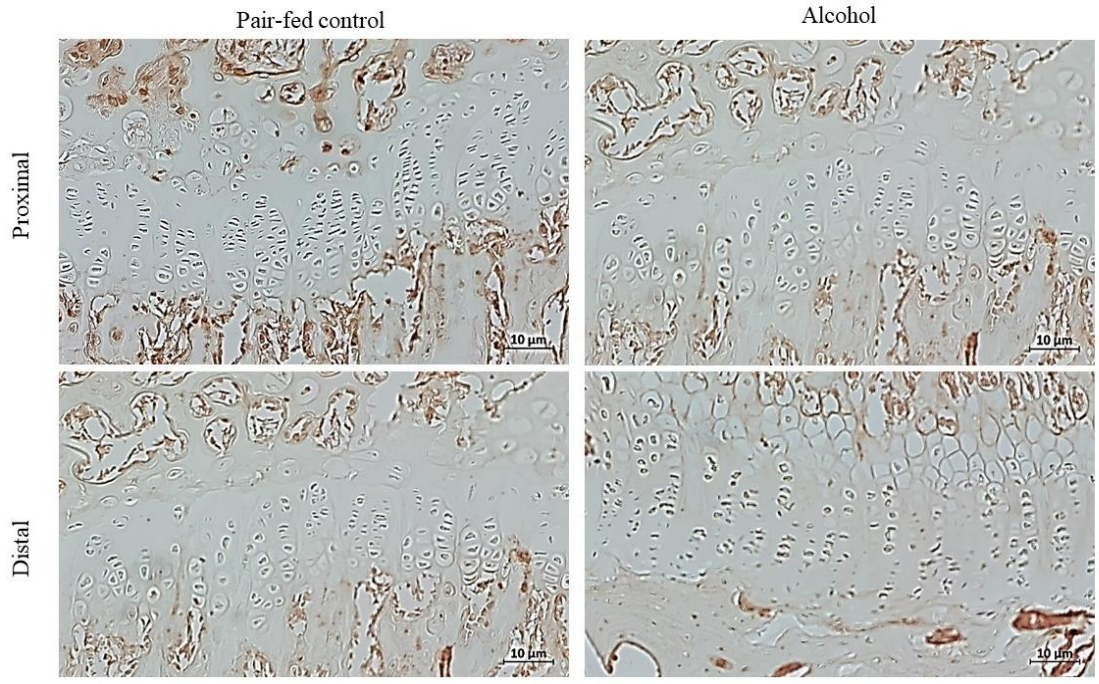


Figure 3.18: Photomicrographs depicting immunolabeled femur chondrocytes using the anti-Ki-67 antibody. The images represent the proximal and distal epiphyseal growth plates for the pair-fed control and alcohol groups in female rats.

3.3 DISCUSSION

The aim of this study was to examine the effects of acute binge alcohol consumption on the growth and development of the femur in adolescent Sprague Dawley rats. We employed micro focus X-ray computed tomography to assess trabecular morphometry in the proximal and distal epiphysis of the femur, osteometric parameters and evaluated cortical dimensions. Histological and immunohistochemical techniques were used to examine the influence of acute binge alcohol consumption on the overall morphology of the epiphyseal growth plate and the proliferation of chondrocytes in the proliferative zone. Also, tensile strength was determined by three- point bending testing was done using a universal bending machine to determine whether an acute binge alcohol drinking model resulted in weaker bones. The study found trabeculae parameters to be affected in the male rats in the distal extremity of the femur. Osteometric measurements, remained unaffected in both the male and female rats. However, the trabecular morphometry was similar in the proximal region in the male rats. On the other hand, the female rats exhibited no detrimental effects of alcohol on both extremities. Tensile strength remained unaffected in both males and female rats. The study observed a decrease in proliferation rate of chondrocytes in both the extremities (proximal and distal) of the femur in male rats. Again, no harmful effects of alcohol were seen in the female rats with regards to chondrocyte proliferation.

Food consumption and body weight gained.

With regards to the food consumed and the percentage of weight gained by the animals, the current study found this to be similar across the groups. In this acute alcohol drinking model, we expected either a decrease in food intake or a reduced weight gained over the week. However, we did not find any group difference in this regard. The lack of differences in food consumption and weight gained in our study may be attributed to the study design. We administered alcohol of 20% (vol/vol) ethanol solution at a dose of 3g/kg, as a single dose via oral gavage for 3 days and then terminated the animal after 7 days. Our dose and duration of alcohol exposure may have been too low and short, respectively to have any adverse effect on food consumption and weight gained. However, some studies have reported a decrease in weight gained caused by prolonged alcohol intake (Milat et al., 2017; Lieber, 2003).

Bone osteometrics

In the current study, the acute binge alcohol consumption model exhibited no significant changes in the length and bicondylar breadth of the femur among the study groups. This finding is similar to a study by Sampson and colleagues in 1996 which showed the femora treated with alcohol exhibiting similar lengths to the pair-fed controls after two weeks of alcohol administration. However, in the same study when alcohol was given for a longer period this resulted in shorter femora (Sampson et al.,1996). This suggests that if alcohol is given for a longer period this could result in a negative impact on bone length (Turner et al., 2001, 1987). Considering the duration of the acute alcohol consumption in the current study, it is plausible to propose that acute binge alcohol consumption duration was too short to cause any detrimental effects on the osteometry of the adolescent femur. This finding is further supported by Turner et al. (1988) in a study which found no changes in femoral length in alcohol-treated rats compared to pair-fed controls, following acute administration of alcohol (Turner et al., 1988).

Femur Trabecular Morphometrics

Regarding, trabecular morphometry it was found that acute binge alcohol consumption led to alterations in the internal architecture and structure of the trabecular bone in the distal epiphysis of male rats. These alterations were characterized by a decrease in bone tissue volume (BV/TV), reduction in trabecular thickness (TbSp), number (TbN) and a decrease in spacing. However, this study found no negative influence of acute binge alcohol consumption in the proximal end of the femur in the male rats. Our findings concur with previous studies on actively young growing rats (Sampson et al., 1996, Sampson, 1997) and in adult rats (Maddalozzo et al., 2009; Turner et al., 2001) which reported changes such as a decrease in bone fraction area (BV/TV), trabecular thinning (TbTh), however, these authors reported the effects of alcohol exposure in the proximal extremity of the osseous tissue (tibia). The higher proportion of trabecular bone and increased mechanical loading in the distal end of the femur maybe likely contributing factors to why alcohol affected trabecular bone in the distal region of male rats more than the proximal end (Kivell, 2016).

Regarding the female adolescent rats, trabecular morphometry was not affected by these animals consuming an acute binge alcohol drinking model in both the extremities, with the exception to trabecular thickness which was significantly thicker in the distal region of female

rats. Hormonal fluctuations in female rats may have influenced the response of trabecular bone to acute binge alcohol consumption. Hormones such as oestrogen play an important role in bone health, and their protective effects may have masked any potential negative impacts of alcohol on trabecular morphometry (Manolagas, et al., 2013; Turner, 2001). Also, the timing of the study in relation to the oestrous cycle of the rats could also have influenced the results.

Femur cross-sectional area, medullary canal area and cortical area

Cortical dimensions, which reflect the thickness and density of the cortical bone, showed no significant changes in either the male or female rats after acute binge alcohol consumption. This may suggest that the acute binge alcohol consumption did not have a noticeable effect on the cortical bone dimensions in the shaft of the femur. This finding concurs with a study by Hogan and colleagues in 1997 which, examined the cortical bone histomorphometry of actively growing rats following alcohol consumption. These authors, revealed in their study that the cross-sectional area, bone marrow area and cortical bone area did not differ significantly between the alcohol and pair-fed control groups after 2 weeks of alcohol consumption (Hogan et al., 1997).

Three-point bend testing of the femur

In the current study, we found no significant differences in the results of bone weight and tensile strength properties, in both male and female rats. The maximum displacement and maximum time results from the present study could not be compared directly to the other studies as no previous studies can be found in the literature that include the effects of acute binge alcohol consumption on these properties. However, Hogan et al. (1997) using a chronic model did investigate the effects of alcohol consumption on both the maximum force and break force and reported a lower maximum force in alcohol-exposed animals compared to the pair-fed controls at all time periods. This trend was also observed in the break force results by Hogan et al, 1997. This discrepancy in findings is likely attributed to differences in study design. In contrast to Hogan et al. (1997), who used three-week-old female Sprague-Dawley rats and fed them a modified Lieber-DeCarli diet ad libitum containing 35% alcohol-derived calories for eight weeks, we administered 20% alcohol via oral gavage to seven-week-old male and female Sprague-Dawley rats for one week in our study. It is possible that if we had used a higher

alcohol concentration, a longer administration period, and younger rats, our results would have been similar to those of Hogan et al. (1997). Considering the cortical dimension results of the midshaft, where no significant differences were found, it is possible that this lack of variation could explain the absence of group differences in bone strength.

Cell morphology of the epiphyseal growth plate

Male study groups

A disrupted cell morphology was observed in the proximal epiphyseal growth plate of the alcohol group, where there appeared to be fewer chondrocytes that were dispersedly arranged which is in agreement with a study by Miralles-Flores and Delgado-Baeza (1992) which found fewer chondrocytes in this zone. Furthermore, the hypertrophic zone which plays a crucial role in regulating the rate of growth in endochondral bones (Hallett et al., 2019), was found to be diminished in the alcohol group, again, similar to the study of Mirrales-Flores and Delgado-Baeza in 1992.

We initially expected similar morphological disturbances in the distal epiphyseal growth plate (due to the negative effects seen in the trabecular parameters in the distal epiphysis), however, an acute binge alcohol consumption resulted in no significant changes to the chondrocytes in the distal end. Both the alcohol and pair-fed male rats exhibited distinct proliferative zones, with similar chondrocyte populations, columnar configuration, and also, an elongated hypertrophic zone containing large chondrocytes undergoing hypertrophy. These indicate a normal progression of the epiphyseal growth plate development (Hallett et al., 2019), particularly in the distal end.

Female study groups

A comparison of the alcohol group with the pair-fed control group, both showed similar chondrocyte density and distinct chondrocyte columnar arrangement, thus indicating normal epiphyseal growth plate development (Hallett et al., 2019). Additionally, the presence of gaps between the chondrocyte stacks of varying width dimensions, spanning the growth plate and, connecting the metaphyseal and epiphyseal ends, was evident in both study groups. This finding aligns with the natural bridging process that occurs in rats as the epiphyseal growth

approaches closure (Roach et al., 2003). Together, these findings indicate that acute administration of alcohol in a binge pattern had no effect on the development and closure of the growth plate located in the proximal region.

However, in the distal epiphyseal growth plate, the acute binge consumption of alcohol was found to increase the chondrocyte population and enhance the compactness and prominence of chondrocyte columns thus, in correlation with a developing growth plate (Hallett et al., 2019; Roach et al., 2003). These results may indicate that acute binge alcohol consumption either accelerates bone growth in female rats or that the resulting accelerated bone growth is a compensatory response to alcohol's adverse effects on bone. Similar phenomena have been reported in menopausal women, where studies have shown a positive association between light to moderate alcohol consumption and bone mass, as well as either no change or a decrease in fracture risk (Turner and Sibonga, 2001; Turner, 2000). However, considering the developmental phase examined in the current study (adolescence), further studies are warranted to understand the impact of alcohol on oestrogen levels in adolescent female rats, as this factor may be crucial in elucidating the observed effects.

Proliferative zone Ki-67 immuno-positive chondrocyte number

Previous studies on the impact of alcohol consumption on adolescent bone tissue development have primarily shown growth inhibition in the tibia and femur (Lauing et al, 2008; Hogan et al, 1997; Sampson et al, 1996, 1997). The reduced number of chondrocytes observed in the current study is a similar finding to that of Miralles-Flores and Delgado-Baeza (1992) who found that both the proliferative and hypertrophic zone had fewer chondrocytes. The authors of this study ascribed this to changes in the composition and organization of the extracellular matrix which may affect the maturation of the chondrocytes.

However, the information about cell markers of proliferation was not part of their investigations (Miralles-Flores and Delgado-Baeza, 1992). The current study found fewer proliferating cells (Ki-67 immuno-positive) in both the proximal and distal epiphyseal growth plates in male rats, suggesting that an acute binge alcohol model affects both regions of the bone.

However, with regards to the female rats our findings showed no significant difference in Ki-67 immuno-positive chondrocytes in the proximal growth plate proliferative zone between the

alcohol and pair-fed control groups. However, we found an increased presence of Ki-67 immunolabelled chondrocytes in the distal epiphyseal growth plate in the alcohol group. This observation contradicts the pattern observed in male rats. This discrepancy, along with the normal cell morphology of the growth plate, suggests the existence of a compensatory or resistance mechanism to alcohol in female rats, at least within the context of acute binge consumption. Similar phenomena have been reported in menopausal women (Turner and Sibonga, 2001), emphasizing the importance of further investigations to elucidate the potential effects of alcohol on oestrogen-bone pathways, particularly in adolescent females.

3.4 CONCLUSION

An acute binge alcohol consumption model resulted in detrimental effects in the distal epiphysis with regards to trabecular morphometry in male rats. Fewer chondrocytes and proliferating cells (Ki-67 immuno-positive) were observed in both the proximal and distal epiphysis of male rats. Female rats' internal architecture as well as chondrocyte number and proliferating cells (Ki-67 immuno-positive) remained unaffected with an acute binge alcohol consumption model.

Chapter 4

The effects of chronic binge alcohol consumption on the development of the femur of adolescent Sprague Dawley rats

ABSTRACT

Although it is well established that chronic alcohol consumption adversely affects bone metabolism, there remains a paucity in literature about bone effects of binge alcohol consumption in adolescents. Therefore, our study aimed to examine the effects of chronic binge alcohol consumption on the development of the adolescent femur. Seven-week-old Sprague Dawley rats (n = 24; 12 male and 12 female rats) were randomly allocated to 1 of the 2 groups; alcohol group (n = 12; 6 male and 6 female rats), receiving 20% of alcohol at 3g/kg bodyweight and the pair-fed control group, receiving isocaloric equivalent of maltose dextrin via oral gavage for 4 weeks (3 days/week on alternative days). Three-dimensional Micro-Focus X-ray Computed Tomography (3D-µCT) and Volume Graphics Studio® software were employed to assess the trabeculae in both the proximal and distal epiphysis, as well as measuring the cortical dimensions of the femur. The morphology of the epiphyseal growth plate was examined by haematoxylin and eosin (H&E) staining, whereas Ki-67 immunostaining was used to quantify the proliferation of chondrocytes in the proliferative zone of the growth plate. A three-point bending test was done to examine the effects of alcohol on bone strength. The results showed disturbances in the trabecular morphometry of the proximal epiphysis in the male alcohol exposed rats, whereas trabecular spacing and trabecular number appeared to have improved after chronic binge alcohol consumption in female rats. In the distal epiphysis, the trabecular morphometry remained unaffected in both male and female rats. Osteometric measurements were also unaffected by chronic binge alcohol consumption. This was consistent across male and female rats. A decrease in proliferation of chondrocytes was observed in the proximal epiphysis of the femur in male rats, while the distal epiphyseal growth plate remained unaffected. Again, no harmful effects of alcohol were seen in the female rats with regards to chondrocyte proliferation. While tensile strength remained unaffected in the male rats, our study revealed improved bone tensile strength in female rats following alcohol consumption. These findings may suggest that chronic binge alcohol consumption has detrimental effects on the trabeculae in the proximal epiphysis. Furthermore, it disrupts the morphology of the proximal epiphyseal growth plate and reduces the proliferation of chondrocytes in the proliferative zone of the growth plate.

4.1 INTRODUCTION

Excessive alcohol consumption is known to have a range of detrimental effects on public health, including alcohol-related accidents, violence, crime and may disturb the integrity of bone development and the internal architecture of the osseous tissue (Pillay and Ndou 2022; Morojele and Ramsoomar, 2016; Reed et al, 2002). South Africa is known to have a high prevalence of dangerous drinking practices, such as binge drinking (Morojele and Ramsoomar, 2016). This is a major public health concern as high levels of binge drinking are observed in the adolescent population, globally (Morojele and Ramsoomar, 2016). Binge alcohol drinking is defined as having had five or more drinks of alcohol in a single drinking episode (Föger-Samwald et al, 2018; National Institute on Alcohol Abuse and Alcoholism, 2004).

The adolescent stage is critical in the development of bone and attaining peak bone mass (Weaver, 2002). Hence, the consumption of alcohol during this period may cause interruptions in bone growth and development (Lauing et al, 2008). Alcohol is known to decrease peak bone mass causing an increased risk of fractures and the early onset of osteoporosis (Reed et al, 2002; Sampson., 1995).

Previous studies have reported that chronic alcohol consumption may have a negative impact with bone growth and development resulting in osteoporosis later in life by inhibiting osteoblastic cells (Mikosch, 2014). However, the mechanism involved in this is not elucidated which needs further investigation. Also, Sampson in 1998 reported that alcohol had an adverse impact on bone mineral content but does not interfere with bone growth (Sampson, 1998). However, a study by Rosa and colleagues in 2019 found that bone growth was reduced in alcohol exposed rats (Rosa et al., 2019).

Although, it is known that alcohol perturbs the osseous tissue there is limited research regarding the damage in the skeletal system of adolescents who partake in chronic binge alcohol consumption in the attainment of growth and peak bone mass.

Thus, the current study sought to evaluate the effect of chronic binge alcohol consumption in growing rats on longitudinal growth of the femur and parameters of bone quality. To achieve this, the current study used three-dimensional micro-focus X-ray computed tomography (3D-µCT) to assess the effects of chronic binge drinking on trabecular parameters and femoral osteometrics. Haematoxylin and Eosin (H&E) staining were employed to study the morphological changes of the epiphyseal growth plate. Immunohistochemistry was used to assess the proliferation of chondrocytes in the epiphyseal growth plate using the anti-Ki-67

antibody. The effects of chronic binge alcohol consumption on bone strength were assessed using a three-point bending test.

4.2 RESULTS

4.2.1 Measurement reliability

The reliability of the measurements was evaluated using Lin's concordance correlation coefficient (p_c), which demonstrated values exceeding 0.7 for all osteometric measurements. These findings indicate a strong level of measurement reliability, suggesting that the measurements are consistently accurate and dependable.

4.2.2 Blood alcohol concentration

The average blood alcohol concentration was 106.04mg/dL (±17.61) in the alcohol groups.

4.2.3 Body weight gain

The chronic binge alcohol consumption model showed a similar pattern in the percentage weight gained in the male rats between the alcohol (mean = 41.61% ± 1.08) and the pair-fed control groups (mean = 40.40 % ± 2.06) (p = 0.24) (Fig 4.1). Conversely, female rats exhibited a different pattern, as the alcohol group displayed a greater percentage of weight gain (mean = 27.96% ± 3.14) compared to the pair-fed control group (mean = 22.74% ± 3.09) (p = 0.019) (Fig 4.1).

Regarding pair-fed control groups, male rats gained more body weight (mean = 40.40 % ± 2.06) compared to female rats (mean = 22.74% ± 3.09) (p < 0.001) (Fog 4.1). This pattern continued in animals exposed to alcohol, with male rats showing higher body weight gains (mean = 41.61% ± 1.08) compared to female rats (mean = 27.96% ± 3.14) (p < 0.001) (Fig 4.1).

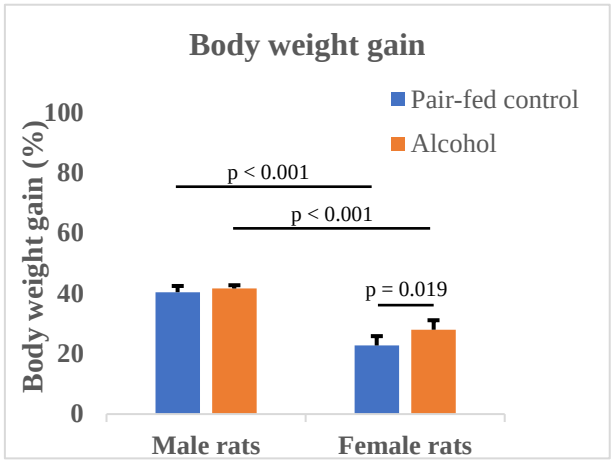


Figure 4.1: Average body weight gain. Body weight gained between the alcohol and pair-fed control represented as a percentage. following chronic binge alcohol consumption in both male and female rats. Error bars represent standard deviation.

4.2.4 Food consumption

Regarding food consumption, all study groups had a similar pattern throughout the course of the study. Male rats showed a similar marginal increase in average food consumption every week, reaching the highest in week 3 (alcohol mean = 51.60g ± 2.29 and pair-fed control mean = 51.07g ± 2.34) ($p = 0.7$) (Fig 4.2). In week 4, there was a slight decrease in the amount of food consumed and this was observed in both the alcohol (mean = 50.43g ± 2.62) and the pair-fed control (mean = 51.52g ± 3.94), however no significance was detected ($p = 0.585$) (Fig 4.2).

A different trend was observed in the female rats, with the daily average of food consumed increasing in week 3 and 4 of alcohol administration (Fig 4.2). However, no significant difference was observed between the alcohol and control groups in week 3 (mean = 34.62g ± 3.21 and mean =36.33 ± 4.56, respectively) and in week 4 (mean = 34.36g ± 3.29 and mean = 35.42g ± 3.32, respectively) ($p = 0.47$ and 0.59, respectively) (Fig 4.2).

A comparison of food consumption between pair-fed control groups, indicated that male rats (mean = 51.30g ± 3.14) significantly consumed more food than female rats (mean = 35.88g ± 3.94) ($p < 0.001$) (Fig 4.2). This was also observed in alcohol groups, with male rats (mean = 51.01g ± 2.46) consuming more food compared to female rats (mean = 34.49g ± 3.25) ($p < 0.001$) (Fig 4.2).

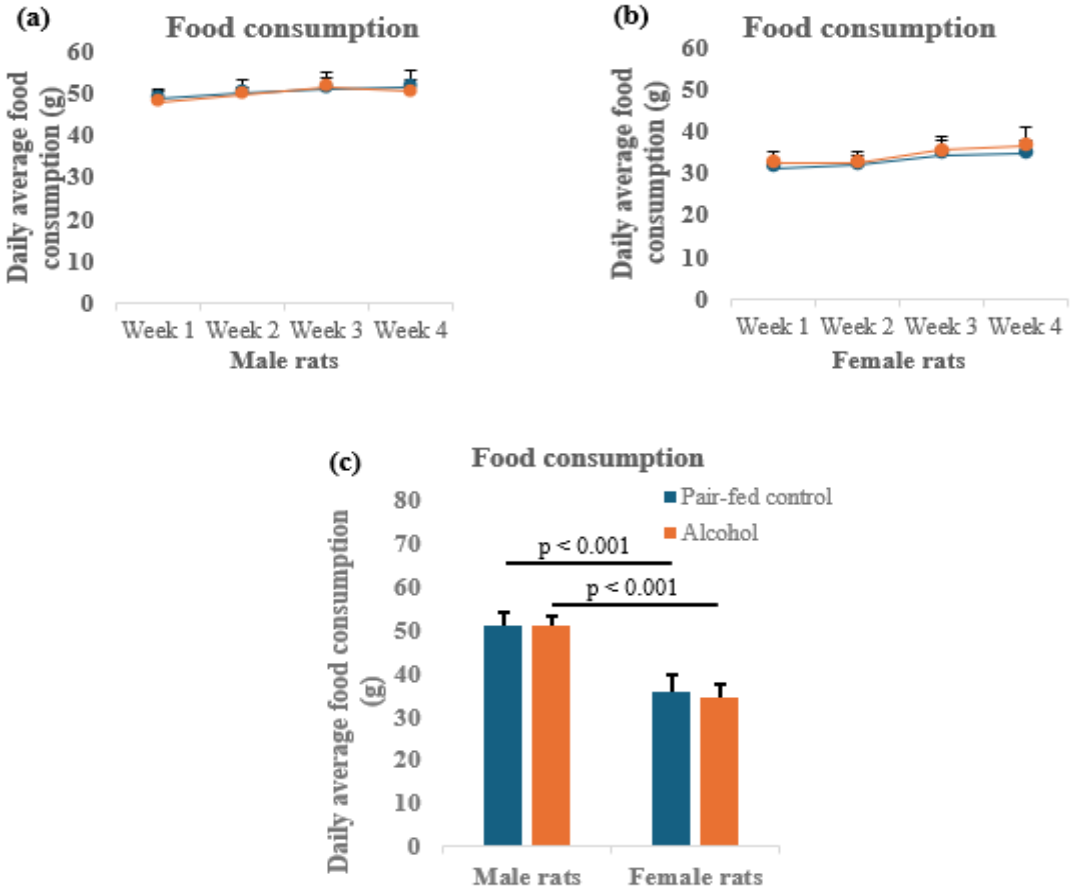


Figure 4.2: Average food consumption. The daily food consumption in grams is shown as an average per week for both alcohol and pair-fed control groups in **(a)**; male rats and **(b)**; female rats, **(c)** shows a comparison between male rats and female rats. Error bars are shown as standard deviation.

4.2.5 Osteometric measurements of the femur

Full femur length

No differences in bone length were detected amongst study groups in the chronic binge alcohol consumption model (Fig 4.3). Similar bone length was observed in male rats, between the alcohol group (mean = 35.18mm ± 0.79) and the pair-fed control group (mean = 35.29mm ± 0.48) (p = 0.790). A similar group comparison was observed in female rats, with the alcohol group (mean 31.84mm ± 0.55) and the pair-fed control (mean = 32.18mm ± 0.24) displaying a similar bone length (p = 0.200) (Fig 4.3)

Male rats, both pair-fed control (mean = 35.29mm ± 0.48) and alcohol group (mean = 35.18mm ± 0.79) had longer femora compared to female rats' pair-fed control (mean = 32.18mm ± 0.24)

and alcohol group (mean = 31.84mm ± 0.55). These differences were statistically significant ($p < 0.001$ for both comparisons) (Fig 4.3).

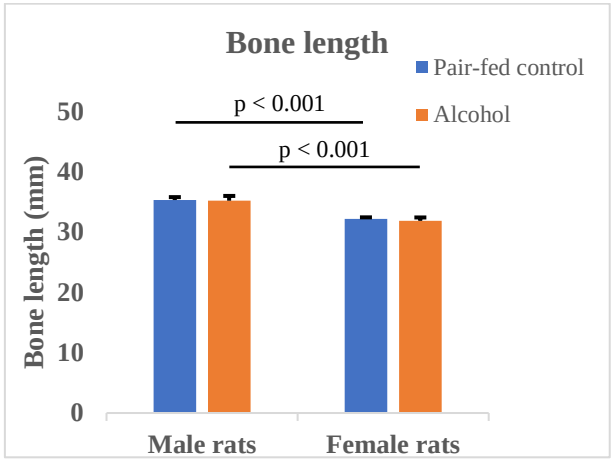


Figure 4.3: Femur length for the chronic binge consumption model. The mean values for the femur length are represented for the alcohol and pair-fed control groups in both male and female rats. Error bars represent standard deviation.

Bicondylar breadth

Bicondylar breadth was similar amongst study groups (Fig 4.4). In male rats, the alcohol (mean = 7.33mm ± 0.22) and the pair-fed control groups (mean = 7.37mm ± 0.15) had a similar bicondylar breadth ($p = 0.721$). This was also observed in female rats, with the alcohol group displaying a similar bicondylar breadth (mean = 6.68mm ± 0.16) to that of the pair-fed control group (mean = 6.77mm ± 0.09) ($p = 0.263$) (Fig 4.4).

Male rats, both pair-fed control (mean = 7.37mm ± 0.15) and alcohol group (mean = 7.33mm ± 0.22) had significantly wider bicondylar breadths compared to female rats' pair-fed control (mean = 6.77mm ± 0.09) and alcohol group (mean = 6.68mm ± 0.16) ($p < 0.001$ for both comparisons) (Fig 4.4).

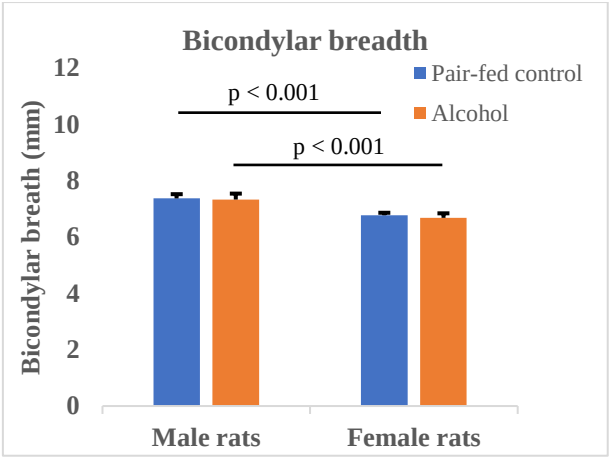


Figure 4.4: Femur bicondylar breadth for the chronic binge consumption model. The mean values for bicondylar breadth are represented for the pair-fed control and alcohol groups. Error bars represent standard deviation.

4.2.6 Femur Trabecular Morphometrics

Femoral bone to total volume ratio (BV/TV)

With regards to bone to total volume ratio (BV/TV), male rats displayed a lower BV/TV in the alcohol group (mean = 60.65% ± 1.31) compared to the pair-fed control group (mean = 66.73% ± 2.36) ($p < 0.001$) (Fig 4.5a). A different pattern was observed in the female rats, with the alcohol group showing a greater BV/TV (mean = 74.71% ± 2.78) than the pair-fed control (mean = 70.83% ± 3.59), in the proximal epiphysis (Fig 4.5a). However, no significance was detected ($p = 0.063$).

Male rats, in both pair-fed control (mean = 66.73% ± 2.36) and alcohol group (mean = 60.65% ± 1.31) appeared to have lesser BV/TV in comparison with female rats' pair-fed control (mean = 70.83% ± 3.59) and alcohol group (mean = 74.71% ± 2.78) ($p = 0.042$ and $p < 0.001$, respectively) (Fig 4.5a).

In the distal epiphysis in male rats the BV/TV was similar between the alcohol group (mean = 27.80% ± 0.04) and the pair-fed control (mean = 28.40% ± 0.04) ($p = 0.800$). Female rats had a marginally lower BV/TV in the alcohol group (mean = 31.90% ± 0.02) compared to the pair-fed control group (mean = 34.40% ± 0.04), however no significance was detected ($p = 0.28$) (Fig 4.5b).

Regarding, pair-fed control groups, male rats had a lesser BV/TV (mean = 28.40% ± 0.04) compared to female rats (mean = 34.40% ± 0.04) ($p < 0.001$). This observation was consistent

in alcohol groups, with male rats (mean = 27.80% ± 0.04) exhibiting lesser BV/TV than female rats (mean = 31.90% ± 0.02) ($p < 0.001$) (Fig 4.5b).

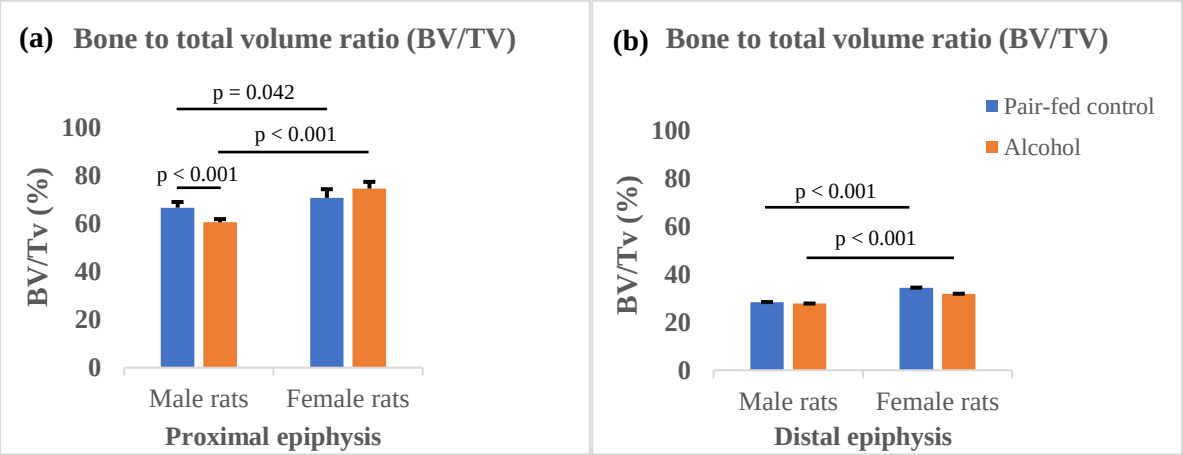


Figure 4.5: Femoral bone to total volume ratio for a chronic binge alcohol consumption model. The mean values for BV/TV are given for both the **(a)**; proximal and **(b)**; distal epiphysis of the pair-fed control and alcohol groups. Error bars represent standard deviation.

Femur trabecular thickness (Tb.Th)

Significant differences in trabecular thickness were detected in the proximal epiphysis amongst study groups. The trabeculae were thinner in the alcohol group (mean = 0.109mm ± 0.005) than the pair-fed control group (mean = 0.131mm ± 0.013) in male rats ($p = 0.005$) (Fig 4.6a). Contrarily, in female rats, the trabeculae was thicker in the alcohol group (mean = 0.173mm ± 0.019) compared to the pair-fed control group (mean = 0.138mm ± 0.026) ($p = 0.040$) (Fig 4.6a).

In pair-fed controls, male rats (mean = 0.131mm ± 0.013) had thinner trabeculae compared to female rats (mean = 0.138mm ± 0.026), however this difference was not statistically significant ($p = 0.597$). Again, the trabecular in male rats exposed to alcohol (mean = 0.109mm ± 0.005) was thinner compared to the female rats' alcohol group (mean = 0.173mm ± 0.019) ($p < 0.001$) (Fig 4.6a).

In the distal epiphysis, the trabecular thickness appeared to be similar in male rats between the alcohol group (mean = 0.079mm ± 0.005) and the pair-fed control (mean = 0.077mm ± 0.005) ($p = 0.561$) (Fig 4.6b). On the contrary, female rats exhibited marginally thinner trabeculae in the alcohol group (mean = 0.080mm ± 0.003) than the pair-fed control group (mean = 0.085mm ± 0.006), but no significance was observed ($p = 0.12$) (Fig 4.6b).

Again, in pair-fed control groups, the trabeculae were thinner in the male rats (mean = 0.077mm ± 0.005) compared to female rats (mean = 0.085mm ± 0.006) (p = 0.04) (Fig 4.6b). Conversely, in rats exposed to alcohol, male rats (mean = 0.079mm ± 0.005) and female rats (mean = 0.080mm ± 0.003) had similar trabecular thickness (p = 0.691) (Fig 4.6b).

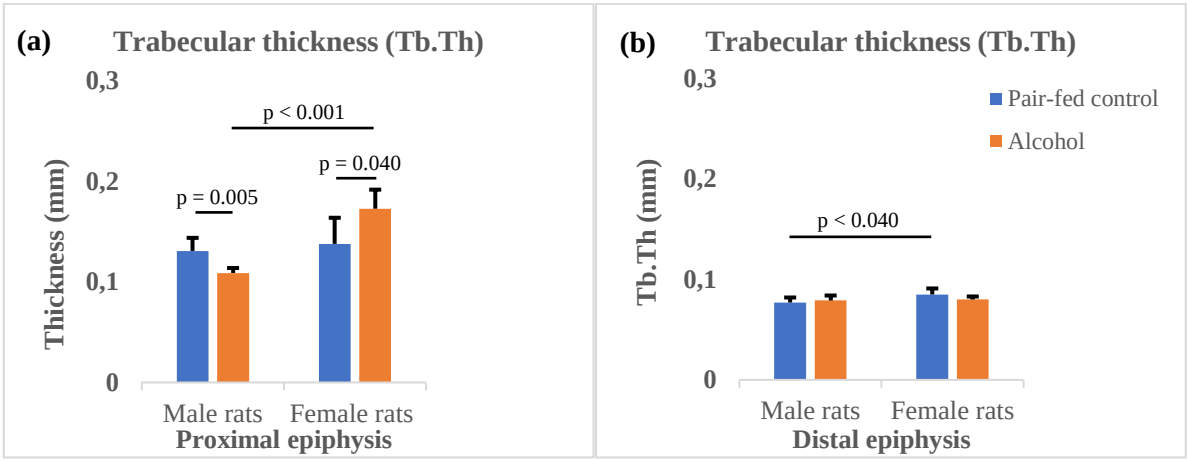


Figure 4.6: Femoral trabecular thickness (Tb.Th) for a chronic binge alcohol consumption model. The mean values for Tb.Th are given for both the **(a)**; proximal and **(b)**; distal epiphysis for the pair-fed control and alcohol groups. Error bars represent standard deviation.

Femur trabecular number (Tb.N)

Regarding the femoral trabecular number in the proximal epiphysis, significant differences were observed amongst study groups. Male rats had significantly fewer trabeculae in the alcohol group (mean = 5.138mm^{-1} ± 0.326) than the pair-fed control (mean = 5.551mm^{-1} ± 0.216) (p =0.030) (Fig 4.7). However, the trabecular number in female rats was significantly greater in the alcohol group (mean = 5.226mm^{-1} ± 0.622) compared to the pair-fed control group (mean = 4.266mm^{-1} ± 0.205) (p = 0.010) (Fig 4.7a).

When comparing pair-fed control groups in the proximal epiphysis, male rats (mean = 5.551mm^{-1} ± 0.216) had a significantly higher trabecular number compared to female rats (mean = 4.266mm^{-1} ± 0.205) (p < 0.001). Conversely, male rats' alcohol group (mean = mean = 5.138mm^{-1} ± 0.326) and female rats' alcohol group (mean = 5.226mm^{-1} ± 0.622) had a similar number of trabeculae (p = 0.688) (Fig 4.7a).

In the distal epiphysis, the male rats exhibited similar number of trabeculae between the alcohol (mean = 3.529mm^{-1} ± 0.315) and the pair-fed control groups (mean = 3.684mm^{-1} ± 0.437) (p = 0.49) (Fig 4.7b). This pattern was also observed in the female rats, with the alcohol (mean =

3.987mm^{-1} ± 0.085) and the pair-fed control group (mean = 4.026mm^{-1} ± 0.438) exhibiting similar trabecular numbers (p = 0.83) (Fig 4.7b).

A comparison across pair-fed control groups, showed male rats (mean = 3.684mm^{-1} ± 0.437) having fewer trabeculae than female rats (mean = 4.026mm^{-1} ± 0.438), however no statistical significance was detected (p = 0.691) (Fig 4.7b). Similarly, across alcohol groups, male rats (mean = 3.529mm^{-1} ± 0.315) had fewer trabeculae compared to female rats (mean = 3.987mm^{-1} ± 0.085). This difference was significant (p = 0.008) (Fig 4.7b).

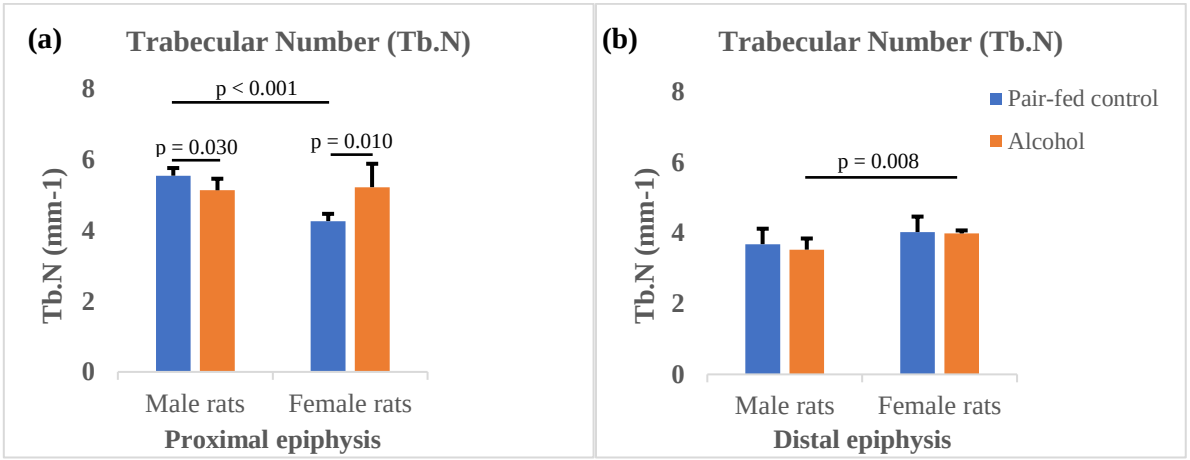


Figure 4.7: Femoral trabecular number (Tb.N) for a chronic binge alcohol consumption model. The mean values for Tb.N are given for both the **(a)**; proximal and **(b)**; distal epiphysis for the pair-fed control and alcohol groups. Error bars represent standard deviation.

Femur trabecular spacing (Tb.Sp)

The trabecular spacing in the proximal epiphysis of male rats was wider in the alcohol group (mean = 0.071mm ± 0.003) than the pair-fed controls (mean = 0.065mm ± 0.001) (p < 0.001) (Fig 4.8a). However, the trabecular spacing appeared to be similar in female rats, between the alcohol group (mean = 0.058mm ± 0.003) and the pair-fed control group (mean = 0,056mm ± 0.004) (p = 0.37) (Fig 4.8a).

Male rats, both pair-fed control (mean = 0.065mm ± 0.001) and alcohol group (mean = 0.071mm ± 0.003) had wider trabecular spacing, in comparison to female rats' pair-fed control (mean = 0,056mm ± 0.004) and alcohol group (mean = 0.058mm ± 0.003), respectively (p < 0.001 for both differences) (Fig 4.8a).

In the distal epiphysis, male rats showed a similar pattern to that of the proximal epiphysis, with the alcohol group (mean = 0.207mm ± 0.027) exhibiting wider trabeculae compared to the pair-fed control group (mean = 0.197mm ± 0.030) (Fig 4.8b). However, this difference was not significant (p = 0.590). Again, the trabecular spacing appeared to be similar in female rats between the alcohol (mean = 0.171mm ± 0.008) and the pair-fed control groups (mean = 0.166mm ± 0.029) (p = 0.684) (Fig 4.8b).

Regarding pair-fed control groups, no difference in trabecular spacing was detected between male rats (mean = 0.197mm ± 0.030) and female rats (mean = 0.166mm ± 0.029) (p = 0.116). However, male rats' alcohol group (mean = 0.207mm ± 0.027) had significantly wider trabecular spacing compared to female rats' alcohol group (mean = 0.171mm ± 0.008) (p = 0.012) (Fig 4.8b).

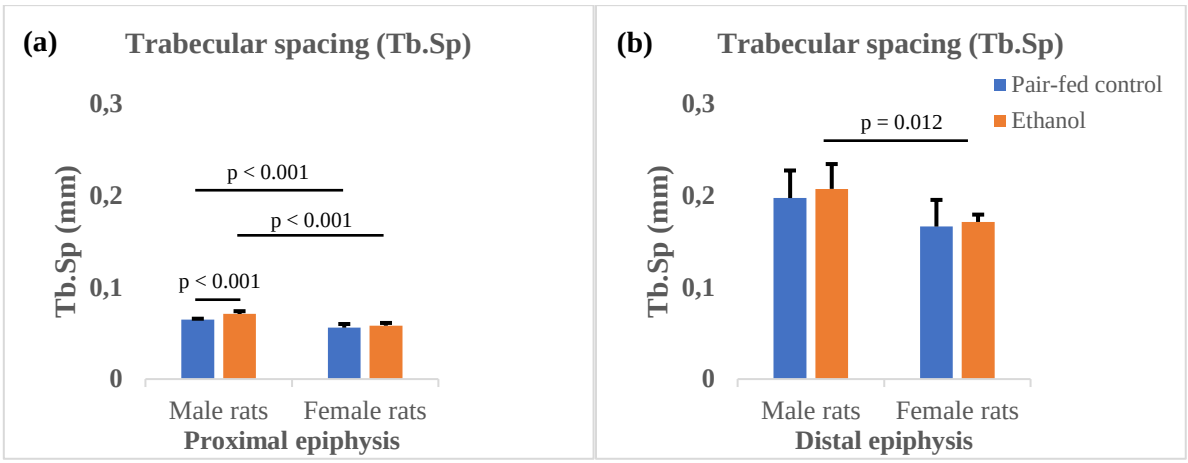


Figure 4.8: Femoral trabecular spacing (Tb.Sp) for a chronic binge alcohol consumption model. The mean values for Tb.Sp are given for both the **(a)**; proximal and **(b)**; distal epiphysis for the pair-fed control and alcohol groups. Error bars represent standard deviation.

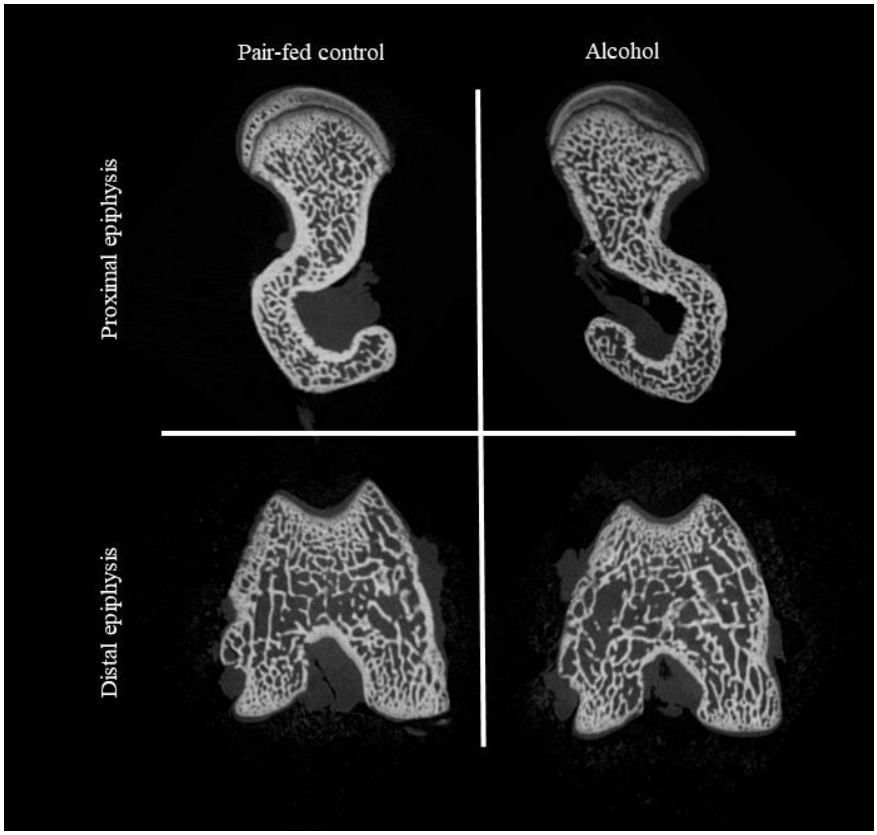


Figure 4.9: Trabecular morphology in the proximal and distal ends of femora for the pair-fed control and alcohol groups in male rats. Representative slices, show a lower BV/TV thinner trabecula, and a decrease in trabecular number, with wider trabecular spaces in the alcohol group, compared to the pair-fed control. In the distal epiphysis, similar trabecular morphometry is observed between the two groups.

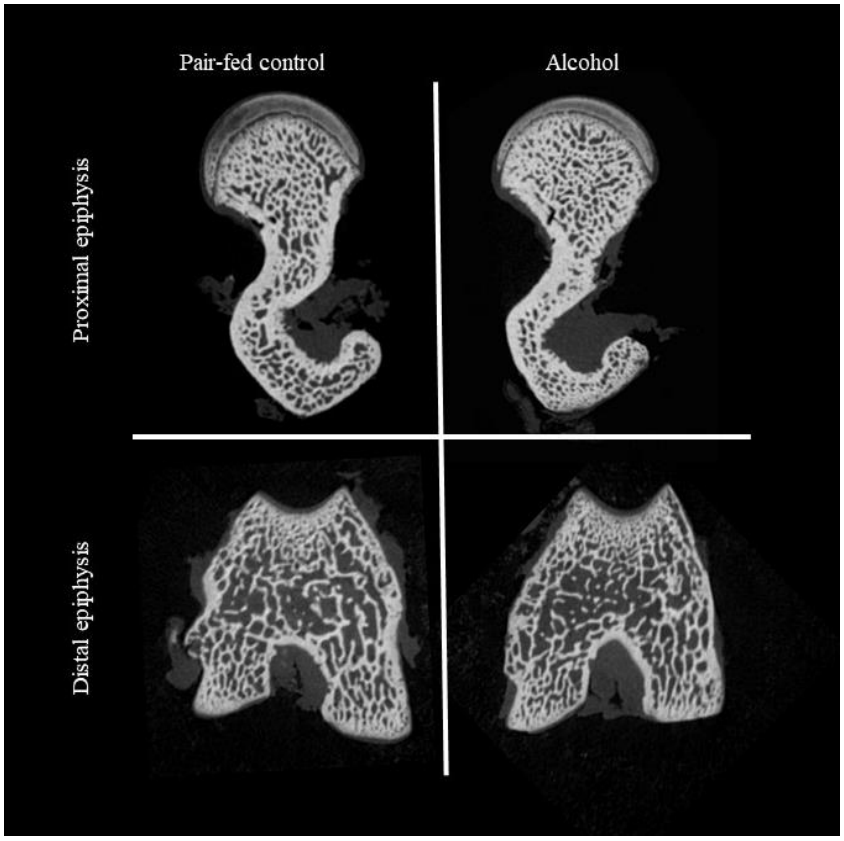


Figure 4.10: Trabecular morphology in the proximal and distal ends of femora for the pair-fed control and alcohol groups in female rats. Representative slices, show thickener trabeculae (Tb.Th) and a greater number of trabeculae (Tb.N) in the proximal epiphysis of the alcohol group. In the distal extremity, no significant difference in trabecular morphometry is observed between the alcohol and pair-fed control groups.

4.2.7 Femur cross-sectional area, medullary canal area and cortical area

25th percentile mark (proximal)

In the male rats, both the cross-sectional area (CSA) and medullary canal (MCA) were lower in the alcohol group (CSA mean =14.937mm^2 ± 0.892 and MCA mean = 5.182mm^2 ± 0.658) compared to the pair-fed control group (CSA mean = 15.796mm^2 ± 2.366 and MCA mean = 5.838mm^2 ± 0.557), however no significance was detected (p = 0.430 and 0.090, respectively) (Fig 4.11a,b) The cortical area (CA) was also marginally lower in the alcohol group (mean = 9.756mm^2 ± 0.580) than the pair-fed control group (mean = 9.958mm^2 ± 1.876) (Fig 4.11c). Again, this difference was not significant (p = 0.800).

A different pattern was observed in female rats, with the alcohol group displaying marginally higher CSA (mean = 11.980mm^2 ± 1.300) and MCA (mean = 3.801mm^2 ± 0.556) compared to the pair-fed control (CSA mean = 11.464mm^2 ± 0.588 and MCA mean = 3.230mm^2 ± 0.250) (Fig 4.14a,b). However, no significance was detected (p = 0.441 and 0.060, respectively). This

was also observed in the CA, with the alcohol (mean = 8.178mm^2 ± 0.803) and the pair-fed control (mean = 8.235mm^2 ± 0.588) (p = 0.90) (Fig 4.11c).

Regarding pair-fed controls, male rats had significantly higher CSA (mean = 15.796mm^2 ± 2.366) and MCA (mean = 5.838mm^2 ± 0.557) compared to female rats' CSA (mean =11.464mm^2 ± 0.588) and MCA (mean = 3.230mm^2 ± 0.250) (p = 0.001 and p < 0.001, respectively) (Fig 4.11a,b). The cortical area was found to be higher in male pair-fed control (mean = 9.958mm^2 ± 1.876) than female pair-fed control group (mean = 8.235mm^2 ± 0.588), however this difference was not statistically significant (p = 0.057) (Fig 4.11c). Across alcohol groups, male rats had significantly higher CSA (mean = 14.937mm^2 ± 0.892), MCA (mean = 5.182mm^2 ± 0.658) and CA (mean = 9.756mm^2 ± 0.580) than female rats' CSA (mean =11.980mm^2 ± 1.300), MCA (mean = 3.801mm^2 ± 0.556), and CA (mean = 8.178mm^2 ± 0.803). These differences were statistically significant (p < 0.001, p = 0.003 and p = 0.003, respectively) (Fig 4.11).

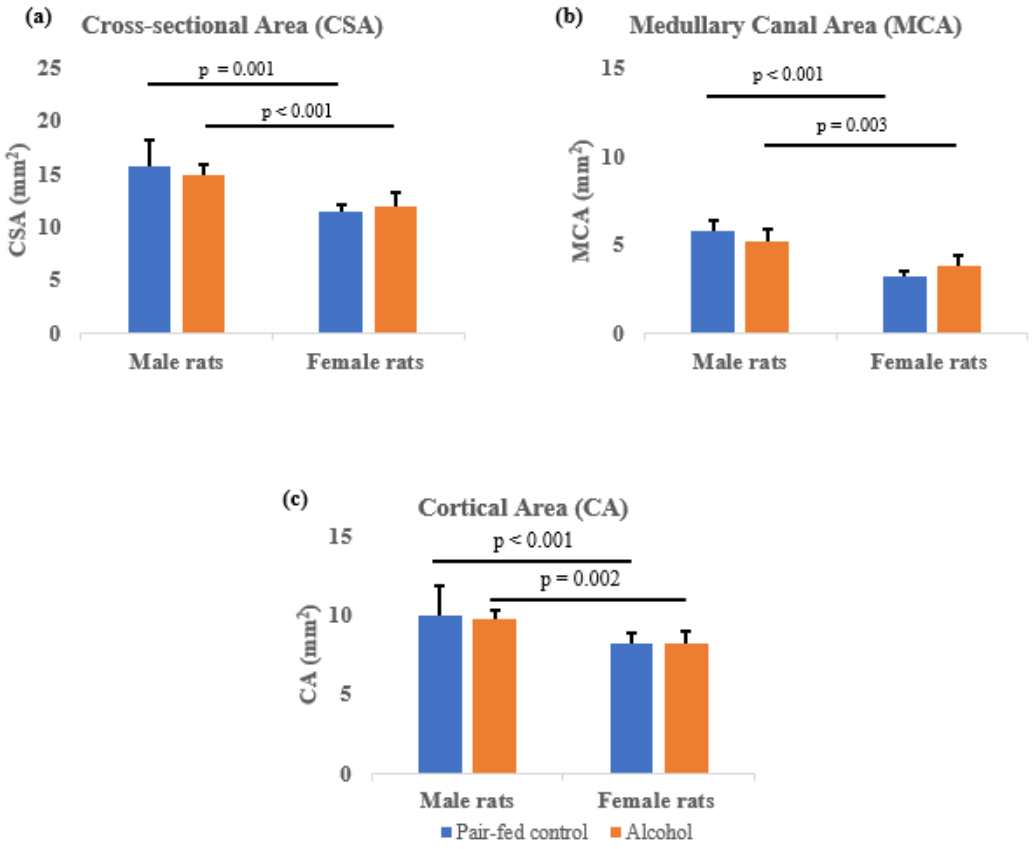


Figure 4.11: 25th percentile mark (proximal) dimensions of the femoral shaft. The mean **(a)**; cross-sectional area (CSA), **(b)**; medullary canal area (MCA) and **(c)**; cortical area (CA) are shown for the two groups studied in both male and female rats. Error bars represent standard deviation.

50^{th} percentile mark (midshaft)

The cortical dimensions in the midshaft of the femur showed no differences amongst study groups. In male rats, the alcohol group had a similar CSA (mean = 12.917mm^2 ± 1.228), MCA (mean = 5.228mm^2 ± 0.692), and CA (mean = 7.689mm^2 ± 0.543) to the pair-fed control group (CSA mean =13.037mm^2 ± 1.723; MCA mean =5.297mm^2 ± 0.593; CA mean = 7.740mm^2 ± 1.196) (p = 0.84; 0.86 and 0.93, respectively) (Fig 4.12). The trend continued in the female rats, with the alcohol group exhibiting similar CSA (mean = 10.567mm^2 ± 0.948), MCA (mean = 4.556mm^2 ± 0.629) and CA (mean = 6.011mm^2 ± 0.331) values to the pair-fed control group's CSA (mean = 9.782mm^2 ± 0.348), MCA (mean = 4.063mm^2 ± 0.239) and CA (mean = 5.719mm^2 ± 0.267) (p = 0.120; 0.141 and 0.163, respectively)(Fig 4.12).

With respect to pair-fed controls, a group comparison showed that male rats had significantly higher CSA (mean = 13.037mm^2 ± 1.723) and MCA (mean = 5.297mm^2 ± 0.593) in comparison to female rats' CSA (mean = 9.782mm^2 ± 0.348) and MCA (mean = 4.063mm^2 ± 0.239) (p = 0.001 and p < 0.001, respectively) (Fig 4.12). Similarly, the male rats' pair-fed control had a higher cortical area (mean = 7.740mm^2 ± 1.196) than that of the female rats' pair-fed control (mean = 5.719mm^2 ± 0.267) (p = 0.002). Similar to group comparisons observed in pair-fed control groups, male rats appeared to have higher CSA (mean = 12.917mm^2 ± 1.228) and CA (mean = 7.689mm^2 ± 0.543) than female rats' CSA (mean = 10.567mm^2 ± 0.948) and CA (mean = 6.011mm^2 ± 0.331) in alcohol exposed animals (p = 0.001 and p < 0.001, respectively) (Fig 4.12a,c). The MCA was also found to be higher in male alcohol groups (mean = 5.228mm^2 ± 0.692) compared to female rats (mean = 4.556mm^2 ± 0.629), however, no statistical significance was detected (p = 0.109) (Fig 4.12b).

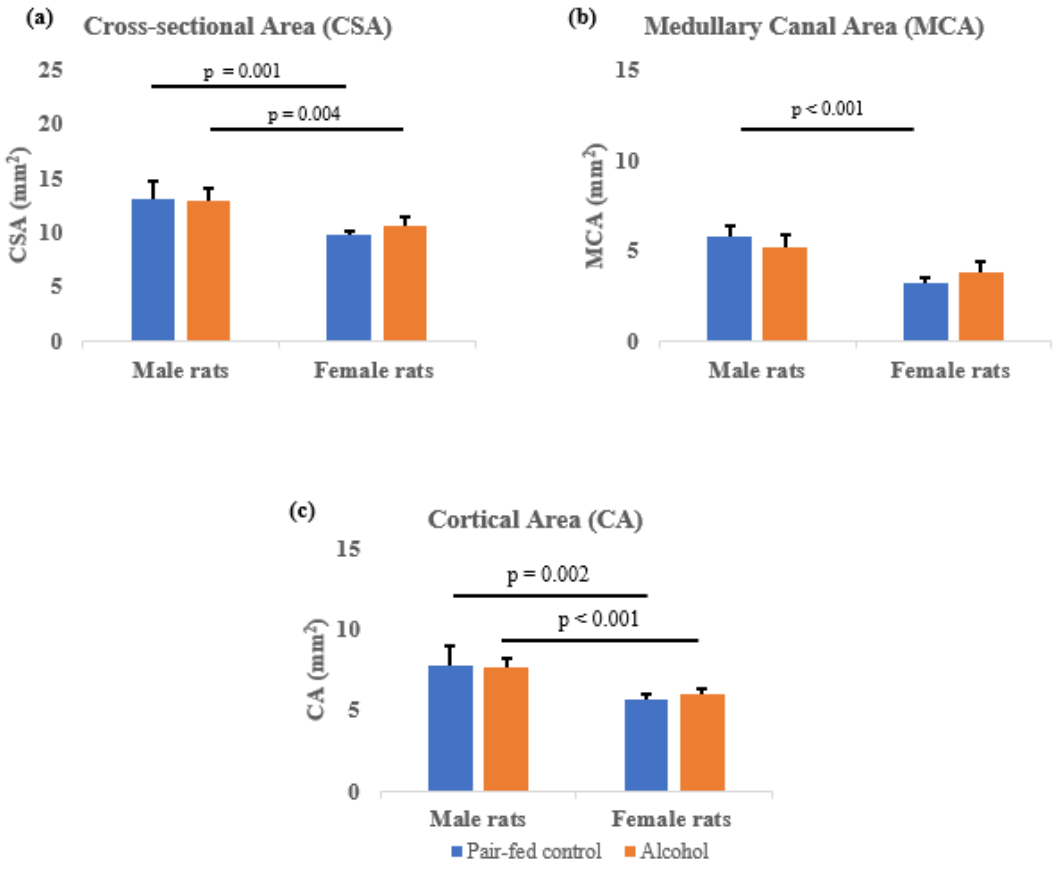


Figure 4.12: 50th percentile mark (midshaft) dimensions of the femoral shaft. The mean **(a)**; cross-sectional area (CSA), **(b)**; medullary canal area (MCA) and **(c)**; cortical area (CA) are shown for the two groups studied in both male and female rats. Error bars represent standard deviation.

75th percentile mark (distal)

The cortical dimensions in the distal region of the bone were similar amongst groups. In male rats, the alcohol group's CSA (mean =18.251mm^2 ± 2.015), MCA (mean = 11.400mm^2 ± 1.684) and CA (mean = 6.852mm^2 ± 0.335) values and the pair-fed control group's CSA (mean = 18.252mm^2 ± 2.056), MCA (mean = 11.490mm^2 ± 1.698) and CA (mean = 6.761mm^2 ± 0.439) values were similar (p = 0.411; 0.673 and 0.111, respectively) (Fig 4.13). In female rats, the alcohol group had a higher CSA (mean = 14.378mm^2 ± 1.446) and MCA (mean = 8.450mm^2 ± 1.235) compared to the pair-fed control group's CSA (mean = 13.770mm^2 ± 0.839) and MCA (mean = 8.057mm^2 ± 0.570), however no significance was detected (p = 0.441 and 0.546, respectively) (Fig 4.13a,b). Again, the cortical area was similar between the alcohol (mean = 5.928mm^2 ± 0.251) and the pair-fed control (mean = 5.713mm^2 ± 0.276) (p = 0.23) (Fig 4.13c).

Regarding pair-fed controls, male rats had significantly higher CSA (mean = 18.252 mm^2 ± 2.056), MCA (mean = 11.490mm^2 ± 1.698) and CA (mean = 6.761mm^2 ± 0.439) compared to female rats' CSA (mean =13.770mm^2 ± 0.839), MCA (mean = 8.057mm^2 ± 0.570) and CA (mean = 5.713mm^2 ± 0.276) ($p < 0.001$ for all differences) (Fig 4.13). This pattern continued in alcohol groups, with male rats exhibiting higher CSA (mean = 18.251mm^2 ± 2.015), MCA (mean = 11.400mm^2 ± 1.684) and CA (mean = 6.852mm^2 ± 0.335) than female rats' CSA (mean =14.378mm^2 ± 1.446), MCA (mean = 18.450mm^2 ± 1.235), and CA (mean = 5.928mm^2 ± 0.251). These differences were statistically significant ($p = 0.003$, $p = 0.006$ and $p < 0.001$, respectively) (Fig 4.13).

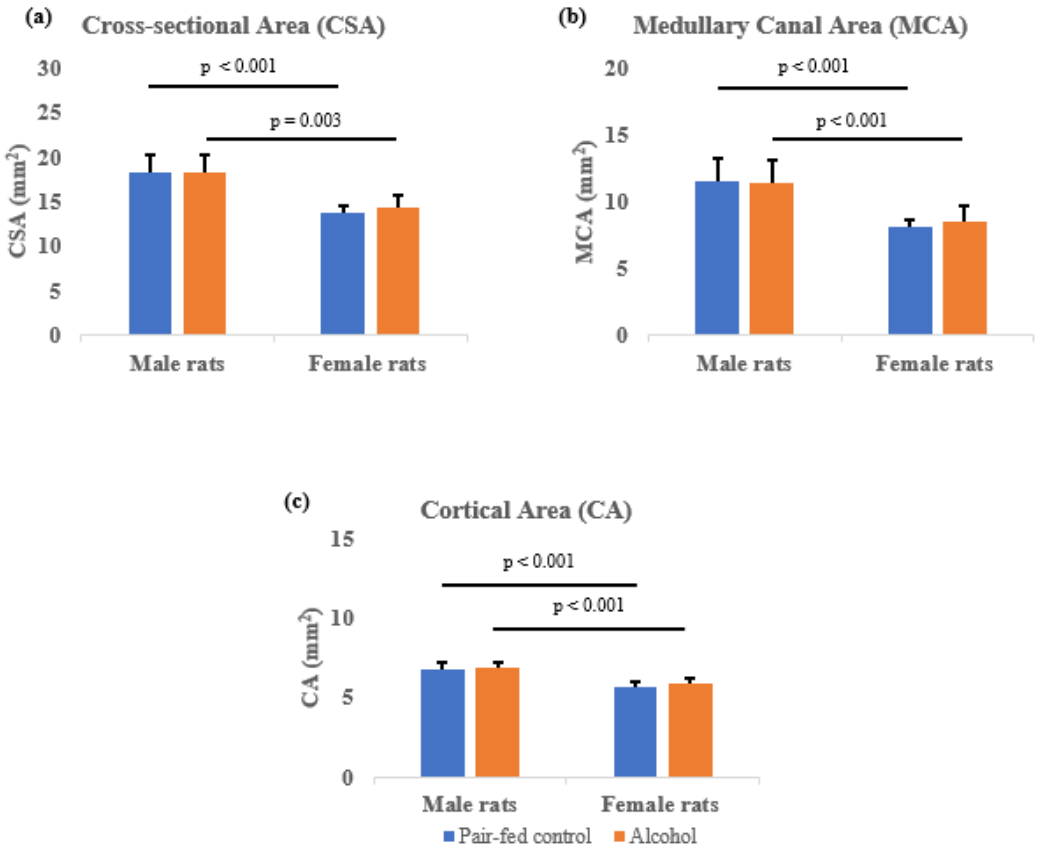


Figure 4.13: 75th percentile mark (distal) dimensions of the femoral shaft. The mean **(a)**; cross-sectional area (CSA), **(b)**; medullary canal area (MCA) and **(c)**; cortical area (CA) are shown for the two groups studied in both male and female rats. Error bars represent standard deviation.

4.2.8 Three-point bend testing of the femur, tensile strength assessment

In the chronic binge alcohol consumption model, no significant difference in bone weight was observed in male rats between the alcohol and pair-fed control groups ($p = 0.230$) (Table 4.1). This observation was also consistent in female rats, with the alcohol group and pair-fed control group exhibiting similar bone weight (Table 4.2) ($p = 0.443$).However, bone weight appeared to be higher in male rats, for both the pair-fed control group and alcohol group, in comparison to female pair-fed control ($p = 0.014$ and $p < 0.001$, respectively).

Regarding bone tensile strength parameters in male rats, the maximum force and maximum displacement were similar between the alcohol and the pair-fed control group ($p = 0.94$ and 0.72, respectively). The maximum time and break force were also similar between the alcohol and the pair-fed controls ($p = 0.72$ and 0.97 respectively) (Table 4.1).

In female rats, the maximum force and maximum displacement were significantly higher in the alcohol group compared to the pair-fed control group in the female rats ($p = 0.04$ and 0.02, respectively) (Table 4.2). The alcohol group also had greater maximum time and break force values than the pair-fed control group ($p = 0.020$ and $p = 0.040$ respectively) (Table 4.2).

When comparing tensile strength parameter across pair-fed groups, male rats had significantly higher maximum force, maximum displacement, and maximum time than female rats ($p = 0.004$, $p = 0.014$ and $p = 0.014$, respectively). This pattern was also observed in the break force, with male rats exhibiting a higher force compared to female rats. Again, this difference was significant ($p = 0.004$). Contrarily, across alcohol exposed groups, tensile strength remained similar between male rats and female rats.

Table 4.1: Weight measurements and tensile strength parameters of the male rat femur.

Parameter		*n*	*Mean*	*SD*
Bone weight (g)	Pair-fed control	6	0.995	0.062
	Alcohol	6	0.997	0.103
Maximum force (N)	Pair-fed control	6	121.389	11.945
	Alcohol	6	120.897	7.959
Maximum displacement (mm)	Pair-fed control	6	1.082	0.158
	Alcohol	6	1.050	0.139
Maximum time (sec)	Pair-fed control	6	21.627	3.168
	Alcohol	6	20.988	2.789
Break force	Pair-fed control	6	120.144	13.062
	Alcohol	6	119.144	7.433

Table 4.2: Weight measurements and tensile strength parameters of the female rat femur

Parameter		*n*	*Mean*	*SD*
Bone weight (g)	Pair-fed control	6	0.756	0.186
	Alcohol	6	0.733	0.056
Maximum force (N)	Pair-fed control	6	102.376	4.138
	Alcohol	6	110.045	6.507
Maximum displacement (mm)	Pair-fed control	6	0.870	0.075
	Alcohol	6	1.089	0.172
Maximum time (sec)	Pair-fed control	6	17.388	1.501
	Alcohol	6	21.778	3.445
Break force	Pair-fed control	6	100.004	3.87
	Alcohol	6	107.122	8.026

4.2.9 Morphological assessment of the femoral epiphyseal growth plate.

Male study group

Differences were observed in the morphology of the proximal epiphyseal growth plate between the alcohol and pair-fed control groups. The alcohol group exhibited a disoriented proximal growth plate displaying irregular chondrocytes, which were dispersedly arranged, compared to the pair-fed control group which showed distinct chondrocyte columns, in the proliferative zone (Fig 4.14). Furthermore, the alcohol group appeared to have a diminished resting zone as well as a diminished hypertrophic zone, whereas in the pair-fed control group, these zones were distinctively unaffected. Nonetheless, both groups exhibited provisional calcified cartilage on both ends of the growth plate (Fig 4.14).

No distinct morphological differences were observed in the distal epiphyseal plate between the two groups, except for a decrease in chondrocyte density observed in the alcohol group. Both groups exhibited clearly defined zones within the growth plate (resting, proliferative, and hypertrophic), and a uniform arrangement of chondrocyte columns was observed (Fig 4.14). Furthermore, calcified cartilage (bone) was visible at both the epiphyseal and metaphyseal ends in both groups.

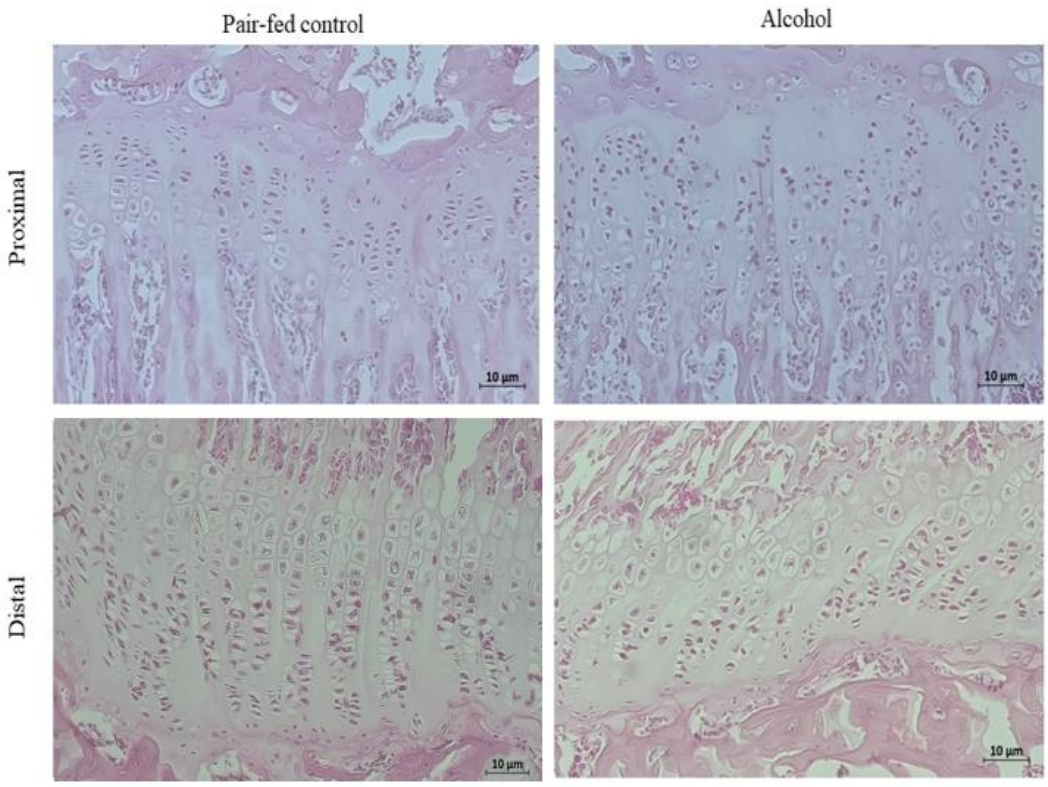


Figure 4.14: Haematoxylin and Eosin-stained longitudinal sections of both the proximal and distal epiphyseal growth plates of femora for the two study groups in male rats.

Female study group

Similar to the male rats, morphological differences in the proximal epiphysis were also observed in female rats. The pair-fed control group showed a slightly disoriented proximal growth plate, evident by few chondrocytes, which were dispersedly arranged, compared to the alcohol group which showed distinct chondrocyte columns, in the proliferative zone (Fig 4.15). In addition, the alcohol group appeared to have round chondrocytes and provisional calcified bone on the proximal end, whereas the pair-fed control group had provisional calcified bone on both ends of the growth plate (Fig 4.15).

In the distal epiphyseal plate, no clear differences were observed as the alcohol and pair-fed controls exhibited a similar morphology. Both groups had well defined growth plate zones (resting, proliferative and hypertrophic), with consistent chondrocyte column arrangements (Fig 4.15). Additionally, the presence of bone (calcified cartilage) was evident at both the distal and the proximal ends in both groups.

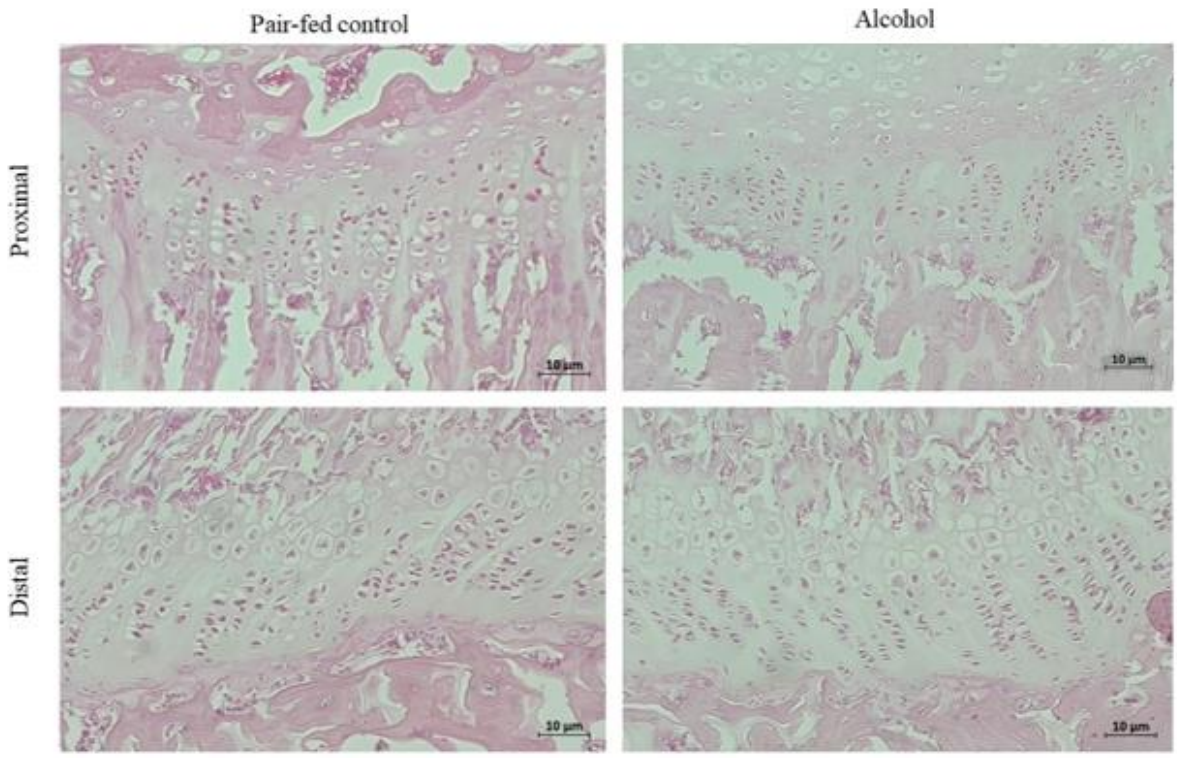


Figure 4.15: Haematoxylin and Eosin-stained longitudinal sections of both the proximal and distal epiphyseal growth plates of femora for the two study groups in female rats

4.2.10 Proliferative zone Ki-67 immuno-positive chondrocyte number

In the proximal growth plate, the alcohol group (mean = 436 ± 89) appeared to have significantly fewer Ki-67 positively stained chondrocytes in the proliferative zone than the pair-fed control (mean = 569 ± 99) in male rats (p = 0.030) (Fig 4.16a). Contrarily, female rats had an increase in the number of proliferative chondrocytes in the alcohol group (mean = 515 ± 59) than in the pair-fed control group (mean = 497 ± 33). However, this difference was not significant (p = 0.529) (Fig 4.16a).

Regarding pair-fed control groups, male rats (mean = 569 ± 99) appeared to have more proliferating chondrocytes compared to female rats (mean = 497 ± 33), in the proximal epiphyseal growth plate. However, this difference was not statistically significant (p = 0.122) (Fig 4.16a). Contrarily, across alcohol groups, fewer number of proliferative chondrocytes were detected in male rats (mean = 436 ± 89) compared to female rats (mean = 515 ± 59). Again, no statistical significance was detected (p = 0.100) (Fig 4.16a).

In the distal epiphyseal growth plate, male rats had similar numbers of Ki-67 immuno-positive chondrocytes between the alcohol group (mean = 497 ± 33) and the pair-fed control group (mean = 513 ± 29) (p = 0.393) (Fig 4.16b). This pattern continued in female rats, with both the

alcohol group (mean = 599 ± 29) and the pair-fed control group (mean = 581 ± 32) having similar numbers of proliferating chondrocytes in the proliferative zone (p = 0.331) (Fig 4.16b).

Both male rats' pair-fed control (mean = 513 ± 29) and alcohol group (mean = 497 ± 33) had fewer number of proliferative chondrocytes than the female rats' pair-fed control (mean = 581 ± 32) and alcohol group (mean = 599 ± 29) (p = 0.003 and p < 0.001, respectively) (Fig 4.16b).

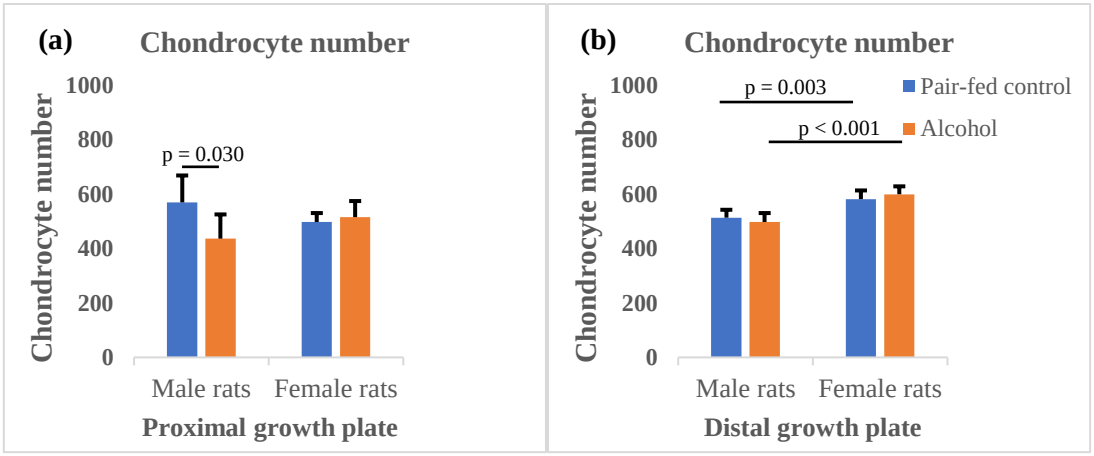


Figure 4.16: Femoral epiphyseal growth plate proliferative zone number of chondrocytes. The mean values are shown for the proliferative zone in the **(a);** proximal and **(b);** distal epiphyseal growth plate for the pair-fed control and the alcohol groups in both male and female rats. Error bars represent standard deviation.

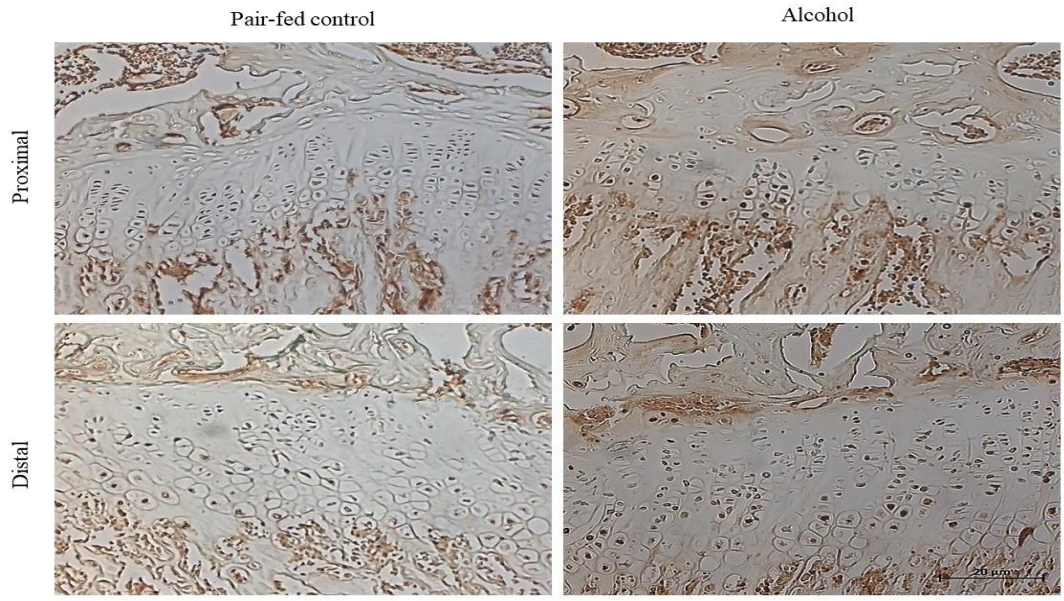


Figure 4.17: Photomicrographs depicting immunolabeled femur chondrocytes using the anti-Ki-67 antibody. The images represent the proximal and distal epiphyseal growth plates for the pair-fed control and alcohol groups in male rats. Scale bar = 20 microns and applies to all images.

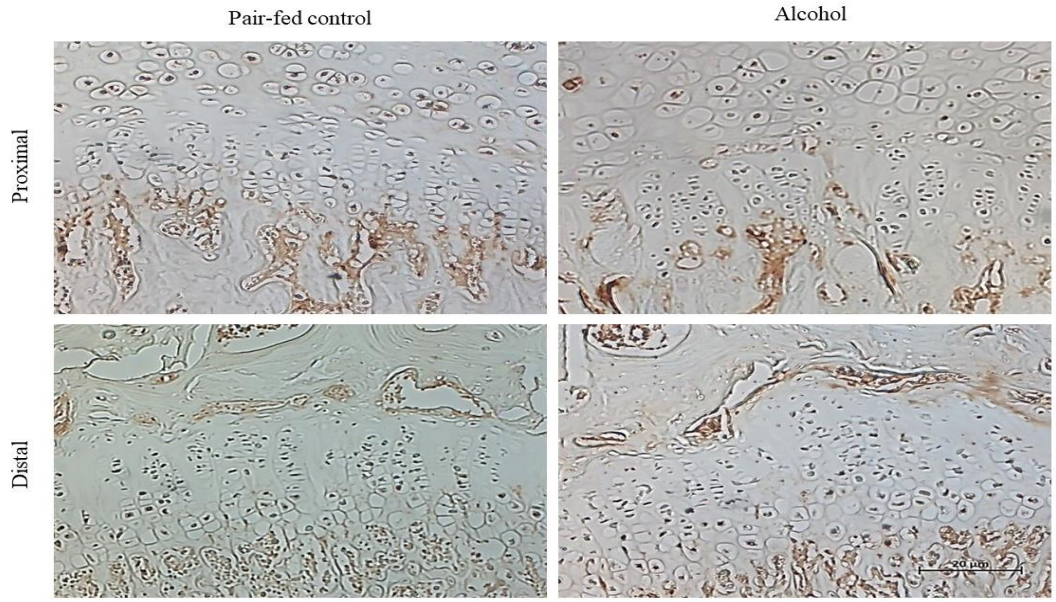


Figure 4.18: Photomicrographs depicting immunolabeled femur chondrocytes using the anti-Ki-67 antibody. The images represent the proximal and distal epiphyseal growth plates for the pair-fed control and alcohol groups in female rats. Scale bar = 20 microns and applies to all images.

4.3 DISCUSSION

The current study sought to investigate whether chronic binge alcohol consumption affects the growth and development of the femur in adolescent Sprague Dawley rats. We employed micro focus X-ray computed tomography to assess trabecular morphometry in the proximal and distal epiphysis of the femur, osteometric parameters and evaluated cortical dimensions. Histological and immunohistochemical techniques were utilized to investigate the effects of chronic binge alcohol consumption on the overall morphology of the growth plate and the proliferation of chondrocytes in the proliferative zone. Furthermore, we conducted three-point bending tests using a universal bending machine to determine the tensile strength of the bones. The current study established disturbances in the trabecular morphometry of the proximal epiphysis in male rats, whereas trabecular spacing and trabecular number appeared to have improved after chronic binge alcohol consumption in female rats. In the distal epiphysis, the trabecular morphometry remained unaffected in both male and female rats. Osteometric measurements were also unaffected by chronic binge alcohol consumption. This was consistent across male and female rats. The study observed a decrease in proliferation of chondrocytes in the proximal epiphysis of the femur in male rats, while the distal epiphyseal growth plate remained unaffected. Again, no harmful effects of alcohol were seen in the female rats with regards to chondrocyte proliferation. While tensile strength remained unaffected in male rats, our study revealed improved bone tensile strength in female rats following alcohol consumption.

Food consumption and body weight gained.

With regards to the percentage of weight gained and daily food consumed by study animals, the current study revealed no significant difference between alcohol and pair-fed control groups, in both male and female rats. We anticipated a decrease in weight gained or a decrease in food consumption following chronic binge alcohol consumption, as previously demonstrated by Lauing and colleagues (2008) however this was not seen in the current study. Although, the study conducted by Lauing et al (2008) and our study administered a similar chronic binge alcohol dosage the difference in findings may be attributed to the differences in the vehicle used for treatment amongst study animals. In our study, alcohol was administered via oral gavage, whereas Lauing and colleagues (2008), employed intraperitoneal injection for delivering alcohol (Lauing et al., 2008). It has been reported that the latter technique may not

replicate the same pathological responses observed with oral administration of alcohol (Turner et al., 2012). The lack of difference in daily food consumption may be explained by the isocaloric intake between the groups (4.2Kcal per kilogram body weight), thus eliminating the potential effects of additional calories in alcohol (7.1Kcal per gram of alcohol). In agreement with this, Callaci et al. (2006), found no significant difference in food intake between the alcohol exposed group (3 g/kg alcohol as a 20% weight to volume alcohol) and the isocaloric control group, however these were significantly different from the saline control group (Callaci et al., 2006). The dose used in our study may have been too low to have an adverse effect on weight and food consumption.

Femur Osteometrics

Based on our findings, the chronic binge alcohol consumption model did not lead to any significant differences in length and bicondylar breadth of the femur in both male and female rats. While we were unable to find comparable studies on the bicondylar breadth of the femur, research investigating the effect of alcohol on the length of long bones (Nwaogu, 2002; Simpson et al., 2005, 1996; Snow and Keiver, 2007; Wezeman et al., 1999) reported a reduction in length in the alcohol-exposed groups. The difference in findings could be attributed to the dosage of alcohol administered to the rats. In the current study, we used 20% alcohol at 3g/kg bodyweight, whereas other studies used higher concentrations ranging from 30% to 36% in their studies (Nwaogu, 2002; Simpson et al., 2005, 1996; Snow and Keiver, 2007). Furthermore, there appears to be a link between the severity of alcohol's impact on bones and the duration of exposure, with longer periods of alcohol intake resulting in more detrimental effects on bone health (Turner et al., 2001; Wezeman et al., 1999). Taken together, the current study suggests that chronic binge alcohol consumption, as administered in our study, may not possess sufficient potency to elicit changes on the osteometry of the adolescent femur seen in previous research (Simpson et al., 2005, 1996; Snow and Keiver, 2007; Wezeman et al., 1999).

Femur Trabecular Morphometrics

Chronic binge alcohol drinking perturbs the trabecular morphometry, we found alterations in the proximal epiphysis of male rats. The current study found a decrease in bone tissue volume (BV/TV), thinner trabeculae (Tb.Th) and fewer trabeculae number (Tb.N), which were wider spaced (Tb.Sp). Our findings are consistent with previous research on both young actively

growing and adult rats (Lauing et al., 2008; Maddalozo et al., 2009; Sampson et al., 1996, 1997; Turner et al., 2001), which demonstrated alterations such as reduction in bone volume area and the thinning of the trabeculae, following alcohol consumption. These authors reported effects of alcohol on bone trabeculae particularly in the proximal epiphysis of the tibiae (Maddalozo et al., 2009; Sampson et al., 1996, 1997; Turner et al., 2001). Our study found alterations in the proximal epiphysis of the femur with no detrimental effects in the distal epiphysis of the femur in male rats, indicating that alcohol is likely to have a site-specific effect in different bones.

With regards to female rats, the trabecular morphometry remained unaffected in both the proximal and distal epiphyses of the adolescent femur, following chronic binge alcohol consumption. However, there was an exception noted in the proximal epiphysis, where the trabecular number and trabecular spacing were significantly enhanced in female rats. Hormonal fluctuations inherent in female rats may have potentially influenced the response of trabecular bone to chronic binge alcohol consumption. Hormones such as oestrogen play a crucial role in maintaining bone health and their protective effects could potentially have masked any detrimental effects of alcohol on trabecular morphometry (Manolagas et al., 20013; Turner, 2001). Furthermore, the timing of the study in relation to the female rat's oestrous cycle might have also played a role in influencing the outcomes observed in the current study.

Femur cross-sectional area, medullary canal area and cortical area

The cortical dimensions such as cross-sectional area, medullary canal area and cortical area remained unaffected in both male and female rats following chronic binge alcohol consumption. This finding differs with the previous research conducted by Hogan et al. (1997), where alcohol consumption resulted in modifications in cortical bone area and marrow area after a 4-week treatment period (Hogan et al., 1997). Despite the similarity in the duration of alcohol exposure between our study and Hogan et al. (1997), the difference in findings could be attributed to the varying alcohol dosages administered. Hogan et al. (1997) administered alcohol through a modified Lieber-DeCarli diet ad libitum, containing 35% alcohol-derived calories (Hogan et al., 1997). In contrast, our study involved the administration of 20% vol/vol alcohol via oral gavage. This discrepancy in dosage might account for the different results. This may suggest that that higher alcohol dosages could potentially have significant effects on the cortical dimensions of the femur.

Three-point bend testing of the femur

Alcohol did not affect bone weight in male rats in our study, this is not in agreement to previous reports which reported a decrease in bone weight. This finding maybe attributed to the amount of alcohol that was administered in our study in comparison to previous reports (Callaci et al., 2006, Lauing et al., 2008, Wezeman et al., 2007). While no comparable studies addressing maximum displacement and maximum time were found, in the current study maximum force and break force remained unaffected. This finding disagrees with a previous investigation conducted by Hogan et al. (1997), in their study, alcohol consumption led to reduced maximum force and break force across various time periods (2, 4, 6, and 8 weeks) (Hogan et al., 1997). This discrepancy in findings may be attributed to the varying alcohol dosages administered. Hogan et al. (1997) employed a modified Lieber-DeCarli diet ad libitum, which contained 35% alcohol-derived calories. Conversely, our study utilized 20% vol/vol alcohol administered via oral gavage. This discrepancy in dosage and duration of alcohol may account for the different findings in studies.

In female adolescent rats, the chronic binge alcohol consumption model resulted in reduced bone weight and enhanced tensile strength parameters. This finding contradicts the findings of previous research (Hogan et al., 1997), that reported adverse impacts of alcohol on these tensile strength parameters. Our study revealed greater maximum force, maximum displacement, maximum time, and break force in female animals exposed to alcohol, thus suggesting enhanced bone strength. These findings may suggest that chronic binge alcohol consumption in female rats either accelerates bone growth or triggers a protective mechanism to counter alcohol's detrimental effects on bone health. A similar phenomenon has been noted in postmenopausal women, where research has revealed a positive correlation between light to moderate alcohol consumption and a reduction in fracture risk (Turner and Sibonga, 2001; Turner, 2000).

Cell morphology of the epiphyseal growth plate

Male study groups

A disrupted cyto-architecture was observed in the proximal epiphyseal growth plate following chronic binge alcohol consumption. The ethanol group exhibited irregular chondrocytes which appeared to be dispersedly arranged. A diminished hypertrophic and resting zone were also

observed. This observation is consistent with those reported by Miralles-Flores and Delgado-Baeza (1992) following alcohol consumption. A disturbed morphology in the proximal epiphyseal growth plate could also explain morphological disturbances observed in the trabeculae of the proximal epiphysis.

Regarding the distal epiphyseal growth plate, minor differences were observed, where the chondrocyte density appeared to be lower in the alcohol group compared to the pair-fed control group. Despite the lower count of chondrocytes in the alcohol group, both the resting zone and the hypertrophic zone remained unaffected, thus suggesting a normal progression of a developing growth plate (Hallett et al., 2019). This could also explain the lack of difference in trabecular morphometry in the distal epiphysis between the alcohol and pair-fed control groups, observed in this study.

Female study groups

In the current study, chronic binge alcohol consumption led to an increased number of chondrocytes, which appeared to be stacked in distinct columns in the proximal epiphyseal growth plate. Periarticular chondrocytes were evident, as well as provisionally calcified bone in the metaphyseal end of the growth plates of animals that consumed alcohol. These observations are consistent with a developing growth plate (Hallett et al., 2019; Roach et al., 2003). These results may infer that chronic binge alcohol consumption promotes bone growth in female rats, particularly in the proximal epiphysis. Furthermore, this could potentially explain the increased trabecular thickness and trabecular number, observed in our study in the female rats. Comparable occurrences have been reported in menopausal women, where a positive correlation exists between light to moderate alcohol consumption and bone mass, coupled with either minimal alterations or a reduction in fracture risk (Turner and Sibonga, 2001; Turner, 2000). Nevertheless, given the developmental stage investigated in the present study (adolescence), further research is warranted to understand the influences of alcohol on oestrogen levels in adolescent female rats which may impact the effects of alcohol on bone growth and development.

A comparison of the alcohol group with the pair-fed control group in the distal epiphyseal growth plate showed similar chondrocyte density and consistent chondrocyte columnar arrangement, thus indicating normal epiphyseal growth plate development (Hallett et al., 2019).

This suggests that chronic binge alcohol consumption had no effect on the distal epiphyseal growth plate.

Proliferative zone Ki-67 immuno-positive chondrocyte number

Previous research on the influence of alcohol consumption on adolescent bone tissue development have predominantly demonstrated growth inhibition in the tibia and femur (Lauing et al, 2008; Hogan et al, 1997; Sampson et al, 1996, 1997). The observed decrease in chondrocyte count in our current study corroborates the findings of Miralles-Flores and Delgado-Baeza (1992), these authors reported a deficiency in chondrocytes within both the proliferative and hypertrophic zones. The authors of our study attribute this phenomenon to alterations in the composition and arrangement of the extracellular matrix, which could potentially influence the maturation process of chondrocytes. However, information regarding cell markers of proliferation was not part of their investigations (Miralles-Flores and Delgado-Baeza, 1992). The current study found fewer proliferating cells (Ki-67 immuno-positive) in the proximal epiphyseal growth plates in male rats, suggesting that a chronic binge alcohol model triggers damages specific to the proximal epiphyseal growth plate. However, in the distal epiphysis, the proliferating chondrocyte population remained unaffected.

Regarding female adolescent rats, our findings showed no significant difference in Ki-67 immuno-positive chondrocytes in both the proximal and distal growth plate proliferative zones between the alcohol and pair-fed control groups. This could explain the lack of differences seen in the trabecular morphometry observed in our study.

4.4 CONCLUSION

Chronic binge alcohol consumption resulted in detrimental effects in the proximal epiphysis with regards to trabecular morphometry in male rats. Disruptions in cellular morphology of the growth plate, as well as fewer proliferating cells (Ki-67 immuno-positive) were also observed in the proximal epiphysis of male rats. Furthermore, female rats' internal architecture in the proximal growth plate appeared enhanced, together with an improved tensile strength.

Chapter 5

General discussion and conclusion

5.1 GENERAL DISCUSSION

We sought to investigate whether an acute and chronic binge drinking model would disturb growth, development, and bone integrity in the femur of adolescent Sprague Dawley rats. To achieve this, we assessed whether a binge drinking model of alcohol causes delayed bone growth through disturbances of epiphyseal growth plate chondrocyte activity, we immunolabelled these chondrocytes for Ki-67 protein expression. Then, we used three-dimensional micro-focus X-ray computed tomography (3D-μCT) to assess trabeculae thickness, volume, number and spacing in the proximal and distal epiphysis of the femur. Finally, we tested the theory that binge alcohol exposure increases fracture risk (weakens bones) by using three-point bending tests to assess tensile strength of the bone.

Our study queried the extent to which binge alcohol consumption would affect bone growth and development in a rat model of moderate binge drinking. This model is appropriate in the South African context where binge drinking is common amongst adolescents and young adults (Morojele and Ramsoomar, 2016, Vellios and Van Walbeek, 2017) No group differences in weight gain and food intake were observed despite one group receiving alcohol. This indicates that the binge alcohol consumption models employed in our study did not affect the feeding behaviors of the animals.

Osteometric measurements

Osteometric dimensions of the femur were included in the parameters to facilitate the estimation of bone size. This study found no difference in osteometric parameters in both the male and female rats in the binge alcohol drinking model, this finding is in agreement with a study by Sampson and colleagues in 1996 which reported the femora treated with alcohol exhibiting similar lengths to the pair-fed controls after two weeks of alcohol administration. However, in the same study when alcohol was given for a longer duration this resulted in shorter femora (Sampson et al.,1996). This suggest that if alcohol is given for a longer period this could result in a negative impact on bone length (Turner et al., 2001, 1987).

Growth plate morphology and cell proliferation

Previous studies attributed the inhibition of growth observed in adolescents due to a smaller epiphyseal growth plate size (Miralles-Flores and Delgado-Baeza, 1992), however this study was done on gestational alcohol exposure. Other researchers (Snow and Keiver, 2007) also found fewer chondrocytes in the epiphyseal growth plate of offspring exposed to binge alcohol using animal studies. Similarly, our study made the same findings of disturbed epiphyseal growth plates with fewer chondrocytes in the male rats from the alcohol treated group in both extremities, with no negative changes seen in female rats. This discrepancy, along with the normal cell morphology of the epiphyseal growth plate, suggests the existence of a compensatory or resistance mechanism to alcohol in female rats, in binge alcohol consumption. Similar phenomena have been reported in menopausal women (Turner and Sibonga, 2001), emphasizing the importance of further investigations to elucidate the potential effects of alcohol on oestrogen-bone pathways, particularly in adolescent females.

We proposed and tested the theory that epiphyseal growth plate chondrocyte proliferation is inhibited by exposure to alcohol using a binge model. Employing immunohistochemical methods (Ki-67), we found that exposure to alcohol using a binge model decreased chondrocyte proliferation in the epiphyseal growth plate in male rats.

Trabecular Morphometry

Trabecular parameters were observed to be worse in the male rats, with no significant changes in the female rats, in both the acute and chronic binge drinking models. We observed that a binge alcohol consumption led to disturbance in the microarchitecture and structure of the trabecular bone of male alcohol exposed rats. These alterations were characterized by a decrease in bone tissue volume (BV/TV), reduction in trabecular thickness (Tb.Sp), and an increase in spacing. Our findings corroborate with previous literature on actively young growing rats (Sampson et al., 1996, Sampson, 1997) and in adult rats (Maddalozzo et al., 2009; Turner et al., 2001) which reported changes such as a decrease in bone fraction area (BV/TV), trabecular thinning (Tb.Th).

Tensile strength

We did not find impairments in bone strength using three-point bending tests in the alcohol group in this study. Conversely, Hogan et al. (1997) using a chronic model reported a lower

maximum and break force in alcohol-exposed animals compared to the pair-fed controls. This discrepancy in findings is likely attributed to differences in study design. Hogan and colleagues (1997) used three-week-old female Sprague-Dawley rats and fed them a modified Lieber-DeCarli diet ad libitum containing 35% alcohol-derived calories for eight weeks, we administered 20% alcohol via oral gavage to seven-week-old male and female Sprague-Dawley rats for one week (acute) and four weeks (chronic) in our study. It is possible that if we had used a higher alcohol concentration, and a longer administration duration, our results would have been similar to those of Hogan et al. (1997).

5.2 Conclusion

The femur exhibited that binge alcohol consumption causes thinner trabeculae that are more widely spaced and with a smaller bone to volume ratio (BV/TV). However, the tensile strength was similar in the alcohol exposed rats and paired fed groups in male rats, whereas it appeared improved in female rats exposed to alcohol. A binge model also affected the number of chondrocytes in the proliferative zone negatively. All the adverse changes observed in the osseous tissue in the current study was shown in the male rats. Our study found alcohol to have no adverse effects on female rats, which could be due to hormonal differences. Oestrogen plays a protective role in bone health by increasing bone mineral density and stimulating osteoblast activity. The absence of this protective effect in male rats may make them more vulnerable to alcohol-induced bone damage. Therefore, an understanding of gender disparities may assist in preventative measure and strategies to mitigate the harmful effects of alcohol abuse.

5.3 Limitations

A limitation of this study was that it involved male rats and female rats aged 7 weeks (equivalent to 49 postnatal days), which corresponds to approximately 14.5 human years and falls within the human adolescence period (Senguta, 2013). It is important to note that female rats typically enter the pubertal phase as early as 32 postnatal days, while male rats do so around 45 postnatal days (McCutcheon and Marinelli, 2009). This difference in pubertal timeframe between male and female rats is likely to impact their response to alcohol exposure.

5.4 Recommendations

Further investigations on the potential effects of alcohol on the oestrogen-bone pathways of adolescent female rats.

REFERENCES

Abrams, S.A. (2003). Normal acquisition and loss of bone mass. *Hormone Research*. 60(Suppl 3), 71–76.

Ağırdil, Y. (2020). The growth plate: A physiologic overview. *Efort Open Reviews*. 5(8), 498-507.

Amirazad, H., Dadashpour, M. and Zarghami, N. (2022). Application of decellularized bone matrix as a bioscaffold in bone tissue engineering. *Journal of Biological Engineering*. 16(1), 1.

Anderson, P. (2007). Binge Britain: Alcohol and the National Response. *Addiction*. 102(5), 830-831.

Astudillo, M., Kuntsche, S., Graham, K., et al. (2010). The Influence of Drinking Pattern, at Individual and Aggregate Levels, on Alcohol-Related Negative Consequences. *European Addiction Research*. 16(3), 115-123.

Augat, P. and Schorlemmer, S. (2006). The role of cortical bone and its microstructure in bone strength. *Age and Ageing.* 35(Suppl 2), 27–31.

Bagi, C. M., Hanson, N., Andresen, C., et al. (2006). The use of micro-CT to evaluate cortical bone geometry and strength in nude rats: Correlation with mechanical testing, pQCT and DXA. *Bone*. 38(1), 136-144.

Barbería-Latasa, M., Gea, A. and Martínez-González, M. A. (2022). Alcohol, Drinking Pattern, and Chronic Disease. Nutrients, 14(9), 1954

Boskey, A.L. and Coleman, R. (2010). Aging and Bones. *Journal of Dental Research*. 89(12), 1333-1348.

Bouxsein, M.L., Boyd, S.K., Christiansen, B.A., et al. (2010). Guidelines for assessment of bone microstructure in rodents using micro-computed tomography. *Journal of Bone and Mineral Research*. 25(7), 1468–1486.

Cashman, K. D. and Ginty, F. (2003). BONE. *Encyclopedia of Food Sciences and Nutrition. Elsevier*, 557–565.

Cederbaum, A.I. (2019). Alcohol Metabolism. *Encyclopedia of Gastroenterology*. (Second Edition). 16(4), 47–55.

Chang. A., Breeland, G., Black, A.C., et al. Anatomy, Bony Pelvis and Lower Limb: Femur. [Updated 2023 Jul 30]. In: StatPearls [Internet]. Treasure Island (FL): StatPearls Publishing; 2023 Jan-. Available from: https://www.ncbi.nlm.nih.gov/books/NBK532982/

Chung, T., Creswell, K.G., Bachrach, R., et al. (2018). Adolescent Binge Drinking: Developmental Context and Opportunities for Prevention. *Alcohol Research : Current Reviews*. 39(1), 5-15.

Courtney, K.E., and Polich, J. (2009). Binge drinking in young adults: Data, definitions, and determinants. *Psychological Bulletin*.135(1), 142–156.

Dawson, D.A., Li, T., and Grant, B.F. (2008). A prospective study of risk drinking: At risk for what?. *Drug and Alcohol Dependence*. 95(1-2), 62-72.

Del Fattore, A., Teti, A., and Rucci, N. (2012). Bone cells and the mechanisms of bone remodelling. *Frontiers in Bioscience* (Elite edition). 4(6), 2302–2321.

Diamond, T., Stiel, D., Lunzer, M., et al. (1989). Ethanol reduces bone formation and may cause osteoporosis. *The American Journal of Medicine*. 86(3), 282–288.

Diana, P., and Ndou. R. (2022). Tensile strength and trabecular parameter disturbances at 12 weeks postnatally in Sprague Dawley rats exposed to gestational alcohol. J*ournal Of Medical Pharmaceutical and Allied Sciences*. 6(11), 5344-5353.

Föger-Samwald, U., Knecht, C., Stimpfl, T., et al. (2018). Bone Effects of Binge Alcohol Drinking Using Prepubescent Pigs as a Model. *Alcoholism, Clinical and Experimental Research*. 42(11), 2123-2135.

French S.W. (2001). Intragastric ethanol infusion model for cellular and molecular studies of alcoholic liver disease. *Journal of Biomedical Science*. 8(1), 20–27.

Gilmore, I. (2007). Binge Britain: Alcohol and the national response. *Clinical Medicine*. 7(1), 86-87.

Gmel, G., and Rehm, J. (2003). Harmful alcohol use. *Alcohol Research & Health*. 27(1), 52–62.

Gordon, C.M., Zemel, B.S., Wren, T.A., et al. (2017). The Determinants of Peak Bone Mass. *The Journal of Pediatrics*. 180, 261–269.

Griswold, M.G., Fullman, N., Hawley, C., et al. (2018). Alcohol use and burden for 195 countries and territories, 1990–2016: A systematic analysis for the global burden of disease study 2016. *The Lancet*. 392(10152), 1015–1035.

Hallett, S.A., Ono, W., and Ono, N. (2019). Growth plate chondrocytes: skeletal development, growth and beyond. *International Journal of Molecular Sciences*. 20(23), 6009.

Ham, L.S., and Hope, D.A. (2003). College students and problematic drinking: a review of the literature. *Clinical Psychology Review*. 23(5), 719–759.

Hernandez, C.J., Beaupré, G.S. and Carter, D.R. (2003). A theoretical analysis of the relative influences of peak BMD, age-related bone loss and menopause on the development of osteoporosis. *Osteoporosis International*. 14(10), 843–847.

Hogan, H.A., Sampson, H.W., Cashier, E., et al. (1997). Alcohol consumption by young actively growing rats: a study of cortical bone histomorphometry and mechanical properties. *Alcoholism: Clinical and Experimental Research*. 21(5), 809-816.

Hsu, J.T., Wang, S.P., Huang, H.L., et al. (2013). The assessment of trabecular bone parameters and cortical bone strength: a comparison of micro-CT and dental cone-beam CT. *Journal of Biomechanics*. 46(15), 2611-2618.

Kanis, J.A., McCloskey, E.V., Johansson, H., et al. (2008). A reference standard for the description of osteoporosis. *Bone.* 42(3), 467–475.

Kierszenbaum AL, Tres L. (2015). Histology and Cell Biology: An Introduction to Pathology E-Book: *Elsevier Health Sciences*. (5th Edition).

Kivell, T.L., (2016). A review of trabecular bone functional adaptation: what have we learned from trabecular analyses in extant hominoids and what can we apply to fossils?. *Journal of Anatomy*. 228(4), 569–594.

Kotha, S.P., and Guzelsu, N. (2007). Tensile behavior of cortical bone: dependence of organic matrix material properties on bone mineral content. *Journal of Biomechanics*. 40(1), 36–45.

Kuntsche, E. and Gmel, G. (2013). Alcohol consumption in late adolescence and early adulthood – where is the problem?. *Swiss Medical Weekly*. 143(2930), w13826.

Kuntsche, E., Kuntsche, S., Thrul, J., et al. (2017). Binge drinking: Health impact, prevalence, correlates and interventions. *Psychology & Health*. 32(8), 976–1017.

Langdahl, B., Ferrari, S., and Dempster, D. (2016). Bone modeling and remodeling: potential as therapeutic targets for the treatment of osteoporosis. *Therapeutic Advances in Musculoskeletal Disease*. 8(6), 225-235.

Lauing, K., Himes, R., Rachwalski, M., et al. (2008). Binge alcohol treatment of adolescent rats followed by alcohol abstinence is associated with site-specific differences in bone loss and incomplete recovery of bone mass and strength. *Alcohol*. 42(8), 649-56.

Leppänen, O.V., Sievänen, H., and Järvinen, T.L. (2008). Biomechanical testing in experimental bone interventions—May the power be with you. *Journal of Biomechanics*. 41(8), 1623-1631.

Lieber, C.S. (2003). Relationships between nutrition, alcohol use, and liver disease. *Alcohol Research & Health*. 27(3), 220–231.

Livy, D.J., Parnell, S.E., and West, J.R. (2003). Blood ethanol concentration profiles: a comparison between rats and mice. *Alcohol*. 29(3), 165-171.

Mackie, E.J., Ahmed, Y.A., Tatarczuch, L., et al. (2008). Endochondral ossification: how cartilage is converted into bone in the developing skeleton. *The International Journal of Biochemistry & Cell Biology*. 40(1), 46–62.

Maddalozzo, G.F., Turner, R.T., Edwards, C.H. et al. (2009). Alcohol alters whole body composition, inhibits bone formation, and increases bone marrow adiposity in rats. *Osteoporosis International*. 20(9), 1529-1538.

Manolagas, S.C., O'Brien, C.A., and Almeida, M. (2013). The role of estrogen and androgen receptors in bone health and disease. *Nature Reviews, Endocrinology*. 9(12):699-712.

Margolis, D.S., Kim, D., Szivek, J.A., et al. (2006). Functionally improved bone in calbindin-D28k knockout mice. *Bone*. 39(3), 477-484.

Marieb, E., and Hoehm, K. (2013). Human Anatomy and Physiology. (9th edition). New York. *Pearson*. 211-212.

Martin, R.M., and Correa, P.H. (2010). Bone quality and osteoporosis therapy. *Arquivos Brasileiros de Endocrinologia e Metabologia*. 54(2), 186–199.

Maurel, D.B., Boisseau, N., Benhamou, C.L. et al. (2012). Alcohol and bone: review of dose effects and mechanisms. *Osteoporosis International*. 23(1), 1–16.

McCalden, R.W., McGeough, J.A., Barker, M.B., et al. (1993). Age-related changes in the tensile properties of cortical bone. The relative importance of changes in porosity, mineralization, and microstructure. *The Journal of Bone & Joint Surgery*. 75(8), 1193-1205.

McCutcheon, J.E., and Marinelli, M. (2009). Age matters. *The European Journal of Neuroscience*. 29(5), 997–1014.

Mikosch P. (2014). Alcohol and bone. *Wiener Medizinische Wochenschrift* (1946). 164(1-2), 15–24.

Milat, A.M., Mudnić, I., Grković, I., et al. (2017). Effects of White Wine Consumption on Weight in Rats: Do Polyphenols Matter?. *Oxidative Medicine and Cellular Longevity*. 2017, 8315803.

Miralles-Flores, C., and Delgado-Baeza, E. (1992). Histomorphometric analysis of the epiphyseal growth plate in rats after prenatal alcohol exposure. *Journal of Orthopaedic Research*. 10(3), 325-336.

Mmereki, B., Mathibe, M., Cele, L., et al. (2022). Risk factors for alcohol use among adolescents: The context of township high schools in Tshwane, South Africa. *Frontiers in Public Health*. 10.

Morojele, N.K. and Ramsoomar, L. (2016). Addressing adolescent alcohol use in South Africa. *South African Medical Journal*. 106(6), 551–553.

Nation, J.R., Burkey, R.T., and Grover, C.A. (1993). Lead/ethanol interactions. II: pharmacokinetics. *Alcohol*. 10(5), 363–367.

National Institute on Alcohol Abuse and Alcoholism (2004). NIAAA Council Approves Definition of Binge Drinking, NIAAA Newsletter, p. 3:3. Available at: http://pubs.niaaa.nih.gov/publications/Newsletter/winter2004/Newsletter_Number3.pdf.

Nilsson, M., Ohlsson, C., Mellström, D., & Lorentzon, M. (2009). Previous sport activity during childhood and adolescence is associated with increased cortical bone size in young adult men. *Journal of Bone and Mineral Research*. 24(1), 125-133.

Penland, S., Hoplight, B., Obernier, J., et al. (2001). Effects of nicotine on ethanol dependence and brain damage. *Alcohol*. 24(1), 45–54.

Pillay, D., and Ndou. R. (2022). Tensile strength and trabecular parameter disturbances at 12 weeks postnatally in Sprague Dawley rats exposed to gestational alcohol. J*ournal Of Medical Pharmaceutical and Allied Sciences*. 6(11), 5344-5353.

Rachner, T.D., Khosla, S. and Hofbauer, L.C. (2011). Osteoporosis: Now and the future. *The Lancet*. 1276–1287.

Raggatt, L.J. and Partridge, N.C. (2010). Cellular and molecular mechanisms of bone remodelling. *Journal of Biological Chemistry*. 285(33), 25103-25108.

Ralston S. H. (2005). Genetic determinants of osteoporosis. *Current Opinion in Rheumatology*. 17(4), 475–479.

Ramchandani, V., Bosron, W., and Li, T. (2001). Research advances in ethanol metabolism. *Pathologie Biologie*. 49(9), 676-682.

Reed, A.H., McCarty, H.L., Evans, G.L., et al. (2002). The effects of chronic alcohol consumption and exercise on the skeleton of adult male rats. *Alcoholism, Clinical and Experimental Research*. 26(8), 1269–1274.

Rehm, J. (2011). The risks associated with alcohol use and alcoholism. *Alcohol Research and Health*. 34(2), 135-143.

Rizzoli, R., Bianchi, M.L., Garabédian, M., et al. (2010). Maximizing bone mineral mass gain during growth for the prevention of fractures in the adolescents and the elderly. *Bone*. 46(2), 294–305.

Roach, H.I., Mehta, G., Oreffo, R.O., et al. (2003). Temporal analysis of rat growth plates: cessation of growth with age despite presence of a physis. *Journal of Histochemistry & Cytochemistry*. 51(3), 373-383.

Sampson, H.W. (1998). Alcohol's Harmful Effects on Bone. *Alcohol Health and Research World*. 22(3), 190-194.

Sampson, H.W., (1997). Alcohol, osteoporosis, and bone regulating hormones. *Alcoholism: Clinical and Experimental Research*. 21(3), 400-403.

Sampson, H.W., Gallager, S., Lange, J., et al. (1999). Binge drinking and bone metabolism in a young actively growing rat model. *Alcoholism, Clinical and Experimental Research*. 23(7), 1228–1231.

Sampson, H.W., Perks, N., Champney, T.H., et al. (1996). Alcohol consumption inhibits bone growth and development in young actively growing rats. *Alcoholism, Clinical and Experimental Research*. 20(8), 1375–1384.

Sengupta, P. (2013). The laboratory rat: Relating its age with human's. *International Journal of Preventive Medicine*. 4(6), 624–630.

Setiawati, R., and Rahardjo, P. (2019). Bone Development and Growth. *Osteogenesis and Bone Regeneration.*

Shield, K.D., Parry, C., and Rehm, J. (2014). Chronic Diseases and Conditions Related to Alcohol Use. *Alcohol Research : Current Reviews*. 35(2), 155-171.

Soliman, A., De Sanctis, V., Elalaily, R., et.al. (2014). Advances in pubertal growth and factors influencing it: Can we increase pubertal growth?. *Indian Journal of Endocrinology and Metabolism*. 18(Suppl 1), S53–S62.

Sun, X. and Kaufman, P. D. (2018). Ki-67: more than a proliferation marker. *Chromosoma*. 127(2), 175–186.

Turner, R.T. (2000). Skeletal Response to Alcohol. *Alcoholism: Clinical and Experimental Research*. 24(11), 1693-1701.

Turner, R.T. and Sibonga, J. D. (2001). Effects of alcohol use and estrogen on bone. *Alcohol Research and Health*. 25(4), 276–281.

Turner, R.T., Aloia, R.C., Segel, L.D., et al. (1988). Chronic alcohol treatment results in disturbed vitamin D metabolism and skeletal abnormalities in rats. *Alcoholism: Clinical and Experimental Research*. 12(1), 159-162.

Turner, R.T., Doran, E., and Iwaniec, U.T. (2012). Detrimental effects of alcohol on bone growth. *Osteogenesis*. 57-82.

Turner, R.T., Greene, V.S., and Bell, N.H. (1987). Demonstration that ethanol inhibits bone matrix synthesis and mineralization in the rat. *Journal of Bone and Mineral Research*. 2(1), 61-66.

Turner, R.T., Kidder, L.S., Kennedy, A., et al. (2001). Moderate alcohol consumption suppresses bone turnover in adult female rats. *Journal of Bone and Mineral Research*. 16(3), 589-594.

Turner, R.T., Wronski, T.J., Zhang, M., et al. (1998). Effects of ethanol on gene expression in rat bone: transient dose-dependent changes in mRNA levels for matrix proteins, skeletal growth factors, and cytokines are followed by reductions in bone formation. *Alcoholism, Clinical and Experimental Research*. 22(7), 1591–1599.

Vellios, N.G. and Van Walbeek, C.P., (2017). Self-reported alcohol use and binge drinking in South Africa: Evidence from the National Income Dynamics Study, 2014-2015. *South African Medical Journal*. 108(1), 33-39.

Weaver, C.M. (2002). Adolescence: The period of dramatic bone growth. *Endocrine*. 17(1), 43–48.

Wezeman, F.H., Emanuele, M.A., Emanuele, N.V., et al. (1999). Chronic alcohol consumption during male rat adolescence impairs skeletal development through effects on osteoblast gene expression, bone mineral density, and bone strength. *Alcoholism, Clinical and Experimental Research*. 23(9), 1534–1542.

White, T and Folkens, P., (2005). The Human Bone Manual. (1st edition). California: *Elsevier Academic Press*. 122-125.

Zakhari, S. (2006). Overview: How is alcohol metabolized by the body?. *Alcohol Research and Health*. 29(4), 245–254.

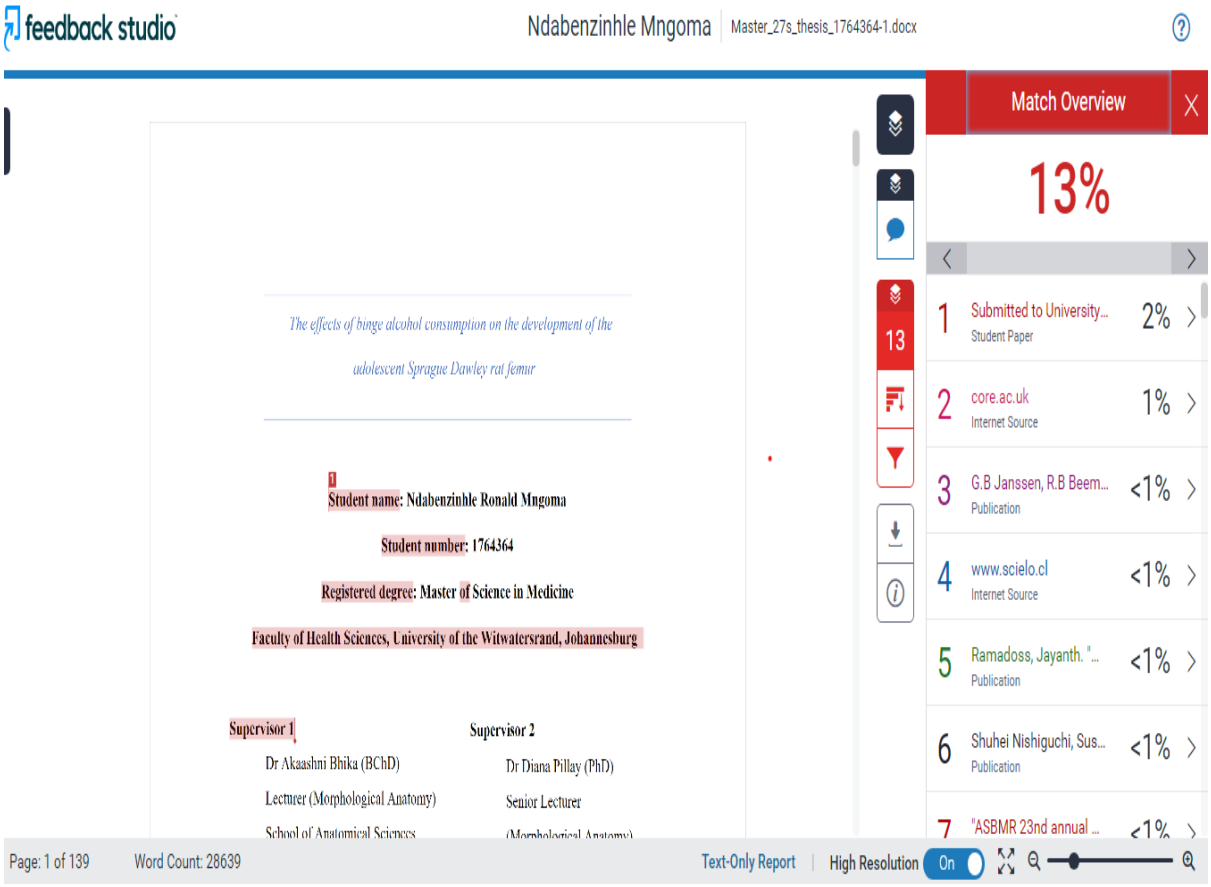
Zhai, G., Andrew, T., Kato, B.S., et al. (2009). Genetic and environmental determinants on bone loss in postmenopausal Caucasian women: a 14-year longitudinal twin study. *Osteoporosis International*. 20(6), 949–953.

Zhu, X., and Zheng, H. (2021). Factors influencing peak bone mass gain. *Frontiers of Medicine*. 15(1), 53–69.

Zorzano, A., and Herrera, E. (1990). In vivo ethanol elimination in man, monkey, and rat: a lack of relationship between the ethanol metabolism and the hepatic activities of alcohol and aldehyde dehydrogenases. *Life Sciences*. 46(3), 223–230.

APPENDICES

Appendix 1: Turnitin report



Appendix 2: Ethical clearance certificate

ANIMALS RESEARCH ETHICS COMMITTEE (AREC)

UNIVERSITY OF THE WITWATERSRAND JOHANNESBURG

STRICTLY CONFIDENTIAL

CLEARANCE CERTIFICATE NUMBER: 2020/11/02/C

APPLICANT: Dr A Bhika
School: School of Anatomical Sciences; Department: N/A; Location: WRAF

PROJECT TITLE: The effect of binge-alcohol consumption on the development of adolescent Sprague Dawley rat mandibles
Category: C; Species and Numbers involved: *72X 7 weeks old male and female, Sprague-Dawley Rats*

Approval is hereby given for the use of animals for the research project named above and described in the application reviewed by a quorate meeting of the AREC held on 1 Dec 2020. This approval remains valid until 4 Mar 2023 and is conditional to the following (if blank there are no special conditions):

Condition 1	Condition 2	Condition 3	Condition 4

All material changes to the approved research must be reported to the AREC before they are implemented. Failure to do so will invalidate this clearance certificate.

An annual progress report must be provided to the AREC.

The use of these animals is subject to AREC guidelines on the use and care of laboratory animals, is limited to the procedures described in the application and is subject to additional conditions listed below:

I, the Chair of the AREC (or my designated representative) am satisfied that the proposed research is ethical as judged by local law, international standards and University policy.

Signed: _____ _____ Date: ___05/03/2021_____

(Chairperson of the AREC)

I am satisfied that the persons listed in this application are competent to perform the procedures described in the application, in the context of Section 23 (1) (c) of the veterinary and Para-veterinary Professions Act (19 of 1982).

Signed: ___ _____ Date: __8 March 2021_____

(Registered Veterinarian)

CC: Student supervisor: «Title1» «Initials1» «Supervisor_surname»
Director Central Animals Service: Dr Kim Jardine

Appendix 3: Reagents used

3-Aminoprpyl triethoxy silane (1010666628, Sigma Aldrich., Germany)

Acetic acid (glacial) (Saarchem 1021020LC., RSA)

Acetone (SAAR1022040LC, Merck Chemicals (Pty.) Ltd., RSA)

Chloroform (CAS NO. 67-66-3, Associated Chemical Enterprise, RSA

Citric Acid (19150 41, Riedel-de Haën AG, Germany)

Disodium hydrogen orthophosphate anhydrate (CAS NO. 7558-79-4, Associated Chemicals Enterprise, RSA)

Entellen (HX 088232, Merck RGA, Germany)

Eosin yellowish (SAAR2186000DC, Merck Chemicals (Pty.) Ltd., RSA)

Formaldehyde (Associated Chemicals Enterprise., RSA)

Hydrochloric acid 1% (HCl) (Associated Chemicals Enterprise., RSA)

Hydrogen peroxide (Catalog. 1037024, Merck (Pty.) Ltd., RSA)

Mayer's solution (SAAR2422001LC, Merck Chemicals (Pty.) Ltd., RSA)

Potassium Alum (CAS NO. 7784-24-9, Associated Chemical Enterprises)

Potassium chloride (CAS NO. 7447-40-7, Associated Chemicals Enterprise, RSA)

Potassium dihydrogen orthophosphate (CAS NO. 7778-77-0, Associated Chemicals Enterprise, RSA)

Rabbit Specific HPR/DAB (ABC) detection IHC kit (Ab64256 Abcam)

Sodium chloride (CAS NO. 7647-14-5, Associated Chemical Enterprise, RSA)

Sodium hydrogen carbonate (CAS NO. 582-28-20, Saarchem (Pty.) Ltd., RSA)

Sodium Iodate (The lab Depot, Inc)

Strept-Avidin HRP (Ab64269 Abcam)

Tween 20 (616-45-00KF, Saarchem, RSA)

Wax (Merck Chemicals (Pty.) Ltd., RSA)

Xylene (CAS NO. 108-38-3, Associated Chemicals Enterprise, , RSA)

Appendix 4: Equipment

Alcohol Colorimetric Assay Kit (Sigma-Aldrich, USA)

Automatic tissue processor (Shandon, Citadel 1000)

Cassettes (Merck Chemicals (Pty.) Ltd, RSA)

Digital Vernier caliper (series 530)

Embedding table (Miles Scientific, serial number 31602-554)

ESCO Laboratory fume hood (Model: EFA-4UDW-8. SN: 2011-60070)

iMark Bio-rad Microplate Absorbance Reader (Bio-rad Laboratories Inc, USA)

Incubator (Model-508-2U, Labcon shaker)

Microfocus computed tomography (µCT) X-ray machine (NIKON XTH 225/320 LC)

Microhaematocrit centrifuge (Haematokrit 210, SN 0031 386-04, Germany)

Microscope (axioscope) (Model Axiocom HRC, identification number 105- 041756)

Microscope Slides (3000F-02-1009, Lasec, RSA)

Microtome (Leica RM 2125RM, Fabr. Nr. 07390329)

Moulds (Merck Chemicals (Pty.) Ltd., RSA)

Water bath (Model number 416, SN: SE 9455)

Weighing scales: (Model- KERN EW600-2M, Germany) (Model- SARTORIUS GMBH, Germany)

Appendix 5: Software packages

Fiji Image-J software

IBM SPSS version 26

Microsoft Excel 2016 (Microsoft Corporation)

Volume Graphics Studio (VGS) software Axiovision (AXIOVs) version 4.7.2.0

Appendix 6: Calculation of the Alcohol (ethanol 20%) dosage administered.

Dose = 3g/kg body weight

Ethanol density = 0.789g/ml

We need to calculate volume

- $Volume = \frac{mass}{density}$

  $= {}^{3g}\Big/_{\frac{0.789g}{ml}}$

  = 3.8ml

- Therefore, the dosage = **3.8ml/kg body weight**

Appendix 7: Calculation of the Maltose dextrin (isocaloric) dosage administered.

- Calculate the caloric equivalent of the alcohol dosage administered.

  1g of ethanol = 7kCal

  3g of ethanol = 21kCal

- 20 % Ethanol was used, therefore;
  - 3g.20% ethanol = 20% of 21kCal

    = **4.2kCal** to match

- 1g Maltose dextrin = **3.89kCal**
  - $= {}^{4.2kCal}/_{3.89kCal}\, x\ 1g\ Maltose\ dextrin$
  - = **1.08g** Maltose dextrin for caloric equivalence

- Dissolve 1.08g Maltose dextrin in 4ml distilled water to make 27% Maltose dextrin solution.
  - 1.08g MD in 4ml distilled water = 4.2kCal/4ml

    = 1.05kCal/ml

- Calculate Maltose dextrin isocaloric dosage in **ml/kg** body weight

$$= \frac{\frac{4.2kCal}{kg}}{\frac{1.05kCal}{ml}} x1$$

= **4ml/kg** body weight

Appendix 8: Preparation of 10% Neutral Buffered Formalin (1000 ml)

1. Measure 100ml of Formaldehyde (37% - 40%)
2. Add 900ml of distilled water
3. Add 3.5g of Sodium dihydrogen phosphate (anhydrous)
4. Add 6.5g of Sodium hydrogen phosphate (anhydrous)
5. Add 8g of Sodium Chloride
6. Store at room temperature

Appendix 9: Preparation of 0.9% Saline solution (1000ml)

1. Weigh 9g of Sodium chloride
2. Add 1000ml of distilled water.
3. Store at room temperature

Appendix 10: Tissue decalcification; EDTA 14%

1. Dissolve 14g of EDTA in 100ml of distilled water.
2. pH the ETDA solution to 7
3. Incubate the tissue in 14% EDTA for 7 days at 45 ^{o}C, with continuous gentle agitation.
4. Replace the decal solution with a fresh supply after 3-4 days.
5. Continually check specimens to make sure decal process is complete.
6. Once decalcification is complete (tissue is pliable) wash specimens in running tap water for 10 mins

Appendix 11: Tissue processing

- Tissues were processed using an automatic tissue processor (Shandon citadel 1000) overnight as follows:
    1. 10% buffered (4hrs)
    2. 70% alcohol (1hr)
    3. 95% alcohol (2hrs)
    4. 95% alcohol (2hrs)
    5. 95% alcohol (2hrs)
    6. 95% alcohol (2hrs)
    7. 100% alcohol (2hrs)
    8. 100% alcohol (2hrs)
    9. 100% alcohol (2hrs)
    10. Chloroform (2hrs)
    11. Chloroform (2hrs)
    12. Wax (2hrs)
    13. Wax (2hrs)

Appendix 12: Paraffin wax embedding

1. Begin by heating both the wax and metal moulds, and also have a pair of forceps ready, ensuring that the temperature remains below 60°C.
2. Once the wax has fully melted, carefully pour it into the metal mould.
3. With the warmed forceps, delicately position the specimens, ensuring that the anterior surface of the bone (proximal and distal ends) faces the bottom of the mould.
4. Allow the contents to cool briefly before appropriately covering them with a plastic cassette.
5. Add additional melted wax swiftly to fill any gaps and allow it to cool for approximately 20 minutes.
6. Finally, separate the metal mould from the plastic cassette.

Appendix 13: Silane coated slides

APES solution (3%)

1. 3-Aminopropytriethoxysilane 6ml
2. Acetone 194ml

Method

1. Immerse slides in 3% APES solution for 30 mins.
2. Rinse in acetone X2
3. Rinse in distilled water
4. Leave to air dry overnight at room temperature.

Appendix 14 : Mayer's Haematoxylin and eosin staining

Haematoxylin solution

For 1000mls

1. Haematoxylin 1g
2. Aluminium potassium sulphate (Potassium alum) 50g
3. Sodium iodate 0.2g
4. Citric acid 1g
5. Chlorate hydrate 50g
6. Allow haematoxylin, aluminium potassium sulphate and sodium iodate to dissolve overnight.
7. Add chloral hydrate and citric acid.
8. Boil solution for 5 minutes and then allow to cool.

Eosin solution

For 1000mls

1. Measure 1000mls of distilled water
2. Add 8g of stock eosin.
3. Add 2g of erythron.
4. Stir using a magnetic stirrer until fully dissolved.

Scott's tap water solutions

For 100mls

1. Sodium hydrogen carbonate 2g
2. Magnesium sulphate 20g
3. Distilled water 1000ml

Dissolve the salts in the water and store in stock solutions at room temperature.

Methods

Hydration

1. Dewax in xylene for 2x10 minutes.
2. Immerse in 2 changes of 100% ethanol for 10 dips

3. Immerse in 95% ethanol for 10 dips
4. Immerse in 70% ethanol for 10 dips
5. Wash in distilled water for 5 minutes

Nuclear staining

1. Stain with Mayer's haematoxylin for 20 minutes
2. Wash in running tap water for 5 minutes
3. Differentiate in 1% acid alcohol for 2 dips
4. Wash in running tap water for 5 minutes
5. Blue in Scott's tap water for 5 minutes
6. Wash in running tap water for 5 minutes

Cytoplasm staining

1. Stain in eosin for 2 minutes
2. Wash briefly in running tap water

Dehydration and mounting

1. Immerse in 70% ethanol for 3 minutes
2. Immerse in 90% ethanol for 10 minutes
3. Immerse in 100% ethanol for 10 minutes
4. Clear in 2 changes of xylene
5. Mount in entellen

Results

Nuclei: Blue-black
Muscle fibers: deep pinky red
Cytoplasm: Varying shades of pin

Appendix 15 : Immunohistochemistry for Ki-67 antibody (NB 500-170)

Method:

Silane coated slides required

Day 1

1.	Deparaffinize sections in Xylene for	2 x10mins
2.	Rehydrate sections through graded alcohols	
3.	Wash slides in running water	5mins
4.	Antigen retrieve sections in Citrate Buffer pH 6 overnight @60° C	

Day 2

5.	Allow to cool at room temperature for	20mins
6.	Rinse in PBS (pH 7.4)	5mins
7.	Block endogenous peroxidase with 1% H_2O_2 in methanol	45 mins
8.	Wash in PBS pH 7.4	3 x 5mins
9.	Incubate with Protein Block	20mins
10.	Wash in PBS	3 x 5mins
11.	Incubate with primary antibody anti Ki-67 NB 500-170 (1: 200) overnight at 4°C	

Day 3

Allow sections to reach room temperature

12. Wash in PBS pH 7.4	4 x 5mins
13. Incubate with biotinylated secondary antibody	10mins
14. Wash in PBS pH 7.4	4 X 5mins
15. Incubate with Strept Avidin HRP	10mins
16. Wash in PBS pH 7.4	4 X 5mins
17. Incubate with DAB working solution	10mins
18. Rinse in running tap water	5mins

19. DO NOT COUNTERSTAIN

20. Hydrate through graded alcohols, clear in Xylene and mount with Entellen.

Solutions to be made

10mM Sodium citrate buffer pH 6 + 0.05% Tween 20

1. Tri- Sodium citrate (di-hydrate) 2.9g
2. Distilled water 1000ml
3. Mix to dissolve sodium citrate and adjust pH to 6 with 1M HCl

1M Phosphate buffer pH7.4

1. NaCl 16g
2. Na2HPO4 3.5g
3. KCl 0.4g
4. KH2PO4 0.4g
5. Distilled water 2000ml

DAB working solution:

In a bijou bottle:

1. 2mg DAB
2. 2ml Tris HCl

In a separate tube add:

1. 29 µl cold distilled water
2. 1 µl hydrogen Peroxide

Add 20 µl of sol Hydrogen Peroxide solution to DAB sol.

Appendix 16: Measurement of cross-sectional area, medullary canal area and cortical area

1. Import image (file > open)

2. Select line tool and draw a line along the entire length of the scale bar

3. Select analyse > set scale

4. Type the known distance 2 and the unit of length (mm) in the box that appeared

5. Check on the global and click “OK”.

6. Select analyse > tools > ROI manager. A window will appear.

7. Select polygonal selection tool

8. Delineate the cross sectional area

9. Click add on the ROI manager

10. Delineate the medullary area

11. Click add on the ROI manager

12. Click measure and calculate the difference

Appendix 17: Measuring the trabecular morphometry on VG studio

1 File
2 Import (import stack)
3 Directory > drive (location of your files)> folder> select folder < Click next
4 Specify resolution (copy all axis on xTekCT file)
5 Histogram
  5.1 Calibration (enlarge size)
    5.1.1 Define background
    5.1.2 Define material
6 Contrast
7 Separation (if you have 2 specimens in a single file)
  7.1 Object < register object < simple registration < align it (to your desired orientation) < finish.
  7.2 Make sure the view is on “Scene”.
8 Extraction
  8.1 Select< rectangle shape < Extract ROI
9 Once extracted, make sure the background is uniform.
10 For trabecular morphometry:
11 Surface determination
    Select Advanced (Classic)
    11.1.1 Move the background far left.
    11.1.2 Move the material far right.
    11.1.3 Adjust the Isovalue so that you perfectly outline the bone material (spaces in the trabeculae should be outlined perfectly to enhance accuracy)
    11.1.4 Click Finish
12 Right click the ROI on the right tab
13 Select properties on the pop up tab.
14 Click “update” (all parameters)
  14.1 Get reading on the Morphometry “page”.